EXPERIMENTS AND NUMERICAL MODELING OF WAVE OVERTOPPING AND OVERFLOW ON DIKES

by

ALI FARHADZADEH, NOBUHISA KOBAYASHI, JEFFREY A. MELBY AND CATERINA RICOTTILLI

RESEARCH REPORT NO. CACR-07-02
OCTOBER, 2007

CENTER FOR APPLIED COASTAL RESEARCH
Ocean Engineering Laboratory
University of Delaware
Newark, Delaware 19711

ACKNOWLEDGEMENT

The study has been supported by the US Army Corps of Engineers, Coastal and Hydraulic Laboratory under Contract No.W912HZ-07-P-0311. The forth author was supported by the University of Calabria, Italy.

TABLE OF CONTENTS

LIST OF TABLES

LIST OF FIGURES

ABSTRACT

Earthen levees are designed for little wave overtopping during a design storm but excessive overtopping and overflow can occur due to the combined effects of an extreme storm, sea level rise and land subsidence. The transition from little wave overtopping to excessive wave overtopping and overflow on an impermeable smooth levee is examined in wave-flume experiments consisting of 107 tests. A numerical model based on time-averaged continuity, momentum and wave action equations is developed to predict the cross-shore variations of the mean and standard deviation of the free surface elevation and depth-averaged fluid velocity of irregular waves in the presence of onshore steady flow. An empirical formula is proposed to express the wave overtopping and overflow rate in terms of the computed variables on the seaward slope of the levee. The formula is shown to predict the measured overtopping and overflow rates within a factor of about 2. The numerical model is applied to an earthen levee in Louisiana to show its practical utility but will need to be verified using field data if available. Furthermore, the numerical model will need to be extended to predict levee erosion and breaching.

CHAPTER 1

INTRODUCTION

Sea defense structures such as levees, dikes, and seawalls are designed to avoid wave overtopping or at least lessen it to an allowable level such that overtopping can not cause failure of coastal structures. Moreover, the structures are expected to protect the landward area and facilities from becoming inundated by water level rise due to combined storms and tides. During the past decades, some levees experienced structural or functional failures, resulting in casualties and damages. This led to many studies on wave overtopping of coastal structures during the last 50 years. The overtopping prediction tools for typical sea defense structures have been continuously improved.

Wave overtopping is defined as a process where waves hit an inclined structure and produce runup over the slope, and then if the crest elevation of the structure is lower than the highest runup level, wave overtopping over the structure occurs. The wave overtopping rate is defined as overtopping volume per unit time per unit width of structure. Nonetheless, wave overtopping cannot be avoided entirely due to the random nature of waves, uncertainties associated with determination of a design water level and the costs of a coastal structure with a high crest.

Attempts have been made to extend our quantitative knowledge of wave overtopping phenomena [Kobayashi and Wurjanto (1989), Kobayashi and Raichle (1994), Waal and van der Meer (1992), van der Meer and Janssen (1995), Herbert (1996), Besley et al. (1998) and Basley (1999), Hedges and Reis (1999), Goda (2000), van Gent (2001), Burchartch and Hughes (2003), Shankar and Jayaratne (2003) and Kobayashi and de los Santos (2007)]. However, combined wave overtopping and overflow have been investigated very little.

After investigating of many damaged dikes and levees in Netherlands in 1953, Germany and Denmark in 1962 and 1976 and recently in the US due to Hurricane Katrina in 2005, it has been shown that during severe storms, most of protective structures failed due to combined wave overtopping and overflow since the structure was designed only for minor wave overtopping. Therefore, the existing overtopping formulas, which do not take account of overflow, can significantly underestimate overtopping discharges.

Schüttrumpf and Oumeraci (2005) have investigated initiation of combined overtopping and overflow. Earthen levee breaching due to combined wave and flow action was also studied by Wang and Bowles (2006), D'Eliso et al. (2006) and Stanczak et al. (2006).

The transition from little wave overtopping to combined wave overtopping and overflow on an impermeable smooth levee is studied in this report by using 107 laboratory tests carried out in a wave flume. The experiments were performed on an impermeable smooth levee with a 1/5 slope mounted on a beach of a 1/34.2 slope. The

experimental results out of 78 overtopping and 29 overflow tests are used to calibrate and verify a time-averaged numerical model for irregular waves by Kobayashi and de los Santos (2007), which is extended here to include wave and current interactions.

In Chapter 2, the time-averaged model is explained in detail and the wave-current interaction is included.

In Chapter 3, the experimental setup and procedure are discussed and the experimental results are tabulated for both wave overtopping and overflow tests.

In Chapter 4, the comparisons between the experimental and the numerical results are presented.

In Chapter 5, the numerical model's ability for modeling of wave overtopping and overflow on a complicated bed profile is shown for Jefferson Perish Lakefront Levee as a prototype.

Finally, in Chapter 6, the conclusions are presented. Additional tables and figures are attached in Appendix A and B.

It is noted that, the summary of this report is presented by Kobayashi, Farhadzadeh and Melby (2007).

CHAPTER 2

NUMERICAL MODEL

The time-averaged numerical model for irregular wave overtopping of permeable slopes based on time-averaged continuity, momentum and energy equations developed by Kobayashi and de los Santos (2007) is extended using linear wave and current theory to account for the interaction of waves and current. In following sections, the governing equations for wave overtopping and overflow of a permeable slope are presented.

2.1 GOVERNING EQUATIONS FOR COMBINED WAVE AND CURRENT

The numerical model described here assumes that incident waves are normal to a shore where the shore is uniform in the longshore direction. The problem can be depicted in Fig. 2-1 where the cross-shore and the vertical coordinate x and z are positive onshore and upward, respectively. The coordinate z is assumed to be zero at the datum. The upper and lower boundaries of a permeable slope are denoted by $z = z_b$ and $z = z_p$, respectively. The lower boundary is considered as an impermeable bed. The water depth and the free surface elevation are denoted by h and η where the water

depth can be written as $h = (\eta - z_b)$. The horizontal fluid velocity U is considered to be depth-averaged. The time-averaged continuity, momentum and energy equations suggested by Kobayashi et al. (2007) for prediction of irregular breaking wave transmission over a submerged porous breakwater are used.

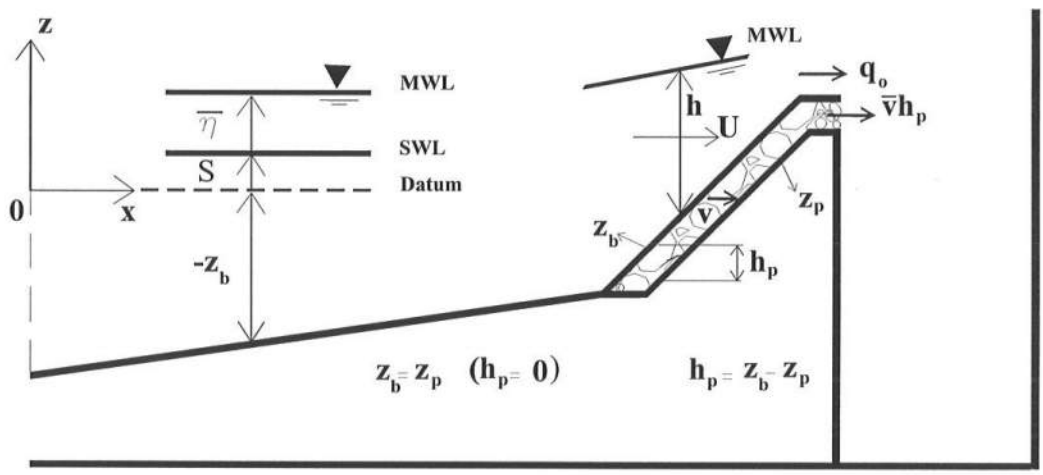

Fig. 2-1. Definition sketch of wave overtopping and overflow model

In Fig. 2-1, z_p =elevation of the lower boundary of a permeable layer; z_b =elevation of the upper boundary of the permeable layer; h_p =(z_b - z_p)= thickness of the permeable layer; S = storm tide (storm surge+tide) which is assumed to be constant in the region of $x \geq 0$ and specified as input at $x = 0$; η =free surface elevation above storm tide; $\overline{\eta}$ =wave setdown or setup above storm tide; $\overline{U}$ =time-averaged, depth-averaged horizontal velocity above z_b; v =vertically-averaged discharge velocity inside the permeable layer; q =time-averaged volume flux above z_b; $d = (S - z_b)$ =still water

depth; and $\bar{h} = (\bar{\eta} + d)$=mean water depth above z_b. For brevity, the overbar of $\bar{h}$ is omitted in the following.

To see how a current can change wave characteristics, based on linear wave theory, the dispersion relationship in presence of a current can be written as follows (e.g., Dean and Dalrymple 1991):

$$\omega_p = \omega + k\, {}^{q}\!/_{h} \quad \text{and} \quad \omega^2 = kg \tanh(kh) \tag{2-1}$$

where g =gravitational acceleration; ω=intrinsic angular frequency based on wave period T; k=wave number; ω_p=absolute angular frequency based on the spectral peak period T_p at the seaward boundary located at $x = 0$.

On the other hand, the dispersion relation of waves in shallow water is approximated as:

$$\omega^2 = kg \tanh(kh) \approx k^2 gh \tag{2-2}$$

Combination of Eqs. (2-1) and (2-2) yields:

$$\omega_p \approx \omega + \omega \frac{q/h}{\sqrt{gh}} = \omega(1 + \frac{q}{h\sqrt{gh}}) \tag{2-3}$$

Using open channel hydraulics (e.g. Henderson 1966), the overflow rate may be estimated as:

$$q \approx h\sqrt{gh} \tag{2-4}$$

Then Eq. (2-3) reduces to:

$$\omega_p = 2\omega \quad \text{or} \quad T \approx 2T_p \tag{2-5}$$

This shows that due to overflow the wave period becomes twice larger, indicating the noticeable effect of the current on waves overtopping on a levee crest. This increase of the wave period T decreases the angular frequency ω, wave celerity C and wave group velocity C_g.

$$C = \frac{\omega}{k}; \quad C_g = nC; \quad n = \frac{1}{2}\left[1 + \frac{2kh}{\sinh(2kh)}\right] \tag{2-6}$$

In order to find the value of k for given h, ω_p and q, Eq. (2-1) is rewritten as:

$$\omega_p = [kg\tanh(kh)]^{0.5} + k\frac{q}{h} \tag{2-7}$$

Expressing the deep water wave number k_o, for $q = 0$ as:

$$k_o = \frac{\omega_p^2}{g} = \frac{(2\pi)^2}{gT_p^2} \tag{2-8}$$

Eq. (2-7) is written as:

$$X\tanh(X) = a(1 - bX)^2 \tag{2-9}$$

where $X = kh$; $a = k_o h$; $b = \frac{1}{\omega_p}\frac{q}{h^2}$; and $\omega_p = \frac{2\pi}{T_p}$. By solving Eq. (2-9) iteratively, all the quantities related to k can be calculated.

2.1.1 TIME-AVERAGED CONTINUITY EQUATION

For linear progressive waves in finite depth relative to the current, the standard deviation of the oscillatory velocity ($U - \overline{U}$) is given by:

$$\sigma_U = C\sigma_* \tag{2-10}$$

where σ_U =the standard deviation of U; $\sigma_* = \sigma_\eta / h$; and σ_η =standard deviation of η.

The wave-induced onshore flux q_{waves} may be written as:

$$q_{waves} = \frac{g\sigma_\eta^2}{C} \tag{2-11}$$

The total volume flux of progressive linear waves and current can be written as:

$$q = h\overline{U} + gC^{-1}\sigma_\eta^2 = h\overline{U} + \frac{gh}{C^2}\sigma_U\sigma_\eta \tag{2-12}$$

Eqs. (2-10) and (2-12) are used to estimate σ_U and $\overline{U}$ for given C, h, σ_η and q.

In shallow water, the wave celerity can be written as $C \approx \sqrt{gh}$, so Eq. (2-12) becomes:

$$q = h\overline{U} + \sigma_U\sigma_\eta \tag{2-13}$$

which was the equation used by Kobayashi and de los Santos (2007).

The time averaged continuity equation in presence of a permeable layer can be written as:

$$\frac{\partial}{\partial x}(q + \bar{v}h_p) = 0 \tag{2-14}$$

where $\bar{v}$=time-averaged horizontal discharge velocity in the permeable layer. Integrating of Eq. (2-14) yields:

$$q + \bar{v}h_p = q_t = q_o + q_s + q_f \tag{2-15}$$

where q_t=total flux on the landward edge of the levee crest; q_o=overtopping rate; q_s=seepage rate; and q_f=overflow rate. Eq. (2-15) with Eq. (2-12) yields:

$$\overline{U} = -\sigma_*^2\frac{gh}{C} + \frac{q_t - \bar{v}h_p}{h} \tag{2-16}$$

where $q_t = q$ for the impermeable slope with h_p=0.

2.1.2 TIME-AVERAGED MOMENTUM EQUATION

In presence of current, time-averaged momentum equation can be written as (e.g., Mei 1989):

$$\frac{d}{dx}(h^{-1}q^2 + \frac{S_{xx}}{\rho}) + gh\frac{d\overline{\eta}}{dx} + \frac{\tau_b}{\rho} = 0 \tag{2-17}$$

where S_{xx}=cross-shore radiation stress defined as:

$$S_{xx} = \rho g \sigma_\eta^2 (2n - 0.5) \tag{2-18}$$

where ρ=fluid density; and $n = [1 + 2kh/\sinh(2kh)]/2$.

The bottom shear stress τ_b in Eq. (2-17) and the corresponding dissipation rate D_f which is used in the next section are expressed using the formulas based on the quadratic drag force (Kobayashi et al. 2007). The Gaussian distribution of U and the equivalency of the time and probabilistic averaging are used to express τ_b and D_f in terms of $\overline{U}$ and σ_U with $U_* = \overline{U}/\sigma_U$.

$$\tau_b = \frac{1}{2}\rho f_b \sigma_U^2 G_2(U_*) \tag{2-19}$$

$$D_f = \frac{1}{2}\rho f_b \sigma_U^3 G_3(U_*) \tag{2-20}$$

where f_b=bottom friction factor. The functions $G_2(r)$ and $G_3(r)$ for an arbitrary r are given by Kobayashi et al. (2007) and can be approximated as $G_2 \approx 1.64r$ and $G_3(r) \approx (1.6 + 2.6r^2)$ for $|r| < 1$. The averaged velocity $\overline{U}$ is estimated using the time-

averaged, vertically integrated continuity equation Eq. (2-16). The mean water level $\overline{\eta}$ computed by Eq. (2-17) is induced by the radiation stress S_{xx} and the volume flux q.

If S_{xx}=0 and τ_b=0, Eq. (2-17) yields $[\overline{U}^2/(2g)+\overline{\eta}]$=constant. This equation is used for steady flow over a wide weir (e.g., Henderson 1966). The mean water level $\overline{\eta}$ decreases landward with the landward increase of $\overline{U}$ in absence of waves.

2.1.3 WAVE ACTION EQUATION

The time-averaged wave energy equation in the absence of waves is replaced by the wave action equation in presence of the current and can be written as (Phillips 1977):

$$\frac{d}{dx}\left[\frac{\rho g\sigma_\eta^2}{\omega}(C_g+h^{-1}q)\right]=-\frac{D_B+D_f+D_r}{\omega} \tag{2-21}$$

where D_r and D_B are the energy dissipation rate inside the permeable layer and the energy dissipation rate due to wave breaking, respectively. In Eq. (2-20), the term $h^{-1}q$ corresponds to the current velocity. In absence of the current, q=0, $\omega=\omega_p$ from Eq. (2-1) and Eq. (2-21) reduces to the wave energy equation used by Kobayashi et al. (2007).

The energy dissipation due to wave breaking, D_B, is estimated as (Battjes and Stive 1985):

$$D_B=\left[\frac{\rho gaQH_B^2}{4T}\right] \tag{2-22}$$

where H_B=breaker height used to estimate D_B; and Q=fraction of breaking waves with Q=0 for no breaking and Q=1 when all waves break. The breaking wave function Q is estimated using the formula by Battjes and Stive (1985):

$$\frac{Q-1}{\ln Q}=\left(\frac{H_{rms}}{H_m}\right)^2 \tag{2-23}$$

with

$$H_m=\frac{0.88}{k}\tanh\left(\frac{\gamma kh}{0.88}\right) \tag{2-24}$$

where H_m=local depth-limited wave height with $H_m=\gamma\bar{h}$ in shallow water; γ=breaker ratio parameter; and a=ratio between wave length and horizontal length scale $\left(3\bar{h}/S_b\right)$ imposed by the small depth $\bar{h}$ and bottom slope S_b near the shoreline. This ratio is assumed $a\geq 1$ and given by:

$$a=\frac{(2\pi/k)}{3h/S_b}\geq 1 \tag{2-25}$$

where S_b=local bottom slope defined as $S_b=dz_b/dx$. The current effect, which modifies wave breaking (Sakai and Kobayashi 1990), is introduced by applying the wave period obtained from Eq. (2-9) into Eq. (2-22). Since the wave period increases due to the following current, D_B decreases. Moreover, the wave number k obtained from Eq. (2-9) is used in Eqs. (2-24) and (2-25).

The energy dissipation rate inside the permeable layer is calculated using the formula developed by Kobayashi et al. (2007) who assumed the discharge velocity v of the Gaussian probability distribution.

$$D_r = \rho h_p \left[\alpha \sigma_v^2 (1 + v_*^2) + \beta \sigma_v^3 G_3(v_*) \right] \tag{2-26}$$

where σ_v=standard deviation of v; and G_3=same function as in Eq. (2-20) except for $r = v_*$.

The parameters in Eq. (2-26) are estimated using the following relations:

$$v_* = \frac{\bar{v}}{\sigma_v} \quad ; \quad \alpha = \alpha_o \left(\frac{1 - n_p}{n_p} \right)^2 \frac{\upsilon}{D_{n50}^2} \quad ; \quad \beta = \left(\beta_1 + \frac{\beta_2}{\sigma_v} \right);$$

$$\beta_1 = \frac{\beta_o (1 - n_p)}{n_p^3 D_{n50}} \quad ; \quad \beta_2 = \frac{7.5 \beta_o (1 - n_p)}{\sqrt{2} n_p^2 T} \tag{2-27}$$

where α_o and β_o=empirical parameters calibrated as $\alpha_o = 1000$ and $\beta_o = 5$; n_p=porosity of the stone; D_{n50}=nominal stone diameter defined as $D_{n50} = (M_{50}/\rho_s)^{1/3}$ with M_{50}=median stone mass and ρ_s=stones density; and υ=water kinematic viscosity. Assuming local force balance between the horizontal gradient of hydrostatic pressure and the flow resistance inside the permeable layer, the values of $\bar{v}$ and σ_v are estimated as:

$$(\alpha + 1.64 \beta \sigma_v) \bar{v} = -g \frac{d\bar{\eta}}{dx} \quad ; \quad \alpha \sigma_v + 1.9 \beta \sigma_v^2 = gkh\sigma_* \tag{2-28}$$

which yields σ_v and $\bar{v}$ for given $k\bar{h}\sigma_*$ and $d\bar{\eta}/dx$.

Since in the present experiments in Chapter 3, an impermeable slope was used, D_r=0 and Eq. (2-21) can be simplified as:

$$\frac{d}{dx} \left[\frac{\rho g \sigma_\eta^2}{\omega} \left(C_g + \frac{q}{h} \right) \right] = -\frac{D_B + D_f}{\omega} \tag{2-29}$$

2.2 COMPUTATIOAL PROCEDURE

The landward-marching computation of the above mentioned equations is made by using an assumed value of the volume flux q. Eqs. (2-17) and (2-29) are solved using a finite-difference method with constant nodal spacing. The assumed q is compared with overtopping and overflow discharge calculated using the following formula:

$$q = P_o q_{SWL} + H_{SWL}\sqrt{gH_{SWL}} \qquad \text{for} \qquad H_{SWL} > 0 \tag{2-30}$$

with

$$H_{SWL} = \bar{\eta} + S - R_c \qquad \text{at} \qquad x = x_{SWL} \tag{2-31}$$

where P_o=wave overtopping probability; q_{SWL} =wave-induced onshore flux q_{wave} given by Eq. (2-11) estimated as $x = x_{SWL}$; and H_{SWL}=water head above the levee crest based on the mean water level $\bar{\eta}$ above SWL at $x = x_{SWL}$. The still water level S and the levee crest height R_c are defined relative to the datum $z = 0$. The still water depth $[S - z_b(x)]$ is zero at $x = x_{SWL}$. If $S > R_c$, the levee crest is located below SWL and x_{SWL} is chosen at seaward edge of the levee crest. For this case, H_{SWL} is the mean water depth and $\sqrt{gH_{SWL}}$ may be regarded as the corresponding velocity. If $H_{SWL} \le 0$, no overflow is assumed to occur and Eq. (2-30) is replaced by $q = P_o q_{SWL}$ corresponding to the wave overtopping formula by Kobayashi and de los Santos (2007) for the impermeable structure. Fig. 2-2 shows the two possible conditions on the crest.

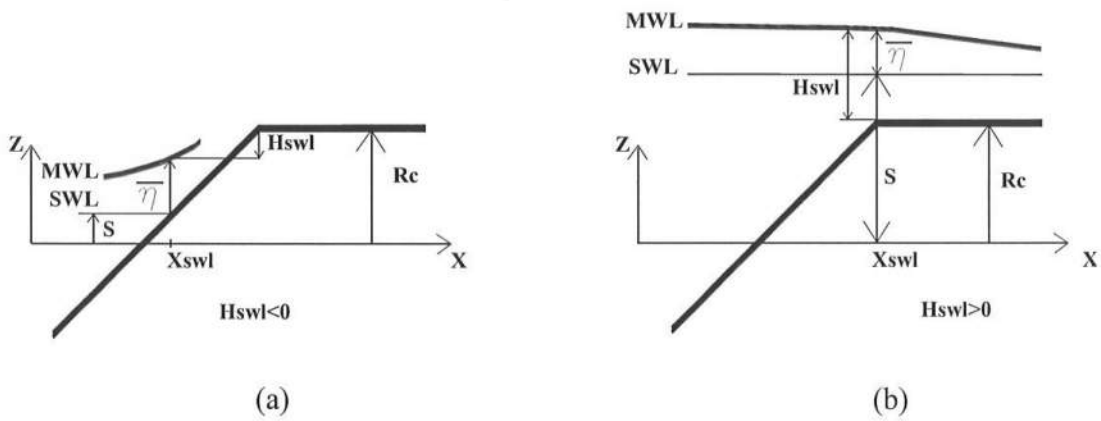

Fig. 2-2. Two possible situations of water level on levee crest

2.3 PROBABILISTIC WAVE OVERTOPPING MODEL

The probabilistic model for irregular wave runup developed by Kobayashi and de los Santos (2007) for a permeable slope is modified to estimate the wave runup probability on an impermeable slope. The model uses the computed $\overline{\eta}(x)$ and $\sigma_\eta(x)$ on the impermeable slope. A runup wire with a vertical elevation above the slope, δ_r, is normally used to measure the water surface oscillations on the slope as shown in Fig. 2-3. The wire measures the instantaneous water surface elevation η_r above SWL on the slope. The mean $\overline{\eta_r}$ and the corresponding standard deviation, σ_r are estimated by the method shown in Fig. 2-3. The probabilities of η surpassing $\overline{\eta}+\sigma_\eta$, $\overline{\eta}$, and $\overline{\eta}-\sigma_\eta$ are assumed equal to the probabilities of η_r exceeding $\overline{\eta_r}+\sigma_r$, $\overline{\eta_r}$, and $\overline{\eta_r}-\sigma_r$. In Fig. 2-3, the elevations z_1, z_2 and z_3 are the intersections of the runup wire with $\overline{\eta}+\sigma$, $\overline{\eta}$, and $\overline{\eta}-\sigma$, using the computed $\overline{\eta}(x)$ and $\sigma_\eta(x)$ along with the runup wire

elevation $[z_b(x)+\delta_r]$. The obtained elevations are assumed to correspond to $z_1=(\overline{\eta_r}+\sigma_r)$, $z_2=\overline{\eta}_r$ and $z_3=(\overline{\eta_r}-\sigma_r)$. The mean and standard deviation of $\eta_r(t)$ are calculated as:

$$\overline{\eta_r}=(z_1+z_2+z_3)/3 \quad ; \quad \sigma_r=(z_1-z_3)/2 \tag{2-32}$$

Since the elevation of z_2 is slightly sensitive to the detailed spatial variation of $\overline{\eta}(x)$, use of z_1, z_2 and z_3 instead of using $\overline{\eta_r}=z_2$ is somewhat more reliable.

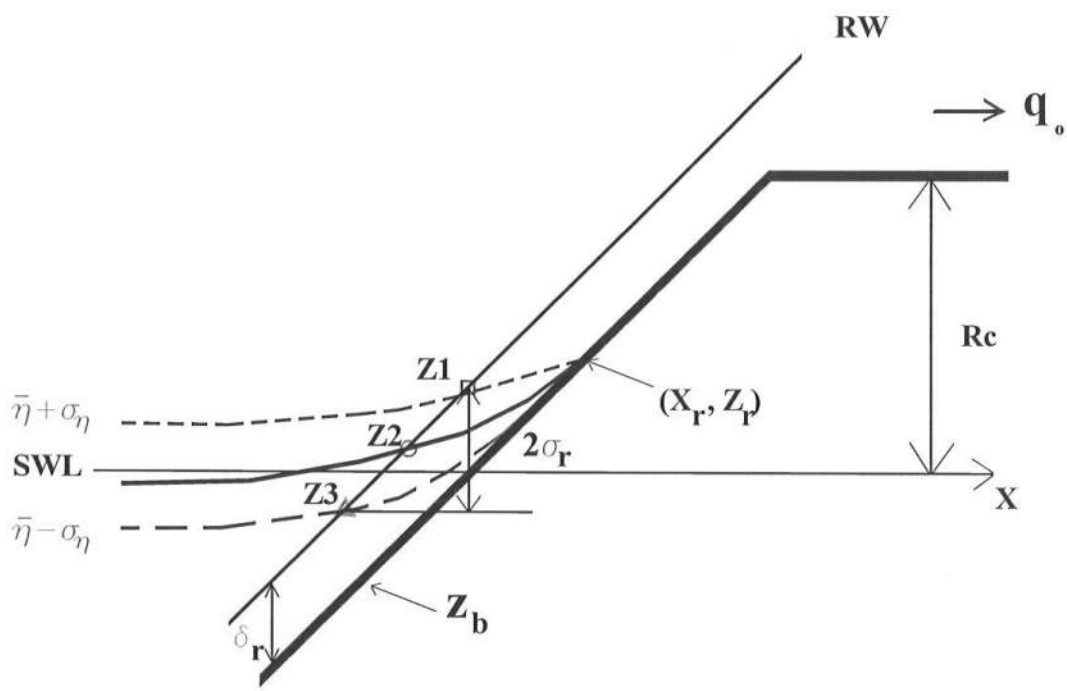

Fig. 2-3. Definition sketch for runup probabilistic model

The runup height R is defined as the crest height above SWL of the temporal variation of η_r. The time series of $[\eta_r(t)-\overline{\eta_r}]$ is analyzed using a zero-upcrossing method to identify the crests in the time series. This procedure is the same as that used for the analysis of the wave crests in the time series of $\eta(t)$ except that the wave crest is defined as the height above the mean water level.

The probability P_o of wave runup exceeding the crest height R_c of a porous structure was proposed by Kobayashi and de los Santos (2007) as:

$$P_o = \exp(-2R_*^{\kappa}) \;\; ; \;\; R_* = \frac{R_c - (\overline{\eta_r} + S)}{R_{1/3} - (\overline{\eta_r} + S)} \tag{2-33}$$

with $$R_{1/3} = (\overline{\eta_r} + S) + (2 + \tan\theta)\sigma_r$$

where $\kappa = 2 + 0.5/R_*^3$ for Weibull distribution with $\kappa = 2$ for Rayleigh distribution; R_c=crest height above the datum $z = 0$; R_*=normalized levee crest height; $R_{1/3}$=significant runup height above $z = 0$, defined as the average of highest 1/3 runups; and $\overline{\eta_r}$ and σ_r=mean and standard deviation of the free surface elevation above SWL measured by the runup wire; θ=slope angle from the horizontal. Eq. (2-33) is applicable only when the crest height R_c exceeds the mean free surface elevation $(S + \overline{\eta_r})$ above z=0. For cases with $R_* \le 0$, the overtopping probability P_o is assumed to be unity (P_o=1). The values of $\overline{\eta_r}$ and σ_r are obtained using Eq. (2-32).

Considering that a runup wire placed above the impermeable slope does not account for a thin layer of uprushing water with its thickness less than the runup wire height δ_r,

the equation of $R_{1/3}$ may be modified as $R_{1/3} = (\overline{\eta} + S) + e\sigma_r$ where e=empirical constant. Using the measured values of P_o, $\overline{\eta_r}$, σ_r, S and R_c, the values of κ and e are calibrated as explained in section 3.5. The Rayleigh distribution (κ=2) and the value of e=4 turn out to gives a better agreement between the calculated and measured wave overtopping probabilities than the Weibull distribution proposed by Kobayashi and de los Santos (2007) for permeable slopes. Therefore, Eq. (2-33) is modified for the impermeable slope:

$$P_o = \exp(-2R_*^2) \quad ; \quad R_* = \frac{R_c - (\overline{\eta_r} + S)}{4\sigma_r} \tag{2-34}$$

Eq. (2-34) is applicable only to the impermeable slopes where a thin layer of water uprushes considerably higher than that on the corresponding permeable slope with infiltration.

The landward-marching computation of the numerical model is started with the initial assumed value of $q = 0$. After the landward-marching computation, Eqs. (2-30) and (2-34) are used to compute q. If the computed q is less than 0.01 cm^2/s, the iteration is assumed to have converged and $q = 0$. Due to numerical oscillations, the simple iteration method by Kobayashi and de los Santos (2007) did not converg for several tests out of the present 107 tests and is replaced by the following bisection method. The initial assumption of $q = 0$ is considered as the minimum value $q_{\min}$. The corresponding computed value of q turns out to be the maximum value $q_{\max}$, indicating that the terms related to q in Eqs. (2-16), (2-17) and (2-29) reduce the wave overtopping and overflow

rate. The landward-marching computation is then made using the assumed value of $q = (q_{\min} + q_{\max})/2$. If the difference between the computed and assumed values of q becomes less than 1%, the iteration is considered to have converged. Otherwise, the range between $q_{\min}$ and $q_{\max}$ is halved. The assumed q is regarded as the new $q_{\max}$ or $q_{\min}$, depending on whether the computed q is less or greater than the assumed q. This iteration found to converge after several iterations. The maximum iteration number was 13 among the 107 tests in the experiments described in Chapter 3.

2.4 EMPIRICAL FORMULA FOR WAVE OVERTOPPING

To compare the numerical model with existing empirical formula, use is made of the Dutch empirical formula for overtopping rates. Reported in the TAW technical report (van der Meer 2002), this widely used formula is expressed separately for breaking and non-breaking waves.

For breaking waves, $\gamma_b \xi_o \le 2$:

$$\frac{q}{\sqrt{gH_{mo}^3}} = \frac{0.067}{\sqrt{\tan\theta}} \gamma \xi_o \exp\left[-4.75 \frac{R_c - S}{H_{mo}} \frac{1}{\xi_o \gamma_b \gamma_f \gamma_\beta \gamma_v}\right] \tag{2-35}$$

For non-breaking waves, $\gamma_b \xi_o > 2$:

$$\frac{q}{\sqrt{gH_{mo}^3}} = 0.2 \exp\left[-2.6 \frac{R_c - S}{H_{mo}} \frac{1}{\gamma_f \gamma_\beta}\right] \tag{4-36}$$

where $H_{mo} = \sqrt{2} H_{rms}$=significant wave height at the toe of a dike; $\tan\theta$=seaward slope of a dike; $\xi_o = \tan\theta / \sqrt{s_o}$; $s_o = 2\pi H_{mo} / (g T_{m-1,o}^2)$; $T_{m-1,o}$=spectral wave period (m_{-1} / m_o)

at the toe of a dike; $T_p = 1.1T_{m-1,o}$ for spectrum with a clear peak; γ_b=berm factor (if no berm γ_b=1); γ_β=wave angle factor (if normally incident waves γ_β=1); γ_f=roughness factor (for smooth slope including grass, γ_f=1.0); γ_v=vertical factor (for no vertical wall γ_v=1.0). It should be noted that Eqs. (2-34) and (2-35) are valid for dikes with the crest elevation ($R_c - S$) above SWL exceeding about $0.5H_{mo}$ and do not account for wave setup explicitly.

For the experiments conditions in Chapter 3, Eqs. (2-34) and (2-35) can be simplified as:

$$\frac{q}{\sqrt{gH_{mo}^3}} = 0.067\sqrt{\frac{\tan\theta}{s_o}}\exp\left[-4.75\frac{R_c - S}{H_{mo}}\frac{\sqrt{s_o}}{\tan\theta}\right] \quad \text{for } \xi_o \le 2 \qquad (2\text{-}37)$$

$$\frac{q}{\sqrt{gH_{mo}^3}} = 0.2\exp\left[-2.6\frac{R_c - S}{H_{mo}}\right] \quad \text{for } \xi_o > 2 \qquad (2\text{-}38)$$

These equations are valid only for the emerged structure, $R_c \ge S$. For the submerged crest tests with $R_c < S$, R_c is simply replaced by $R_c = S$.

CHAPTER 3

EXPERIMENTAL PROCEDURES

This chapter describes the experimental setup and the procedure of performing 107 tests on an impermeable smooth levee with a 1/5 slope placed on a sloped beach, using irregular waves. The experiments consisted of 78 tests of wave overtopping in which the still water level increased incrementally up to the levee crest and 29 combined overtopping and overflow tests in which the still water level was increased to surpass the levee crest elevation. In the following sections, the details of the experiments are explained.

3.1 EXPERIMENTAL SETUP

The experiments were conducted in a wave flume in the Ocean Engineering Laboratory of University of Delaware, which was 33 m long, 0.6 m wide and 1.5 m high as shown in Fig. 3-1. An impermeable smooth beach with a 1.29 m horizontal length and a slope of 1/14.8 was installed in the flume at a distance of 9.06 m from the wave paddle. As shown in Fig. 3-3, a beach with a 1/34.2 slope and a levee with a 1/5 slope and a crest width of 0.3 m was placed landward of the 1/14.8 slope. A basin of

1.85 m length and 0.6 m width built on the lee side of the levee crest collected the overtopped and overflowed water. A submerged pump placed in the collection basin circulated the overtopped water back to the flume to keep the water level in the flume approximately constant. The pumped water was discharged into the zone behind the paddle to lessen flow disturbance (Fig. 3-1). A propeller-type flowmeter was installed in the pipe to measure the flow rate of the pumped water.

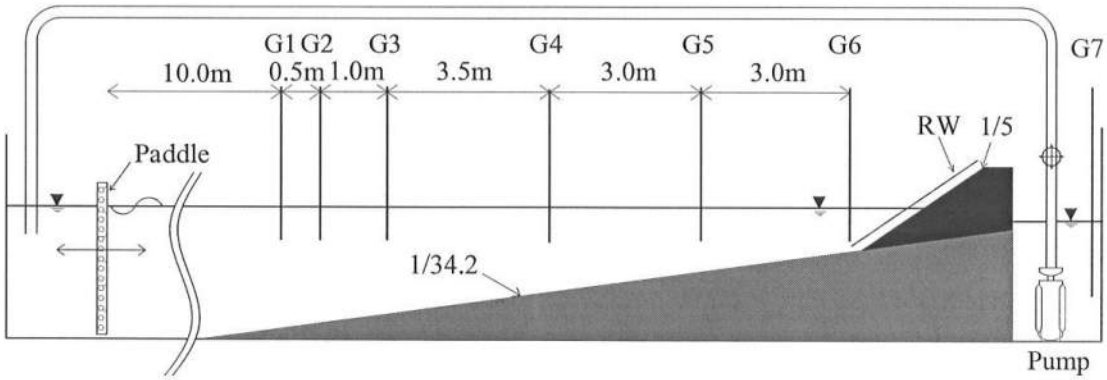

Fig. 3-1. The experimental setup

Seven capacitance gages (G1-G7) and a runup wire (RW) were placed as shown in Fig. 3-1. Wave gages G1- G3 were used to separate the incident and reflected waves and estimate the average reflection coefficient r outside of the surf zone (Kobayashi et al. 1990). Wave gages G4-G6 measured the wave transformation on the 1/34.2 slope and gage G7 was used to record the water level in the collection basin for measuring the wave overtopping and overflow rates. A capacitance runup wire (RW) mounted at the vertical elevation of $\delta_r = 2 \ cm$ on the levee was used to measure the shoreline oscillations.

In this study, the cross-shore coordinate x is taken to be positive landward with $x = 0$ at wave gage G1. The vertical coordinate z is taken to be positive upward with $z = 0$ at the lowest still water level used in the wave overtopping experiments where the still water level (SWL) in the flume was lower than the levee's crest elevation. In Fig. 3-2, dh=water depth (m) on the horizontal bottom of the flume in front of the wave paddle; dt=water depth (m) at the toe of the 1/5 slope; and $d1$=water depth (m) at gage G1.The datum $z = 0$ is chosen such that the bottom elevation $z_b = -0.456\ m$ at $x = 0$, $z_b = -0.12\ m$ at the toe of the 1/5 slope at $x = 11.0\ m$, and $z_b = 0.165\ m$ on the levee crest at $x = 12.5 - 12.8\ m$.

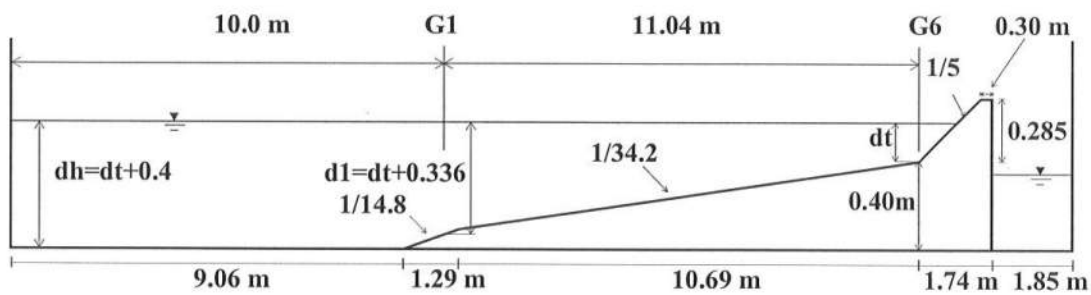

Fig. 3-2. Experimental setup dimensions

3.2 CALIBRATION OF INSTRUMENTS

The flowmeter, seven wave gages G1-G7 and runup wire were calibrated before the tests to ensure the reliability of the instruments.

3.2.1 FLOWMETER CALIBRATION

The flowmeter was calibrated once at the beginning of the experiments. For this purpose a known amount of water in the basin was pumped. The output voltage of the

flowmeter was recorded where the voltage depended on the frequency of the propeller spinning. The water level change in the basin was recorded by gage G7. The rate of water volume change in the basin can be written as $M = dV_b/dt = A(-d\eta/dt)$ where M =pumping rate based on the volume change, V_b = water volume in the basin, A =basin area (A=1.1 m^2 in Fig. 3-2), and η=instantaneous water level in the basin. This pumping rate M is compared with the flow rate R recorded by the flowmeter. Fig. 3-3 shows the measurements of R and η for 8 calibration tests where the flow rate was controlled by a valve. The mean value of R and the constant decrease rate $(-d\eta/dt)$ for each calibration test were used for the correlation between R and $M = A(-d\eta/dt)$. As can be seen in Fig. 3-4, the equation of $M = 1.16R$ explained the calibration tests data well. This relation was used to convert the measured flowmeter rate R to the actual pumping rate M in the following.

3.2.2 CALIBRATION OF WAVE GAGES AND RUNUP WIRE

Gages G1-G7 were moved upward and downward in water every 1 cm in the range of -15 cm and +15 cm about SWL, using motors controlled by a computer program written in LABVIEW. The program controlled the motors for all the seven gages. The voltage of each gage was recorded every 1 cm by the computer program. The calibration line for each gage was produced as a linear relationship between the gage elevation and the voltage. When the calibration line was not linear, the procedure was repeated. Each calibration relation was automatically applied to the corresponding time series of voltage of each gage by the program whose output was the free surface elevation time series.

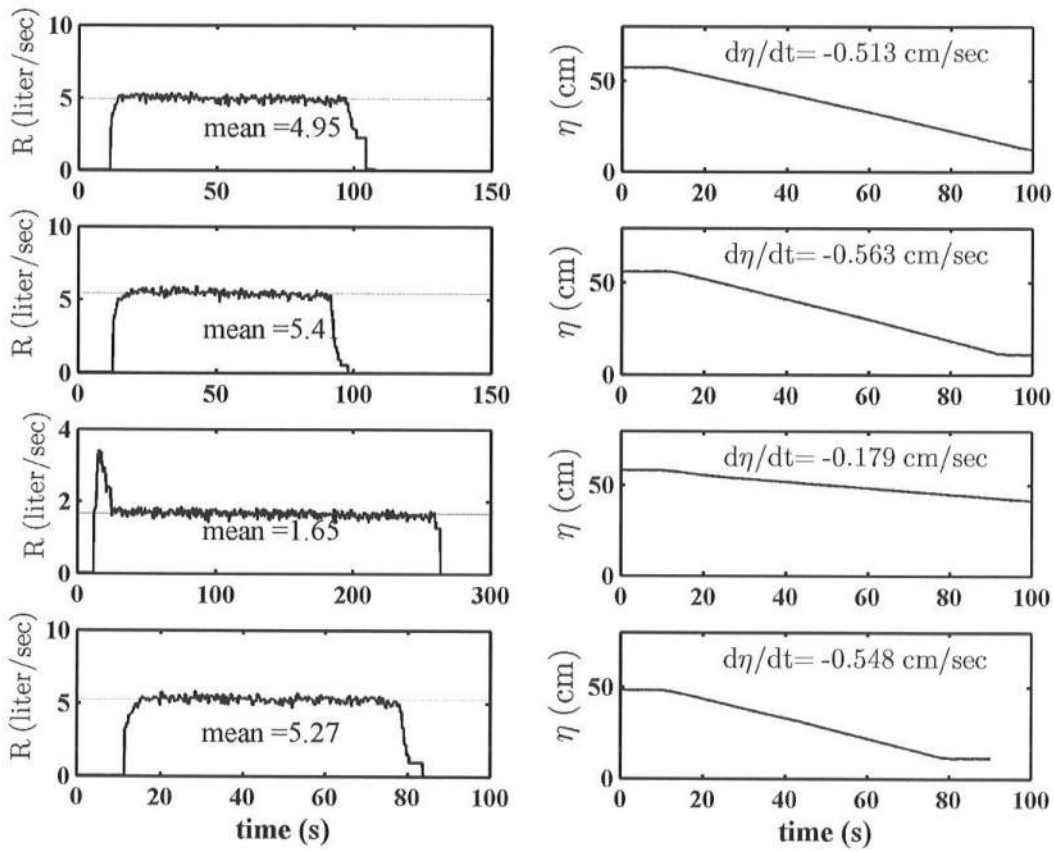

(a) (b)

Fig. 3-3. (a) Flowmeter rate (R) versus time; (b) Water level (η)in the collection basin versus time for 4 calibration tests

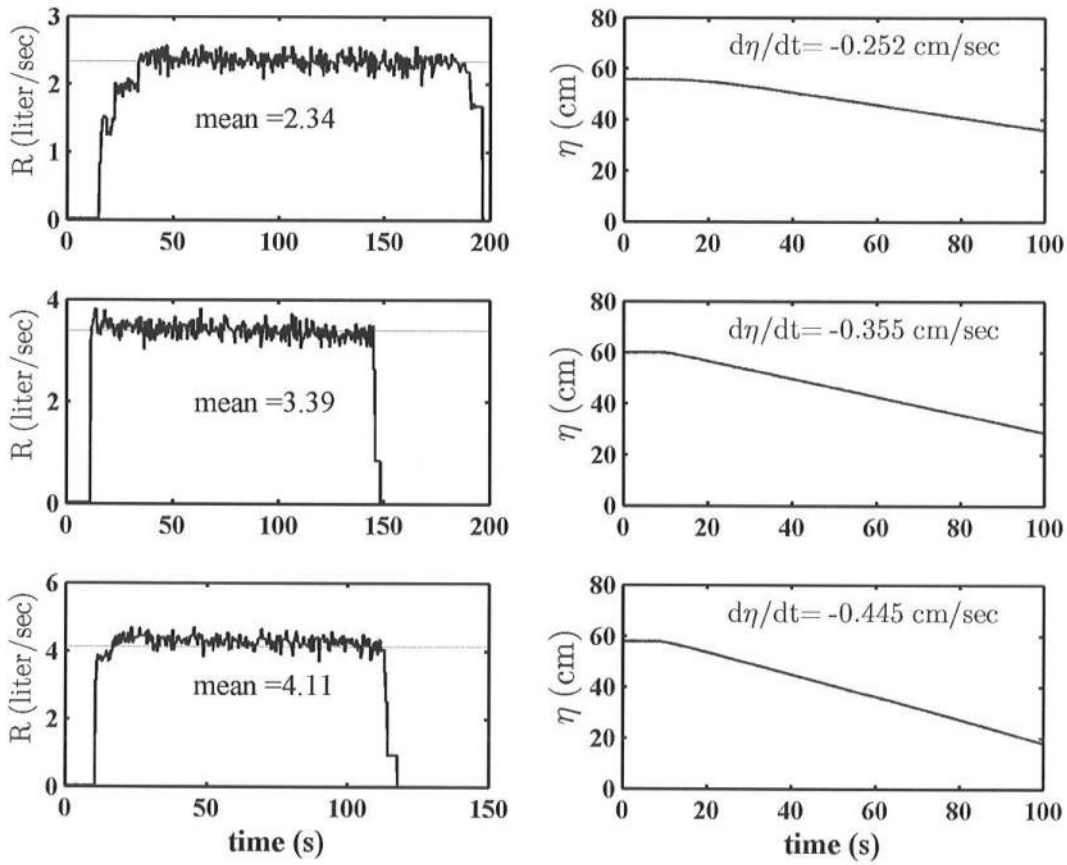

(a) (b)

Fig. 3-3. (Continued). (a) Flowmeter rate (R) versus time; (b) Water level (η) in the collection basin versus time for additional 3 calibration tests

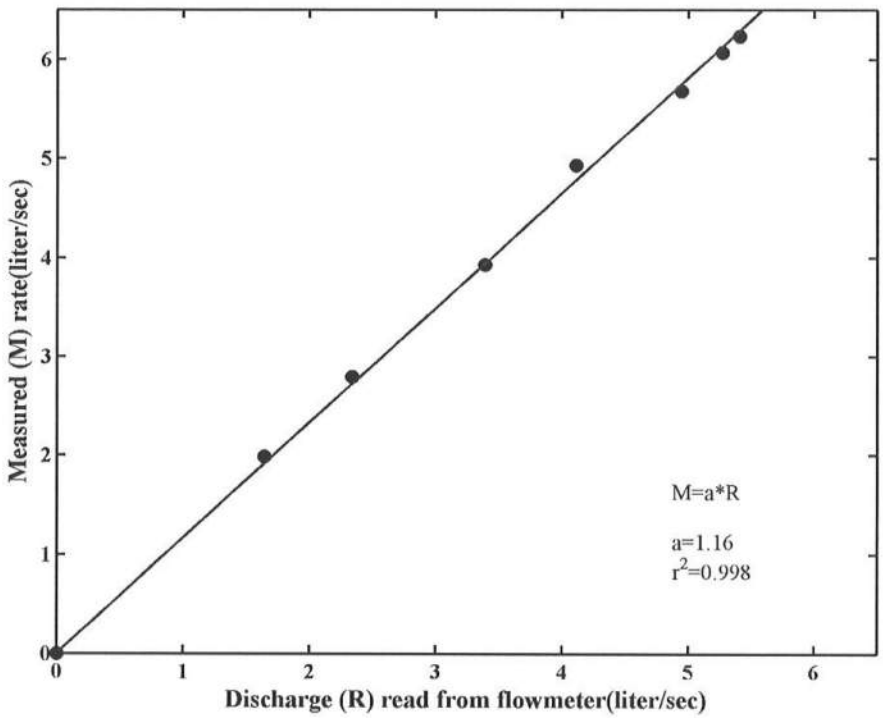

Fig. 3-4. Measured pumping rate M versus flowmeter rate R

The calibration of the runup wire fixed on the 1/5 slope was done by varying the water level inside the tank and recording the voltage for each water level. The calibration curve obtained from the water level-voltage pairs was used to convert the voltage data from the runup wire to the runup wire water level. Since the runup wire was too long, a capacitor was added to facilitate the data acquisition. Fig 3-5 shows an example of the third order calibration curve of the runup wire. The calibration of the runup wire was time-consuming and was performed only at the beginning of each day during the experiments. Wave gages G1-G7 were calibrated before each test.

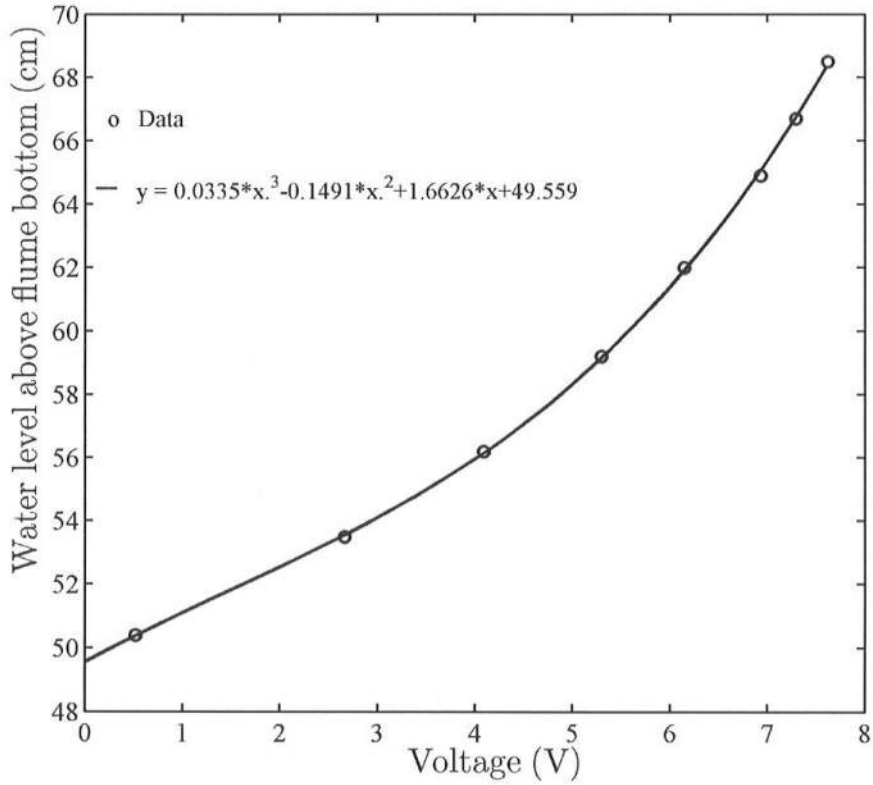

Fig. 3-5. Calibration curve for the runup wire

3.3 OVERTOPPING TESTS

The procedure of 78 overtopping tests was based on the following sequence. After the runup wire calibration, the flume was filled with water to the specified still water level. After a few minutes, the water level became stationary. The seven wave gages were then calibrated as explained above. Irregular waves were generated on the basis of the TMA spectrum whose root-mean-square (RMS) wave height H_{rms} and the significant wave height H_{mo} are defined as $H_{rms} = \sqrt{8}\sigma_\eta$ and $H_{mo} = 4\sigma_\eta$. The measured values of the free surface standard deviation σ_η and the spectral peak period T_p, at wave gage G1,

ranged from 0.84 cm to 4.58 cm and 1.33 s to 3.5 s, respectively. The still water level S above the datum $z = 0$, ranged from 0 m to 0.165 m, corresponding to the toe depth dt =0.12-0.285 m in Fig. 3-2.

Generated waves traveled along the flume, uprushed on the 1/5 slope and overtopped on the crest. The overtopped water was collected in the basin. The collected water was pumped through the pipe to the area behind the wave paddle. The pump was turned on automatically when a float was lifted to a certain water level. When overtopping was excessive, the pump was manually started to reduce the initial accumulation of water in the collection basin.

The waves were generated in a burst of 400 s by a piston-type perforated paddle. The time series of all the gages, the runup wire and the flowmeter were sampled at a rate of 50 Hz. The incident and reflected waves were separated using gages G1, G2 and G3 as discussed earlier. The initial transient of 40 s in each burst was removed from the measured time series. The remaining 360 s time series were used to obtain the mean $\bar{\eta}$ and the standard deviation σ_η of the measured free surface elevation η above still water level for wave gages G1-G6 and the runup wire. Table 3-1 lists the still water level S, the still water depth d, the spectral peak period T_p and the average reflection coefficient r at wave gages G1 as well as the measured values of $\bar{\eta}$ and σ_η at wave gages G1-G6 for the 78 overtopping tests. The overtopping tests were numbered from the lowest ($S = 0$) SWL to the highest ($S = 0.165$ m) SWL. It should be noted that in Table 3-1,

"NR" stands for "Not Reliable", indicating unreliable data due to the instrument malfunction.

In Table 3-2 N_i=total number of incident waves at gage G1, calculated using a zero up-crossing method; $\overline{\eta}_r$=mean water level of the runup wire; σ_r=standard deviation of the free surface oscillation of the runup wire; N_o=number of overtopped waves counted visually; P_o=wave overtopping probability defined as $P_o = N_i / N_o$; and q=average overtopping rate per unit width for the 360-s duration. The overtopping rate q was obtained from the pumped water volume and the water volume change in the collection basin during the 360-s duration. The overtopping rates per unit width and the wave overtopping probabilities for the 78 overtopping tests varied in the range of 0-71.6 cm^2/s and 0.0-1.0, respectively.

Table 3-1a: Free surface statistics for overtopping tests 1-27

Test	G1						G2		G3		G4		G5		G6	
No.	d_1 cm	S cm	T_p sec	r	$\bar{\eta}$ cm	σ_η cm	$\bar{\eta}$ cm	σ_η cm	$\bar{\eta}$ cm	σ_η cm	$\bar{\eta}$ cm	σ_η cm	$\bar{\eta}$ cm	σ_η cm	$\bar{\eta}$ cm	σ_η cm
1	45.8	0.0	1.37	0.33	-0.04	2.64	-0.02	2.40	-0.02	2.67	-0.04	2.59	-0.03	2.55	0.09	2.42
2	45.8	0.0	1.98	0.29	-0.23	4.16	-0.14	4.16	-0.28	4.22	-0.24	4.02	-0.14	3.70	0.27	3.08
3	45.8	0.0	2.31	0.31	-0.32	4.58	-0.31	4.58	-0.36	4.64	NR	4.47	-0.13	3.71	0.38	3.03
4	45.8	0.0	1.4	NR	-0.01	1.96	NR	NR	-0.01	1.98	-0.03	1.99	-0.05	2.00	0.03	2.03
5	45.6	0.0	2.05	0.39	-0.12	3.27	-0.09	2.70	-0.13	3.29	-0.15	3.23	-0.13	3.11	0.16	2.74
6	45.6	0.0	2.35	0.34	-0.15	3.67	0.02	3.43	-0.19	3.76	NR	3.76	-0.21	3.42	0.12	2.90
7	45.6	0.0	1.36	0.32	0.00	1.41	-0.01	1.35	0.00	1.39	-0.03	1.37	-0.02	1.41	0.00	1.55
8	45.6	0.0	1.97	0.34	-0.08	2.25	-0.07	2.26	-0.08	2.27	-0.19	2.32	-0.14	2.46	-0.03	2.43
9	45.6	0.0	2.34	0.36	-0.12	2.82	-0.12	2.70	-0.12	2.87	-0.15	2.74	-0.16	2.54	-0.01	2.26
10	47.6	2.0	1.43	0.26	-0.04	2.35	-0.02	2.35	-0.05	2.36	-0.07	2.32	-0.10	2.31	-0.05	2.37
11	47.6	2.0	2.05	0.3	-0.36	3.88	-0.32	3.87	-0.35	3.82	NR	3.77	-0.21	3.49	0.00	3.07
12	47.6	2.0	2.22	0.33	-0.60	4.56	-0.53	4.46	-0.68	4.59	-0.51	4.36	-0.44	3.92	-0.14	3.20
13	47.6	2.0	1.45	0.26	-0.03	1.90	0.00	1.88	-0.03	1.88	-0.08	1.89	-0.06	1.96	-0.05	1.99
14	47.6	2.0	1.98	0.33	-0.31	2.89	-0.29	2.84	-0.29	3.00	NR	3.13	-0.32	3.02	-0.25	2.91
15	47.6	2.0	2.12	0.34	-0.38	3.68	-0.35	3.68	-0.42	3.65	NR	3.73	-0.22	3.32	-0.20	2.88
16	47.6	2.0	1.4	0.31	0.00	1.35	0.01	1.31	-0.01	1.32	-0.14	1.32	-0.02	1.33	-0.02	1.43
17	47.6	2.0	2.01	0.36	-0.23	2.07	-0.22	2.06	-0.24	2.11	-0.28	2.17	-0.29	2.22	-0.26	2.46
18	47.6	2.0	2.32	0.38	-0.30	2.69	-0.29	2.69	-0.32	2.68	-0.38	2.79	-0.39	2.64	-0.34	2.55
19	49.6	4.0	1.33	0.24	-0.10	2.35	-0.10	2.35	-0.13	2.38	-0.12	2.36	-0.16	2.33	-0.16	2.36
20	49.6	4.0	1.95	0.28	-0.66	3.79	-0.62	3.76	-0.73	3.84	-1.00	3.85	-0.61	3.56	-0.39	3.37
21	49.6	4.0	2.22	0.34	-0.81	4.50	-0.79	4.49	-0.81	4.62	NR	4.34	-0.71	4.01	-0.56	3.34
22	49.6	4.0	1.34	0.27	-0.05	1.72	-0.05	1.72	-0.06	1.71	-0.07	1.74	-0.08	1.71	-0.06	1.77
23	49.6	4.0	2.02	0.3	-0.76	3.08	-0.71	3.10	-0.75	3.08	-0.79	3.17	-0.79	3.22	-0.66	3.13
24	49.6	4.0	2.45	0.36	-0.64	3.42	-0.57	3.49	-0.64	3.52	NR	3.65	-0.66	3.44	-0.48	3.12
25	49.6	4.0	1.43	0.33	0.00	1.23	0.00	1.22	0.00	1.21	-0.01	1.23	-0.01	1.25	-0.04	1.27
26	49.6	4.0	2.03	0.35	-0.37	2.15	-0.35	2.10	-0.38	2.20	-0.40	2.21	-0.41	2.26	-0.42	2.56
27	49.6	4.0	2.5	0.39	-0.61	2.41	-0.56	2.48	-0.61	2.41	-0.61	2.56	-0.61	2.49	-0.62	2.61

Table 3-1b: Free surface statistics for overtopping tests 28-54

Test	G1						G2		G3		G4		G5		G6	
No.	d_1 cm	S cm	T_p sec	r	$\bar{\eta}$ cm	σ_η cm	$\bar{\eta}$ cm	σ_η cm	$\bar{\eta}$ cm	σ_η cm	$\bar{\eta}$ cm	σ_η cm	$\bar{\eta}$ cm	σ_η cm	$\bar{\eta}$ cm	σ_η cm
28	51.6	6.0	1.4	NR	-0.21	2.34	-0.21	NR	-0.22	2.33	-0.21	2.32	-0.21	2.25	-0.29	2.18
29	51.6	6.0	2.03	0.39	-0.71	3.82	-0.69	NR	-0.71	3.89	-0.69	3.96	-0.68	3.83	-0.52	3.61
30	51.6	6.0	2.28	0.42	-0.76	4.56	-0.75	NR	-0.75	4.64	NR	4.61	-0.68	4.31	-0.52	3.65
31	51.6	6.0	1.4	NR	-0.08	1.80	-0.09	NR	-0.10	1.79	-0.14	1.76	-0.10	1.70	-0.10	1.65
32	51.6	6.0	1.96	0.4	-0.57	3.03	-0.55	NR	-0.58	3.02	-0.64	3.00	-0.60	3.14	-0.54	3.16
33	51.6	6.0	2.42	0.43	-0.71	3.45	-0.68	NR	-0.72	3.46	-0.73	3.51	-0.72	3.36	-0.70	3.07
34	51.6	6.0	1.37	NR	-0.03	1.24	-0.03	NR	-0.03	1.23	-0.03	1.23	-0.03	1.22	-0.02	1.15
35	51.6	6.0	2.01	0.45	-0.67	1.99	-0.63	NR	-0.65	2.03	-0.66	2.08	-0.66	2.20	-0.66	2.36
36	51.6	6.0	2.28	0.46	-0.61	2.42	-0.59	NR	-0.62	2.45	-0.63	2.55	-0.64	2.53	-0.61	2.64
37	53.8	8.0	1.37	0.24	-0.39	2.25	-0.35	NR	-0.42	2.22	-0.38	2.21	-0.47	2.16	-0.48	2.04
38	53.6	8.0	1.97	0.29	-0.60	3.74	-0.56	NR	-0.59	3.70	-0.68	3.62	-0.58	3.74	-0.52	3.50
39	53.6	8.0	2.42	0.32	-0.78	4.08	-0.69	NR	-0.80	4.03	-0.60	4.16	-0.77	3.96	-0.64	3.69
40	53.6	8.0	1.4	0.26	-0.25	1.66	-0.25	1.65	-0.23	1.69	-0.30	1.65	-0.51	1.66	-0.24	1.55
41	53.6	8.0	1.88	0.32	-0.62	2.78	-0.56	2.84	-0.63	2.73	-0.66	2.92	-0.64	3.00	-0.60	3.02
42	53.6	8.0	2.17	0.32	-0.61	3.33	-0.49	3.30	-0.59	3.30	-0.62	3.52	-0.62	3.30	-0.56	3.17
43	53.6	8.0	1.38	0.33	-0.04	1.13	-0.05	1.12	-0.06	1.15	-0.07	1.14	-0.05	1.14	0.02	1.05
44	53.6	8.0	1.96	0.38	-0.61	2.02	-0.58	1.95	-0.63	2.00	-0.65	2.06	-0.63	2.10	-0.60	2.19
45	53.6	8.0	2.38	0.4	-0.51	2.32	-0.45	2.30	-0.53	2.29	-0.53	2.42	-0.54	2.40	-0.51	2.56
46	55.8	10.0	1.36	0.24	-0.41	2.17	-0.39	2.14	-0.40	2.15	-0.42	2.19	-0.42	2.15	-0.43	1.89
47	55.6	10.0	2.05	0.28	-0.55	3.44	-0.53	3.30	-0.57	3.39	-0.58	3.37	-0.54	3.40	-0.51	3.20
48	55.6	10.0	1.96	0.3	-0.69	4.05	-0.62	4.01	-0.72	4.06	1.50	4.11	-0.87	3.94	-0.61	3.48
49	55.6	10.0	1.36	0.27	-0.43	1.58	-0.41	1.51	-0.43	1.57	-0.43	1.55	-0.41	1.53	-0.40	1.36
50	55.6	10.0	1.94	0.3	-0.55	2.73	-0.47	2.69	-0.55	2.71	-0.59	2.79	NR	2.87	-0.54	2.69
51	55.6	10.0	2.4	0.34	-0.62	3.13	-0.53	3.16	-0.63	3.12	-0.64	3.29	-0.59	3.17	-0.65	2.98
52	55.6	10.0	1.32	0.36	-0.08	1.13	-0.05	1.11	-0.08	1.13	-0.05	1.10	NR	1.06	-0.07	0.98
53	55.6	10.0	1.97	0.37	-0.45	1.93	-0.40	1.92	-0.44	1.95	-0.49	2.03	-0.45	2.06	-0.45	2.01
54	55.6	10.0	2.34	0.4	-0.48	2.19	-0.44	2.15	-0.47	2.22	-0.53	2.29	-0.48	2.32	-0.46	2.33

Table 3-1c: Free surface statistics for overtopping tests 55-78

Test	G1						G2		G3		G4		G5		G6	
No.	d_1 cm	S cm	T_p sec	r	$\bar{\eta}$ cm	σ_η cm	$\bar{\eta}$ cm	σ_η cm	$\bar{\eta}$ cm	σ_η cm	$\bar{\eta}$ cm	σ_η cm	$\bar{\eta}$ cm	σ_η cm	$\bar{\eta}$ cm	σ_η cm
55	57.6	12.0	1.36	0.38	-0.26	1.11	-0.27	1.13	-0.27	1.10	-0.39	1.12	-0.36	1.13	-0.24	0.94
56	57.6	12.0	2.05	0.39	-0.31	1.76	-0.32	1.70	-0.32	1.77	-0.40	1.74	-0.32	1.83	-0.33	1.66
57	57.6	12.0	2.18	0.39	-0.51	2.08	-0.56	2.08	-0.48	2.10	-0.49	2.17	-0.48	2.14	-0.49	2.07
58	57.6	12.0	1.39	0.29	-0.33	1.58	-0.32	1.58	-0.33	1.59	-0.33	1.59	-0.31	1.55	-0.33	1.35
59	57.6	12.0	2.02	0.29	-0.64	2.56	-0.63	2.57	-0.65	2.59	-0.64	2.63	-0.67	2.69	-0.63	2.46
60	57.6	12.0	2.14	0.32	-0.56	2.93	-0.63	2.91	-0.55	2.90	-0.59	2.94	NR	2.96	-0.55	2.80
61	57.6	12.0	1.35	0.26	-0.43	2.13	-0.43	2.08	-0.43	2.11	-0.43	2.10	-0.55	2.10	-0.39	1.87
62	59.6	14.0	1.64	0.41	-0.58	0.93	-0.59	0.92	-0.57	0.95	-0.60	0.93	-0.59	0.96	-0.62	0.88
63	59.6	14.0	1.94	0.34	-0.37	1.56	-0.33	1.57	-0.37	1.55	-0.39	1.62	-0.37	1.70	-0.41	1.59
64	59.6	14.0	2.13	0.37	-0.43	1.74	-0.41	1.76	-0.41	1.70	-0.44	1.73	-0.41	1.81	-0.45	1.82
65	59.6	14.0	1.63	0.29	-0.36	1.38	-0.37	1.40	-0.37	1.35	-0.38	1.37	-0.37	1.37	-0.39	1.26
66	59.6	14.0	2.05	0.29	-0.36	2.11	-0.37	2.10	-0.37	2.15	-0.39	2.09	-0.39	2.20	-0.41	2.15
67	59.6	14.0	1.36	0.25	-0.28	1.70	-0.30	1.72	-0.28	1.71	-0.32	1.68	-0.28	1.71	-0.33	1.61
68	61.1	15.5	1.34	0.33	-0.63	0.94	-0.63	0.95	-0.63	0.94	-0.61	0.90	-0.65	0.92	-0.65	0.86
69	61.1	15.5	1.96	0.31	-0.66	1.48	-0.67	1.50	-0.69	1.47	-0.66	1.47	-0.63	1.60	-0.69	1.46
70	61.1	15.5	1.62	0.27	-0.61	1.24	-0.61	1.25	-0.61	1.24	-0.62	1.20	-0.61	1.23	-0.64	1.16
71	61.1	15.5	1.94	0.24	-0.41	2.09	-0.42	2.11	-0.42	2.07	-0.43	2.09	-0.35	2.20	-0.44	2.05
72	61.1	15.5	1.63	0.23	-0.41	1.72	-0.41	1.72	-0.41	1.71	-0.42	1.66	-0.45	1.66	-0.44	1.57
73	62.1	16.5	1.32	0.24	-0.22	0.84	-0.21	0.85	-0.22	0.83	-0.23	0.81	-0.22	0.81	-0.23	0.76
74	62.1	16.5	1.97	0.25	-0.45	1.40	-0.48	1.44	-0.46	1.39	-0.48	1.42	-0.48	1.50	-0.48	1.36
75	62.1	16.5	2.29	0.27	-0.33	1.53	-0.34	1.56	-0.32	1.53	-0.35	1.56	-0.35	1.61	-0.36	1.59
76	62.1	16.5	1.59	0.2	-0.19	1.22	-0.18	1.25	-0.17	1.22	-0.17	1.21	-0.17	1.21	-0.18	1.12
77	62.1	16.5	1.67	0.2	-0.45	1.66	-0.46	1.67	-0.45	1.65	-0.47	1.61	-0.47	1.60	-0.49	1.52
78	62.1	16.5	1.91	0.2	-0.31	1.99	-0.31	2.02	-0.33	1.97	-0.33	1.94	-0.31	2.02	-0.36	1.90

3.4 COMBINED OVERTOPPING AND OVERFLOW TESTS

The combined wave overtopping and overflow tests were conducted in manners similar to the overtopping tests. The runup wire was calibrated and then the water level in the flume was raised up to the levee crest level, before the water level was increased above the crest. Water was put in the collection basin to be pumped into the flume to establish overflow. The gages G1-G7 were then calibrated. The rate of pumping was adjusted by the pump valve but it was almost impossible to determine the water level in the flume precisely before each test. After the pumping was started, it took about 800 s to establish a steady current. Waves were then generated for each of 29 combined overtopping and overflow tests. The wave gages G1-G7, the runup wire and the flowmeter were recorded in the same way as in the wave overtopping tests.

Tables 3-3 and 3-4 summarize the 29 combined overtopping and overflow tests. The still water level S was in the range of 17.3-19.4 cm. The value of S in Table 3-3 corresponds to the still water level at wave gage G1 before the generation of irregular waves. The measured values of σ_η at wave gage G1 were in range of 0.73-2.23 cm for the 29 tests because of the limited space between the water level and the carriages supporting the wave gages. In Table 3-4 the number of overtopped waves (N_o) is taken to be equal to the number of waves at gage G1 (N_i) because all the incident waves appear to have propagated over the levee crest. The overtopping probability is equal to 1 for all the 29 tests. In Table 3-4, the combined overtopping and overflow rate q per unit width of the flume was in range of 34.3-107.48 cm^2/s.

Table 3-2a: Wave runup and overtopping statistics for overtopping tests 1-36

Test No.	N_i	RW $\bar{\eta}_r$ (cm)	RW σ_r (cm)	N_o	P_o (N_o/N_i)	q (cm^2/s)
1	258	1.09	3.14	32	0.12	0.26
2	211	1.29	5.27	96	0.45	2.20
3	208	1.37	5.57	96	0.46	1.96
4	265	0.90	2.13	22	0.08	0.11
5	215	1.47	3.58	51	0.24	1.27
6	199	1.63	4.34	44	0.22	2.13
7	257	0.17	1.62	0	0.00	0.00
8	212	0.91	3.15	27	0.13	0.89
9	202	1.11	3.57	38	0.19	1.40
10	268	0.91	2.59	32	0.12	0.64
11	222	1.70	4.12	70	0.32	3.29
12	206	1.67	5.19	45	0.22	6.84
13	269	0.53	2.18	18	0.07	0.27
14	212	1.14	3.94	72	0.34	3.95
15	204	1.38	4.63	79	0.39	5.59
16	260	0.22	1.60	4	0.02	0.03
17	212	0.66	3.21	61	0.29	2.30
18	197	1.04	4.14	72	0.37	4.71
19	263	1.18	2.67	NM	NM	2.06
20	217	1.61	4.34	NM	NM	10.40
21	212	1.84	5.34	NM	NM	13.19
22	272	1.02	2.05	NM	NM	0.65
23	211	1.10	3.97	NM	NM	8.57
24	205	1.44	4.85	NM	NM	11.08
25	264	0.33	1.53	NM	NM	0.02
26	208	0.70	3.24	176	0.85	5.77
27	206	0.69	3.88	167	0.81	6.98
28	263	0.82	2.42	67	0.25	3.16
29	208	1.90	4.34	153	0.74	18.75
30	200	2.37	5.34	131	0.66	25.40
31	261	0.54	2.06	45	0.17	1.23
32	203	1.58	4.03	140	0.69	15.17
33	198	1.72	4.89	133	0.67	17.06
34	274	0.44	1.63	19	0.07	0.29
35	208	0.46	3.35	103	0.50	7.13
36	198	0.97	4.08	100	0.51	11.17

(NM: Not measured)

Table 3-2b: Wave runup and overtopping statistics for overtopping tests 37-67

Test No.	N_i	RW $\bar{\eta}_r$ (cm)	RW σ_r (cm)	N_o	P_o (N_o/N_i)	q (cm^2/s)
37	254	0.94	2.56	114	0.45	5.85
38	211	2.28	4.38	173	0.82	29.78
39	197	2.22	5.19	168	0.85	36.76
40	263	0.54	2.05	72	0.27	2.62
41	216	1.60	3.99	140	0.65	21.05
42	216	1.56	4.47	147	0.68	28.42
43	271	0.41	1.42	24	0.09	0.51
44	208	0.40	3.12	112	0.54	9.74
45	203	0.82	3.69	127	0.63	14.12
46	258	0.84	2.35	138	0.53	9.40
47	219	1.51	3.80	171	0.78	36.60
48	206	1.48	4.61	191	0.93	48.71
49	272	0.22	1.86	81	0.30	3.72
50	212	1.13	3.45	168	0.79	26.32
51	210	1.17	4.31	173	0.82	34.63
52	255	0.22	1.41	40	0.16	1.09
53	214	0.52	2.85	119	0.56	12.39
54	207	0.61	3.46	125	0.60	17.46
55	256	0.09	1.46	91	0.36	3.32
56	216	0.48	2.60	149	0.69	16.42
57	203	0.47	3.17	151	0.74	23.53
58	264	0.38	1.91	154	0.58	7.81
59	213	0.66	3.21	171	0.80	34.79
60	212	0.74	3.67	172	0.81	41.10
61	267	0.65	2.34	170	0.64	13.33
62	263	-0.48	1.40	142	0.54	6.10
63	212	0.29	2.46	172	0.81	24.02
64	198	0.16	2.84	176	0.89	28.91
65	255	0.15	1.88	183	0.72	12.86
66	219	0.48	2.89	196	0.89	40.03
67	262	0.49	2.10	207	0.79	21.56

Table 3-2c: Wave runup and overtopping statistics for overtopping tests 68-78

Test No.	N_i	RW $\bar{\eta}_r$ (cm)	RW σ_r (cm)	N_o	P_o (N_o/N_i)	q (cm^2/s)
68	253	-0.51	1.26	194	0.77	10.00
69	203	-0.44	2.04	179	0.88	33.46
70	263	-0.38	1.53	214	0.81	18.50
71	208	0.03	2.42	199	0.96	57.44
72	252	0.10	1.79	222	0.88	33.51
73	259	-0.39	1.08	253	0.98	20.35
74	204	-0.51	1.89	212	1.00	43.87
75	203	-0.43	2.15	215	1.00	51.39
76	261	-0.19	1.41	256	0.98	33.82
77	255	-0.41	1.60	238	0.93	42.56
78	218	-0.47	2.04	212	0.97	71.64

Fig. 3-6 shows the measured rate q_o as a function of the head H_1 at wave gage G1 for all the 107 tests. The head H is defined as $H = (S + \bar{\eta} - R_c)$ with S=still water level above $z = 0$; $\bar{\eta}$=mean water level above SWL; and R_c=levee crest elevation above $z = 0$ where R_c=16.5 cm for the these tests. The solid line in Fig. 3-6 is based on $q_o = (2/3)^{1.5} H_1 \sqrt{gH_1}$ for steady flow over a broad-crested weir for the positive head H_1 above the weir crest (e.g., Henderson 1966). The combined overtopping and overflow rate q_o increased rapidly with the increase of the positive head H_1. Fig. 3-6 shows the importance of the wave contribution to the measured q_o unless the head H_1 becomes large.

3.5 WAVE OVERTOPPING PROBABILITIES

The measured overtopping probabilities $P_o = N_i / N_o$ are compared with the formula given by Eq. (2-33) with $R_{1/3} = \left(\overline{\eta_r} + S\right) + e\sigma_r$ with e=3, 4, 4.5 and 5 for the Weibul distribution with $\left(\kappa = 2 + 0.5/R_*^3\right)$ and the Rayleigh distribution $\left(\kappa = 2\right)$ as shown in Fig. 3-7 to 3-10. The adopted formula given by Eq. (2-34) is based on e=4 and $\kappa = 2$. This simple formula incorporated into the time-averaged numerical model is compared with the present experiments in Chapter 4.

Table 3-3: Free surface statistics for overflow tests 79-107

Test	WG1						WG2		WG3		WG4		WG5		WG6	
No.	d_1 cm	S cm	T_p sec	r	$\bar{\eta}$ cm	σ_η cm	$\bar{\eta}$ cm	σ_η cm	$\bar{\eta}$ cm	σ_η cm	$\bar{\eta}$ cm	σ_η cm	$\bar{\eta}$ cm	σ_η cm	$\bar{\eta}$ cm	σ_η cm
79	62.8	17.2	2.03	0.30	-1.91	1.58	-1.91	1.62	-1.93	1.59	-1.88	1.58	-1.89	1.70	-1.91	1.57
80	62.8	17.2	1.69	0.23	-1.23	1.37	-1.22	1.39	-1.29	1.36	-1.23	1.34	-1.20	1.33	-1.23	1.27
81	62.8	17.2	1.89	0.34	-2.48	2.09	-2.51	2.05	-2.52	2.06	-2.46	2.05	-2.44	2.23	-2.52	2.21
82	63.0	17.4	1.62	0.22	-0.66	0.89	-0.65	0.89	-0.69	0.88	-0.66	0.85	-0.64	0.86	-0.65	0.82
83	63.1	17.5	1.88	0.27	-1.59	1.48	-1.58	1.50	-1.60	1.49	-1.62	1.44	-1.56	1.55	-1.59	1.41
84	63.1	17.5	1.64	0.22	-1.03	1.22	-1.02	1.24	-1.06	1.22	-1.00	1.18	-0.98	1.21	-1.02	1.14
85	63.1	17.5	1.97	0.28	-2.67	2.23	-2.65	2.27	-2.67	2.24	-2.61	2.21	-2.62	2.35	-2.64	2.27
86	63.3	17.7	1.61	0.18	-0.58	0.81	-0.56	0.82	-0.53	0.80	-0.51	0.76	-0.56	0.77	-0.57	0.73
87	63.6	18.0	1.57	0.14	-0.28	0.79	-0.28	0.82	-0.28	0.79	-0.28	0.76	-0.24	0.76	-0.27	0.73
88	63.6	18.0	1.69	0.16	-0.69	1.19	-0.66	1.14	-0.71	1.18	-0.69	1.15	-0.65	1.15	-0.65	1.15
89	63.6	18.0	1.88	0.25	-2.26	2.07	-2.16	1.98	-2.28	2.06	-2.24	2.03	-2.24	2.18	-2.27	2.08
90	63.7	18.1	1.87	0.22	-1.19	1.41	-1.11	1.32	-1.19	1.40	-1.17	1.35	-1.15	1.46	-1.18	1.32
91	63.7	18.1	1.65	0.15	-0.27	0.81	-0.26	0.83	-0.27	0.80	-0.27	0.78	-0.25	0.77	-0.26	0.74
92	64.1	18.5	1.96	0.19	-0.74	1.30	-0.70	1.25	-0.76	1.31	-0.75	1.27	-0.72	1.35	-0.73	1.27
93	64.1	18.5	1.56	0.13	-0.45	1.17	-0.41	1.12	-0.47	1.15	-0.45	1.10	-0.42	1.11	-0.44	1.06
94	64.1	18.5	1.88	0.21	-1.76	1.87	-1.68	1.77	-1.79	1.83	-1.76	1.81	-1.60	1.94	-1.78	1.85
95	64.4	18.8	1.59	0.11	-0.37	1.19	-0.38	1.22	-0.37	1.18	-0.37	1.13	-0.35	1.14	-0.36	1.08
96	64.4	18.8	1.93	0.17	-0.57	1.23	-0.54	1.19	-0.59	1.24	-0.58	1.18	-0.55	1.22	-0.58	1.16
97	64.4	18.8	1.65	0.13	-0.29	1.13	-0.28	1.09	-0.33	1.12	-0.32	1.08	-0.30	1.07	-0.31	1.04
98	64.4	18.8	2.06	0.20	-1.50	1.97	-1.44	1.88	-1.54	1.97	-1.52	1.91	-1.49	2.05	-1.53	1.94
99	64.7	19.1	1.57	0.10	-0.04	0.79	-0.07	0.80	-0.08	0.78	-0.06	0.74	-0.04	0.74	-0.10	0.70
100	64.8	19.2	1.97	0.13	-0.36	1.34	-0.35	1.38	-0.40	1.34	-0.40	1.29	-0.33	1.37	-0.45	1.31
101	64.8	19.2	1.64	0.10	-0.07	0.73	-0.08	0.74	-0.10	0.72	-0.10	0.69	-0.08	0.68	-0.08	0.65
102	64.9	19.3	1.63	0.12	-0.54	1.60	-0.51	1.63	-0.55	1.59	-0.55	1.54	-0.54	1.54	-0.62	1.49
103	65.0	19.4	1.62	0.10	-0.04	0.73	-0.03	0.74	-0.04	0.72	-0.04	0.69	-0.02	0.68	-0.08	0.66
104	65.0	19.4	2.03	0.13	-0.35	1.16	-0.35	1.18	-0.36	1.16	-0.36	1.12	-0.35	1.19	-0.41	1.16
105	65.0	19.4	1.58	0.11	-0.17	1.12	-0.16	1.13	-0.19	1.12	-0.19	1.06	-0.17	1.06	-0.22	1.02
106	65.0	19.4	1.95	0.15	-1.03	1.80	-1.03	1.83	-1.04	1.83	-1.05	1.76	-0.88	1.87	-1.07	1.77
107	65.0	19.4	1.60	0.09	-0.05	0.72	-0.02	0.73	-0.04	0.71	-0.04	0.67	-0.04	0.67	-0.08	0.65

Table 3-4: Wave runup and overtopping statistics for overflow tests 79-107

Test No.	N_i	RW $\bar{\eta}_r$ (cm)	RW σ_r (cm)	P_o (N_o/N_i)	q (cm^2/s)
79	213	-1.66	2.05	1	33.13
80	256	-1.19	1.46	1	27.15
81	217	-1.62	2.80	1	26.27
82	264	-0.74	1.02	1	24.20
83	210	-1.46	1.78	1	40.32
84	266	-0.98	1.32	1	33.08
85	217	-2.08	2.60	1	48.79
86	263	-0.53	0.86	1	29.61
87	261	-0.35	0.75	1	42.66
88	257	-0.68	1.08	1	46.46
89	214	-1.77	2.21	1	58.89
90	211	-1.11	1.52	1	52.10
91	261	-0.33	0.75	1	44.30
92	210	-0.50	1.26	1	66.37
93	261	-0.42	0.90	1	62.74
94	213	-1.31	1.88	1	69.06
95	262	-0.30	0.90	1	82.36
96	211	-0.73	1.05	1	73.53
97	263	-0.11	0.81	1	73.17
98	214	-1.12	1.83	1	84.18
99	257	-0.01	0.50	1	94.70
100	212	-0.36	1.11	1	105.63
101	271	-0.01	0.51	1	87.07
102	253	-0.31	1.09	1	104.11
103	260	0.11	0.51	1	98.76
104	212	-0.18	0.97	1	100.89
105	257	-0.04	0.79	1	102.41
106	206	-0.81	1.62	1	107.48
107	260	0.10	0.51	1	99.18

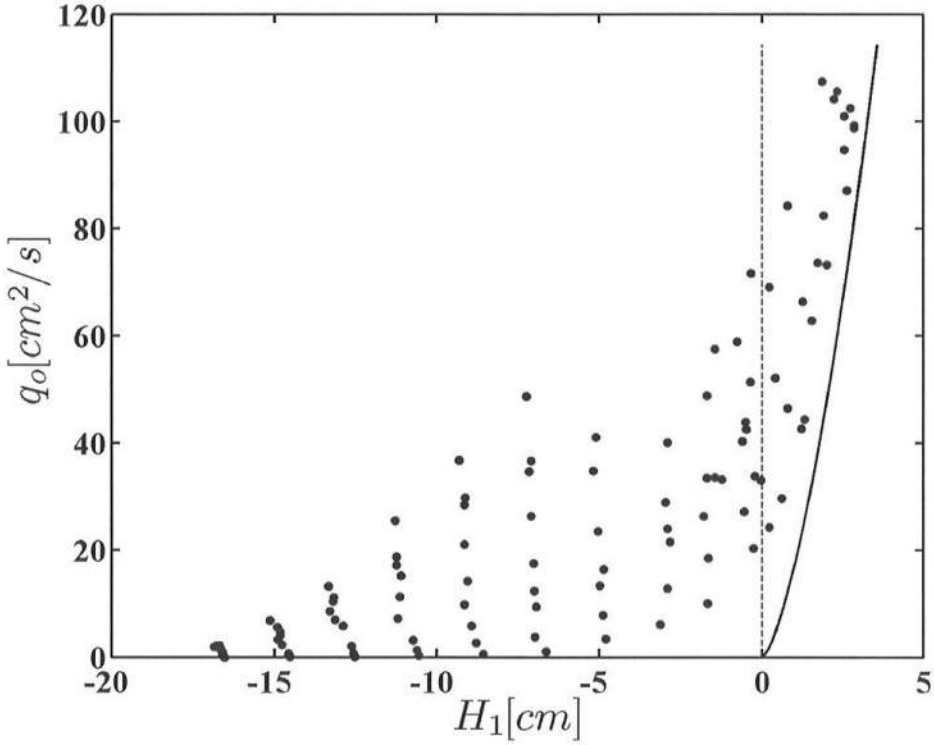

Fig. 3-6. Overtopping and overflow rate q_o versus head H_1

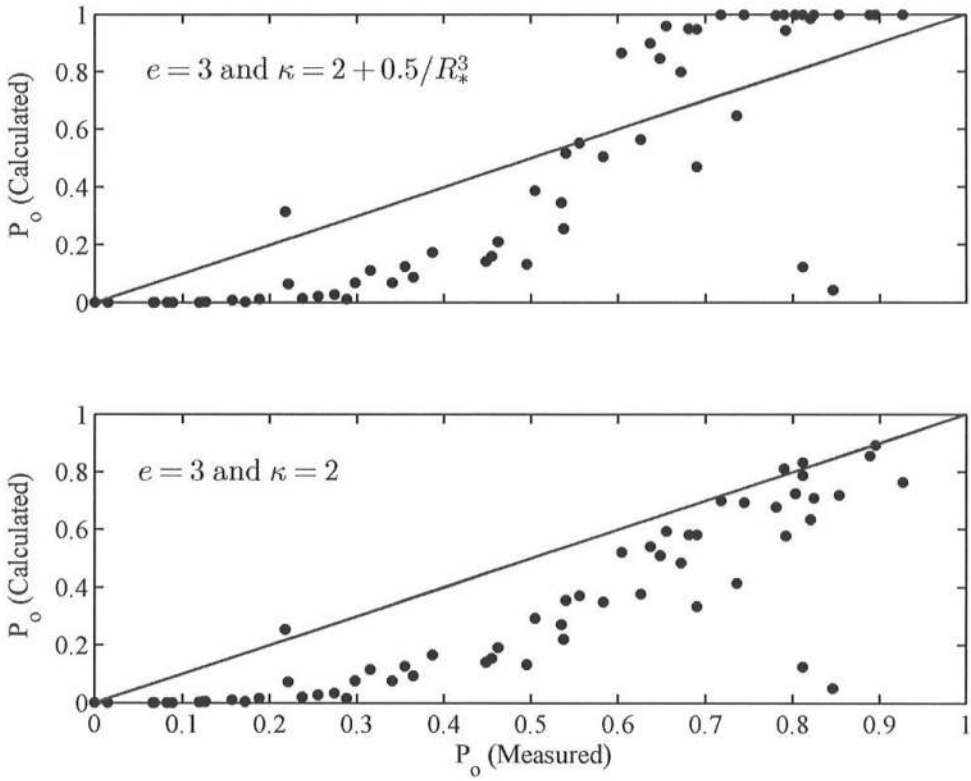

Fig. 3-7. Comparison of measured and calculated probabilities based on $e = 3$ for $\kappa = 2 + 0.5/R_*^3$ and $\kappa = 2$

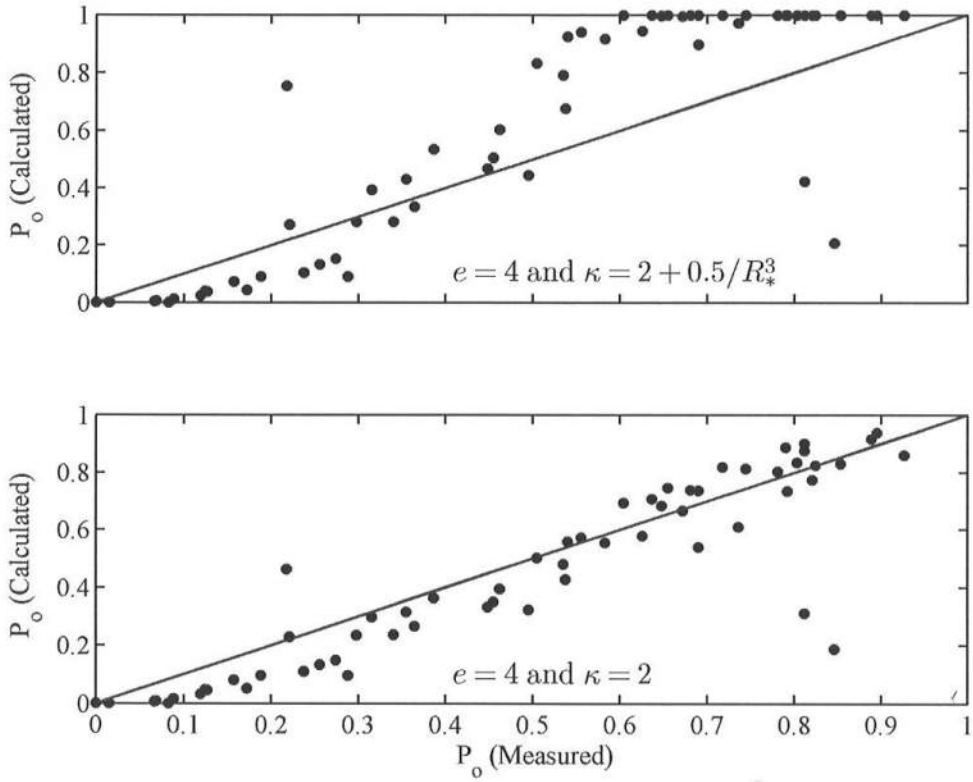

Fig. 3-8. Comparison of measured and calculated probabilities based on $e = 4$ for $\kappa = 2 + 0.5/R_*^3$ and $\kappa = 2$

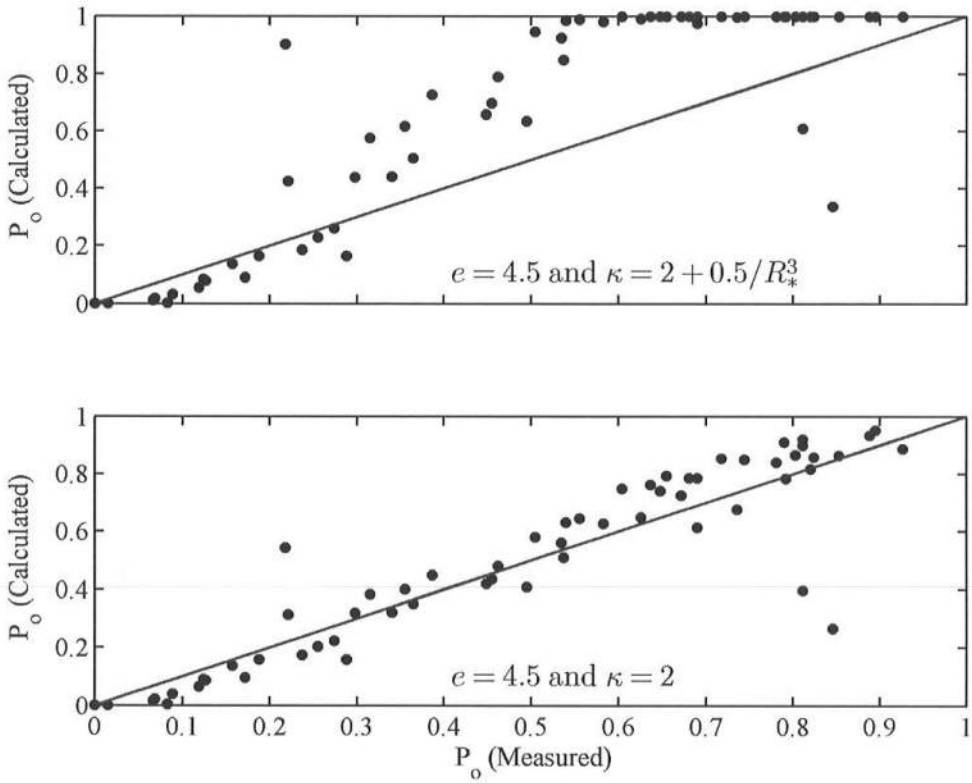

Fig. 3-9. Comparison of measured and calculated probabilities based on $e = 4.5$ for

$\kappa = 2 + 0.5/R_*^3$ and $\kappa = 2$

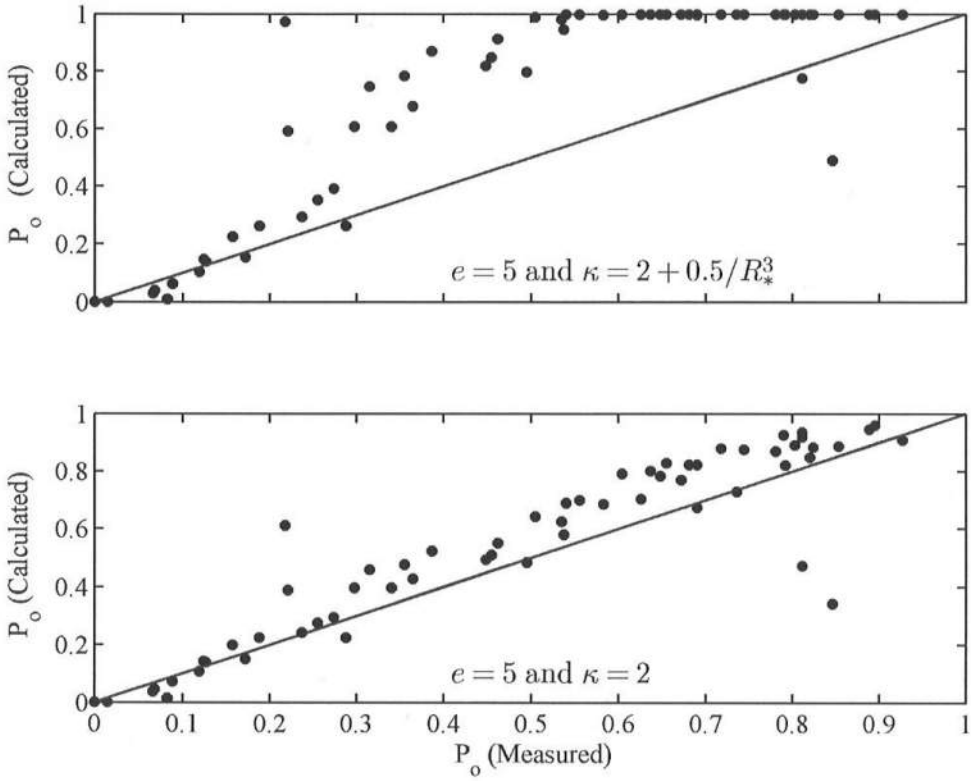

Fig. 3-10. Comparison of measured and calculated probabilities based on $e = 5$ for $\kappa = 2 + 0.5/R_*^3$ and $\kappa = 2$

CHAPTER 4

COMPARISON OF MODEL WITH EXPERIMENTS

4.1 SENSITIVITY OF NUMERICAL MODEL

The beach and levee geometry was simulated using 1279 nodes of constant spacing from wave gage G1 at $x = 0$ to the landward end of the levee crest located at $x = 12.8\ m$. The numerical model input was modified to allow the computation of the 107 tests in a single run. The computation time was of the order of $10\,s$. The breaker ratio parameter γ was selected as $\gamma = 0.7$ or 0.8 on the basis of the previous comparisons by Kobayashi et al. (2007) and Kobayashi and de los Santos (2007). By increasing γ, the breaking process is delayed so that the wave height represented by σ_η increases. During the experiments, the landward current occurred due to wave overtopping and overflow. The current following the waves causes the delay in breaking. This may explain why $\gamma = 0.8$ gives slightly better agreement with the present experiments.

The experiments consisting of 107 tests are compared with the numerical model. The bottom friction factor f_b is chosen as $f_b = 0$ on the beach and $f_b = 0$ or 0.01 on the levee where f_b may increase in shallow water. The computed q changed less than 10% for $f_b = 0.0$ and 0.01. This difference is within accuracy of the numerical model which is

a factor of about 2 as shown later. The runup wire elevation above the slope is chosen as δ_r=2 cm, as measured in the experiments. During the experiments, many waves broke right on the 1/5 slope where the flexible runup wire was mounted. It was hence difficult to maintain δ_r=2 cm in the experiments. The runup wire elevation might have been reduced somewhat during the experiments. As a result, computation was made for δ_r=1 cm as well. The computed results for δ_r=1 cm indicate that q increases by a factor of about 2 only for tests with the computed q less than about 5 cm^2/s. Accordingly, the results presented in Chapter 4 and 5 are based on δ_r=2 cm, γ=0.8 and f_b=0.

The comparisons of the numerical model with all the 107 tests are summarized in Table 4-1 and are explained in the following. The computed results discussed above for the different values of γ, δ_r and f_b are presented in Appendix A.

4.2 COMPARISONS FOR WAVE RUNUP AND OVERTOPPING STATISTICS

Fig 4-1 compares the computed and measured mean water level $(\overline{\eta_r}+S)$ above $z=0$ at the runup wire. The levee crest elevation above MWL, ($R_c-\overline{\eta_r}-S$), is normalized in Eq. (2-34) and R_c=16.5 cm for the present tests. The agreement in Fig. 4-1 is excellent mainly because $\overline{\eta_r}$ due to waves and overflow is small relative to the still water level increase S, due to storm surge and tide in the present experiments. The numerical model underpredicts $(\overline{\eta_r}+S)$ somewhat when $(\overline{\eta_r}+S)$ exceeds R_c=16.5 cm.

Fig. 4-2 shows the comparison of the computed and measured standard deviation of the free surface fluctuations along the runup wire denoted by σ_r and σ_m, respectively. In Eq. (2-34), σ_r is used to normalize $\left(R_c - \overline{\eta_r} - S\right)$. The agreement is within a range of errors of 30 % where the numerical model prediction is fairly good up to about σ_m=2.5 cm.

Table 4-1a: Comparisons for tests 1-18

Test No.	Numerical Model							Measured				
	H_{SWL} cm	q_{SWL} cm^2/s	P_o	q_o cm^2/s	q_o (empirical) cm^2/s	$S+\overline{\eta_r}$ cm	σ_r cm	H_1 cm	P_o	q_m cm^2/s	$S+\overline{\eta_r}$ cm	σ_m cm
1	0.00	40.83	0.0025	0.10	0.01	0.77	2.27	-16.57	0.12	0.26	1.09	3.14
2	0.00	61.60	0.0486	2.99	0.74	1.65	3.02	-16.76	0.46	2.20	1.29	5.27
3	0.00	69.18	0.0872	6.03	2.48	2.00	3.29	-16.85	0.46	1.96	1.37	5.57
4	0.00	37.21	0.0012	0.05	0.01	0.57	2.18	-16.54	0.08	0.11	0.90	2.13
5	0.00	58.59	0.0420	2.46	0.89	1.42	3.00	-16.65	0.24	1.27	1.47	3.58
6	0.00	65.88	0.0748	4.93	2.58	1.75	3.25	-16.68	0.22	2.13	1.63	4.34
7	0.00	28.94	0.0000	0.00	0.00	0.29	1.79	-16.53	0.00	0.00	0.17	1.62
8	0.00	48.50	0.0165	0.80	0.48	0.90	2.73	-16.61	0.13	0.89	0.91	3.15
9	0.00	58.62	0.0486	2.85	2.14	1.32	3.09	-16.65	0.19	1.40	1.11	3.57
10	0.00	42.55	0.0253	1.08	0.09	2.79	2.53	-14.57	0.12	0.64	2.91	2.59
11	0.00	62.75	0.1521	9.55	2.54	3.59	3.33	-14.89	0.32	3.29	3.70	4.12
12	0.00	66.81	0.1858	12.42	4.44	3.77	3.48	-15.13	0.22	6.84	3.67	5.19
13	0.00	37.92	0.0129	0.49	0.07	2.60	2.36	-14.56	0.07	0.27	2.53	2.18
14	0.00	54.76	0.1047	5.73	1.70	3.13	3.15	-14.84	0.34	3.95	3.14	3.94
15	0.00	62.34	0.1541	9.61	3.10	3.53	3.36	-14.91	0.39	5.59	3.38	4.63
16	0.00	27.01	0.0004	0.01	0.01	2.28	1.79	-14.53	0.02	0.03	2.22	1.60
17	0.00	45.93	0.0542	2.49	1.27	2.73	2.86	-14.76	0.29	2.30	2.66	3.21
18	0.00	57.06	0.1278	7.29	4.43	3.17	3.29	-14.83	0.37	4.71	3.04	4.14

q_{SWL} =wave-induced flux at SWL; $H_1 = \left(S + \overline{\eta} - R_c\right)$ at gage G1; q_m =measured rate of overtopping/overflow; σ_m =measured standard deviation of free surface oscillation along the runup wire

Table 4-1b: Comparisons for tests 19-45

Test No.	Numerical Model							Measured				
	H_{SWL} cm	q_{SWL} cm^2/s	P_o	q_o cm^2/s	q_o (empirical) cm^2/s	$S+\overline{\eta_r}$ cm	σ_r cm	H_1 cm	P_o	q_m cm^2/s	$S+\overline{\eta_r}$ cm	σ_m cm
19	0.00	41.45	0.0619	2.57	0.16	4.70	2.51	-12.63	NM	2.06	5.18	2.67
20	0.00	59.84	0.2585	15.47	4.34	5.28	3.42	-13.19	NM	10.40	5.61	4.34
21	0.00	67.06	0.3196	21.43	9.74	5.62	3.61	-13.34	NM	13.19	5.84	5.34
22	0.00	33.58	0.0191	0.64	0.07	4.44	2.15	-12.58	NM	0.65	5.02	2.05
23	0.00	54.47	0.2274	12.38	4.70	4.89	3.38	-13.29	NM	8.57	5.10	3.97
24	0.00	64.47	0.3118	20.10	14.41	5.39	3.65	-13.17	NM	11.08	5.44	4.85
25	0.00	24.90	0.0011	0.03	0.03	4.21	1.66	-12.53	NM	0.02	4.33	1.53
26	0.00	48.14	0.1489	7.17	3.20	4.72	3.03	-12.90	0.85	5.77	4.70	3.24
27	0.00	53.03	0.2177	11.54	11.35	4.80	3.36	-13.14	0.81	6.98	4.69	3.88
28	0.00	43.32	0.1825	7.90	0.79	6.70	2.67	-10.74	0.26	3.16	6.82	2.42
29	0.00	62.63	0.4277	26.79	12.39	7.34	3.53	-11.24	0.74	18.75	7.90	4.34
30	0.00	71.14	0.4820	34.29	23.17	7.74	3.64	-11.29	0.66	25.40	8.37	5.34
31	0.00	36.60	0.0926	3.39	0.39	6.50	2.30	-10.61	0.17	1.23	6.54	2.06
32	0.00	56.85	0.3793	21.56	8.96	7.08	3.39	-11.10	0.69	15.17	7.58	4.03
33	0.00	64.76	0.4529	29.33	26.10	7.34	3.65	-11.24	0.67	17.06	7.72	4.89
34	0.00	24.36	0.0066	0.16	0.07	6.17	1.63	-10.56	0.07	0.29	6.44	1.63
35	0.00	41.83	0.2155	9.01	5.29	6.32	2.91	-11.20	0.50	7.13	6.46	3.35
36	0.00	52.04	0.3403	17.71	13.93	6.79	3.32	-11.14	0.51	11.17	6.97	4.08
37	0.00	38.59	0.2873	11.09	1.78	8.45	2.56	-8.92	0.45	5.85	8.94	2.56
38	0.00	62.83	0.5789	36.37	22.49	9.36	3.43	-9.13	0.82	29.78	10.28	4.38
39	0.00	70.78	0.6318	44.72	52.31	9.55	3.64	-9.31	0.85	36.76	10.22	5.19
40	0.00	31.50	0.1486	4.68	0.85	8.23	2.12	-8.78	0.27	2.62	8.54	2.05
41	0.00	51.82	0.4977	25.79	14.09	8.85	3.25	-9.15	0.65	21.05	9.60	3.99
42	0.00	62.19	0.5806	36.11	30.81	9.27	3.48	-9.14	0.68	28.42	9.56	4.47
43	0.00	21.86	0.0174	0.38	0.18	8.10	1.48	-8.57	0.09	0.51	8.41	1.42
44	0.00	41.02	0.3608	14.80	9.56	8.38	2.86	-9.14	0.54	9.74	8.40	3.12
45	0.00	50.32	0.4804	24.18	27.55	8.81	3.19	-9.04	0.63	14.12	8.82	3.69

Table 4-1c: Comparisons for tests 46-67

Test	Numerical Model							Measured				
No.	H_{SWL} cm	q_{SWL} cm^2/s	P_o	q_o cm^2/s	q_o (empirical) cm^2/s	$S+\overline{\eta_r}$ cm	σ_r cm	H_1 cm	P_o	q_m cm^2/s	$S+\overline{\eta_r}$ cm	σ_m cm
46	0.00	34.67	0.4446	15.41	4.40	10.36	2.42	-6.94	0.54	9.40	10.84	2.35
47	0.00	61.62	0.7310	45.04	48.50	11.26	3.33	-7.08	0.78	36.60	11.51	3.80
48	0.00	63.81	0.7417	47.33	45.70	11.34	3.36	-7.22	0.93	48.71	11.48	4.61
49	0.00	26.37	0.2443	6.44	1.85	9.97	1.95	-6.96	0.30	3.72	10.22	1.86
50	0.00	50.79	0.6649	33.77	31.18	10.87	3.13	-7.08	0.79	26.32	11.13	3.45
51	0.00	61.02	0.7322	44.68	72.55	11.17	3.40	-7.15	0.82	34.63	11.17	4.31
52	0.00	20.74	0.0739	1.53	0.52	10.04	1.42	-6.61	0.16	1.09	10.22	1.41
53	0.00	37.94	0.5148	19.53	17.57	10.42	2.65	-6.98	0.56	12.39	10.52	2.85
54	0.00	45.05	0.6118	27.56	40.62	10.67	2.95	-7.01	0.60	17.46	10.61	3.46
55	0.00	18.31	0.2479	4.54	2.49	11.86	1.40	-4.79	0.36	3.32	12.09	1.46
56	0.00	33.24	0.6867	22.83	33.71	12.40	2.38	-4.84	0.69	16.42	12.48	2.60
57	0.00	38.58	0.7549	29.12	53.59	12.47	2.71	-5.04	0.74	23.53	12.47	3.17
58	0.00	24.64	0.5009	12.34	6.63	12.07	1.90	-4.86	0.58	7.81	12.38	1.91
59	0.00	45.67	0.8094	36.96	60.87	12.65	2.99	-5.17	0.80	34.80	12.66	3.21
60	0.00	54.42	0.8519	46.36	84.72	12.97	3.14	-5.09	0.81	41.10	12.74	3.67
61	0.00	30.59	0.6471	19.80	11.35	12.27	2.28	-4.96	0.64	13.33	12.65	2.34
62	0.00	12.64	0.5052	6.39	13.90	13.50	1.30	-3.11	0.54	6.10	13.52	1.40
63	0.00	25.47	0.8467	21.57	50.60	14.14	2.07	-2.90	0.81	24.02	14.29	2.46
64	0.00	29.55	0.8833	26.10	72.97	14.24	2.30	-2.96	0.89	28.91	14.16	2.84
65	0.00	20.42	0.7700	15.72	26.67	13.97	1.77	-2.89	0.72	12.86	14.15	1.88
66	0.00	37.38	0.9270	34.65	88.83	14.54	2.55	-2.89	0.90	40.03	14.48	2.89
67	0.00	23.09	0.8178	18.88	22.66	14.14	1.88	-2.81	0.79	21.56	14.49	2.10

Table 4-1d: Comparisons for tests 68-91

Test No.	Numerical Model							Measured				
	H_{SWL} cm	q_{SWL} cm^2/s	P_o	q_o cm^2/s	q_o (empirical) cm^2/s	$S+\overline{\eta_r}$ cm	σ_r cm	H_1 cm	P_o	q_m cm^2/s	$S+\overline{\eta_r}$ cm	σ_m cm
68	0.00	8.38	0.7860	6.58	23.59	14.92	1.16	-1.66	0.77	10.00	14.99	1.26
69	0.05	19.87	0.9550	19.37	88.88	15.31	2.02	-1.69	0.88	33.46	15.06	2.04
70	0.00	14.34	0.9115	13.07	50.76	15.13	1.62	-1.64	0.81	18.50	15.12	1.53
71	0.42	30.32	0.9901	38.62	131.45	15.87	2.35	-1.44	0.96	57.44	15.53	2.42
72	0.18	22.86	0.9748	24.66	77.57	15.61	2.04	-1.44	0.88	33.51	15.60	1.79
73	0.36	6.59	0.9942	13.22	33.33	16.31	1.02	-0.25	0.98	20.35	16.11	1.08
74	0.63	15.24	0.9983	30.81	94.73	16.34	1.63	-0.48	1.00	43.87	15.99	1.89
75	0.71	21.13	1.0000	39.81	122.70	16.59	1.72	-0.36	1.00	51.40	16.07	2.15
76	0.56	12.45	0.9993	25.62	63.00	16.43	1.32	-0.22	0.98	33.82	16.31	1.41
77	0.68	17.20	0.9997	34.66	91.32	16.45	1.71	-0.48	0.93	42.56	16.09	1.60
78	0.88	26.92	1.0000	52.61	129.37	16.77	1.91	-0.34	0.97	71.64	16.03	2.04
79	0.56	13.43	0.9841	26.25	152.48	15.80	2.05	-1.21	1.00	33.13	15.57	2.05
80	0.56	13.15	0.9959	26.21	105.56	16.24	1.62	-0.54	1.00	27.15	16.04	1.46
81	0.63	16.16	0.9828	31.47	185.16	15.59	2.53	-1.79	1.00	26.27	15.61	2.80
82	0.57	10.19	1.0000	23.49	64.82	16.75	1.06	0.24	1.00	24.20	16.69	1.02
83	0.61	15.14	0.9970	30.19	129.44	16.26	1.76	-0.60	1.00	40.32	16.07	1.78
84	0.62	13.45	1.0000	28.77	90.43	16.61	1.37	-0.03	1.00	33.08	16.55	1.32
85	0.70	19.07	0.9894	37.28	206.96	15.78	2.58	-1.68	1.00	48.79	15.44	2.60
86	0.69	10.19	1.0000	28.05	58.57	17.08	0.92	0.61	1.00	29.61	17.20	0.86
87	0.99	10.47	1.0000	41.28	55.25	17.56	0.76	1.22	1.00	42.66	17.68	0.75
88	0.93	16.29	1.0000	44.29	90.88	17.29	1.12	0.80	1.00	46.46	17.34	1.08
89	0.81	22.67	0.9994	45.49	181.46	16.39	2.13	-0.76	1.00	58.89	16.26	2.21
90	0.88	19.03	1.0000	44.69	121.63	17.04	1.39	0.41	1.00	52.10	17.01	1.52
91	1.06	11.09	1.0000	45.47	39.83	17.64	0.75	1.33	1.00	44.30	17.79	0.75

Table 4-1e: Comparisons for tests 92-107

Test No.	Numerical Model							Measured				
	H_{SWL} cm	q_{SWL} cm^2/s	P_o	q_o cm^2/s	q_o (empirical) cm^2/s	$S+\overline{\eta_r}$ cm	σ_r cm	H_1 cm	P_o	q_m cm^2/s	$S+\overline{\eta_r}$ cm	σ_m cm
92	1.25	21.42	1.0000	65.01	117.53	17.66	1.12	1.26	1.00	66.37	18.03	1.26
93	1.34	17.23	1.0000	66.09	80.01	17.84	0.93	1.55	1.00	62.74	18.11	0.90
94	1.01	25.37	1.0000	57.37	162.53	17.05	1.66	0.24	1.00	69.06	17.22	1.88
95	1.53	17.20	1.0000	76.60	83.71	18.10	0.85	1.91	1.00	82.36	18.50	0.90
96	1.50	20.49	1.0000	78.12	109.34	17.99	1.02	1.72	1.00	73.54	18.10	1.05
97	1.57	16.49	1.0000	78.19	82.97	18.15	0.82	2.00	1.00	73.17	18.72	0.81
98	1.28	30.71	1.0000	75.90	190.04	17.51	1.58	0.80	1.00	84.18	17.71	1.83
99	1.84	9.89	1.0000	87.78	54.13	18.46	0.56	2.56	1.00	94.70	19.11	0.50
100	1.91	22.87	1.0000	105.34	121.62	18.44	1.04	2.33	1.00	105.63	18.86	1.11
101	1.87	9.02	1.0000	89.15	32.88	18.49	0.53	2.62	1.00	87.07	19.21	0.51
102	1.89	25.46	1.0000	107.00	115.13	18.41	1.12	2.22	1.00	104.11	18.97	1.09
103	2.04	8.85	1.0000	99.95	32.87	18.64	0.54	2.86	1.00	98.76	19.53	0.51
104	2.00	19.31	1.0000	108.08	71.00	18.55	0.94	2.55	1.00	100.89	19.25	0.97
105	2.07	15.87	1.0000	109.31	77.07	18.63	0.84	2.72	1.00	102.41	19.39	0.79
106	1.76	31.55	1.0000	104.76	161.24	18.21	1.32	1.87	1.00	107.48	18.61	1.62
107	2.03	8.54	1.0000	99.19	31.77	18.63	0.53	2.85	1.00	99.18	19.53	0.51

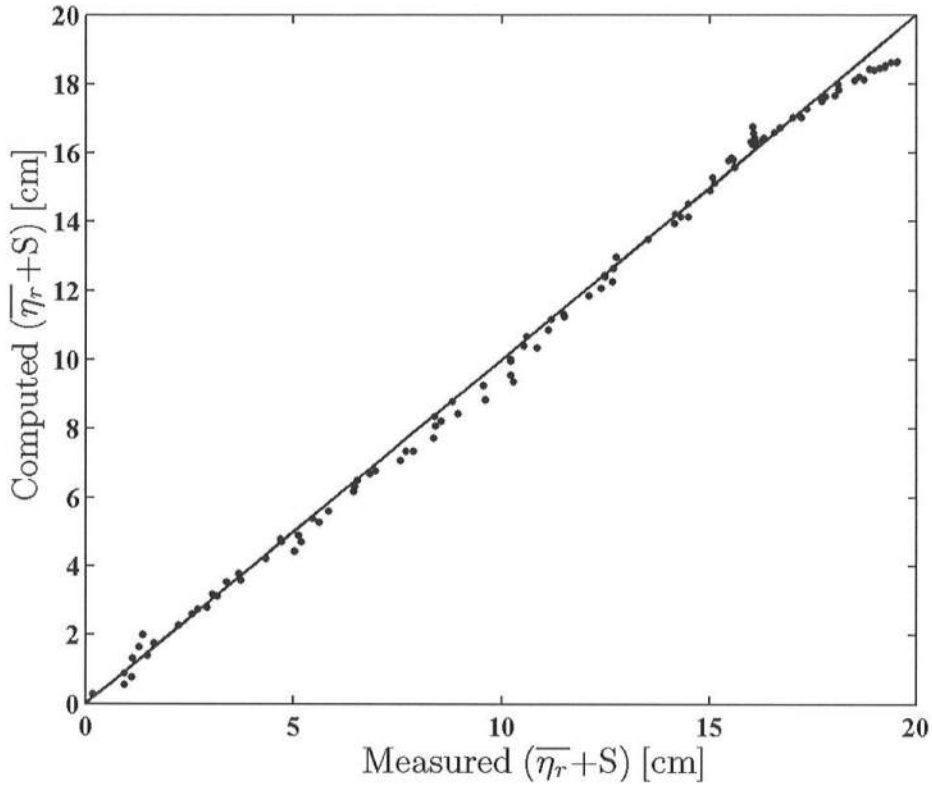

Fig. 4-1. Computed ($\overline{\eta_r} + S$) versus measured ($\overline{\eta_r} + S$)

Fig. 4-3 shows the computed P_o for all the tests against the measured P_o. The measured wave overtopping probability, which is the ratio of the overtopped waves to the number of incident waves at gage 1, was measured visually. Some incident waves broke on the 1/5 slope and generate thin layers of uprushing water on the slope which might not have been counted as overtopped waves. In any event, the visual judgment was somewhat subjective.

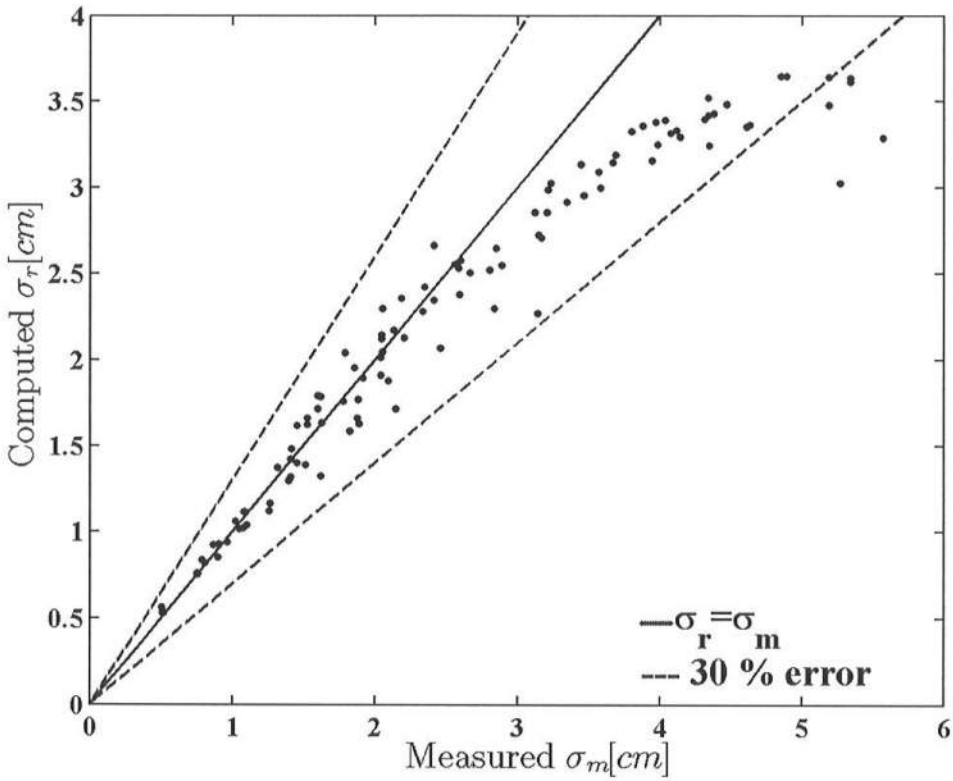

Fig. 4-2. Computed standard deviation σ_r of free surface versus measured σ_m

The computed and measured rates of wave overtopping and overflow are compared in Fig 4-4. The agreement between the computed q_o and the measured q_m is found to be better for the high rates when the overflow dominated. The proposed formula for the wave overtopping rate on the impermeable structure, $q_o = P_o q_{SWL}$, in Eq. (2-30), which is actually the modified form of the wave overtopping formula developed by Kobayashi and de los Santos (2007) for permeable structures, does not predict the small rates of wave

overtopping accurately unlike the formula for steady overflow. Nevertheless, the agreement is within a factor of 2.

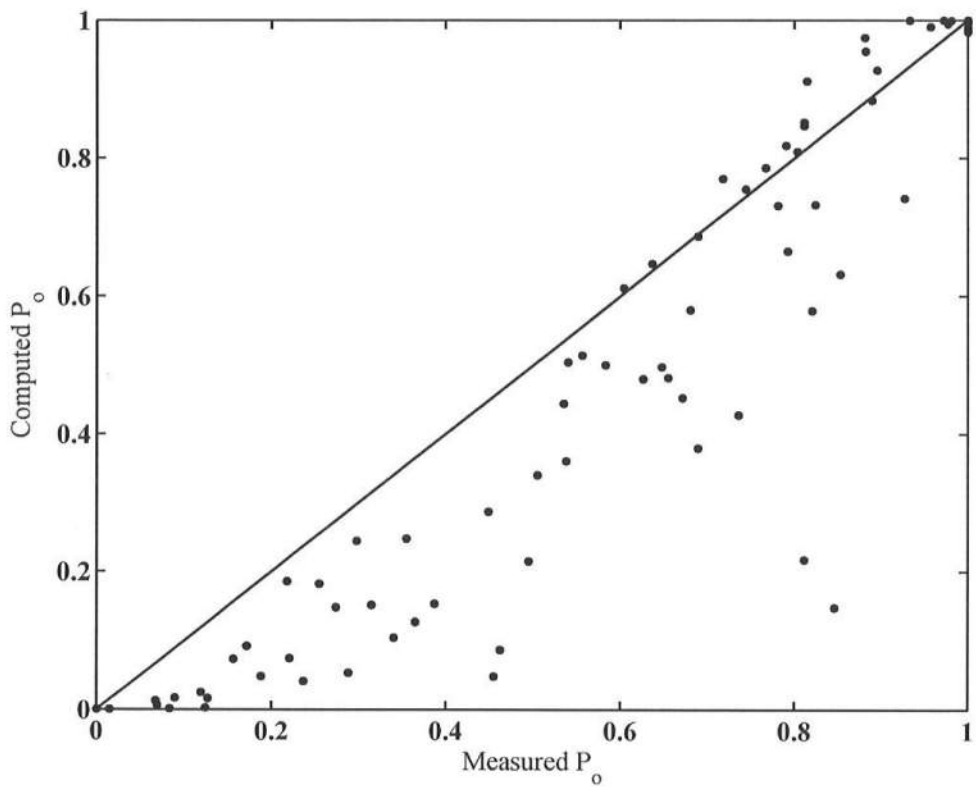

Fig. 4-3. Computed wave overtopping probabilities versus measured probabilities

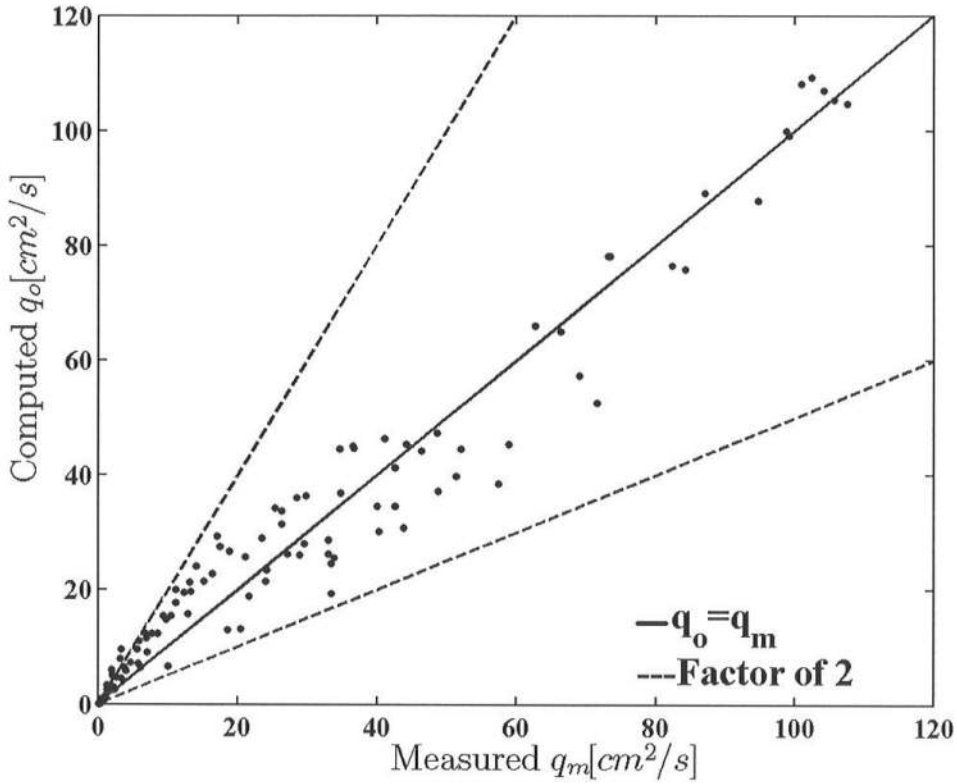

Fig. 4-4. Computed wave overtopping and overflow rates versus measured rates

Fig 4-5 compares the empirical wave overtopping rates q_e using the Dutch formula given by Eqs. (2-37) and (2-38), with the measured overtopping /overflow rates q_m. For the low rates ($q_m < 20\ cm^2/s$) the agreement of the empirical and measured rates in Fig. 4-5 is as good as in Fig. 4-4. For the high rates, the empirical formula tends to overpredict the wave overtopping rate. The agreement becomes poor for the overflow tests because the empirical formula is not valid for submerged structures.

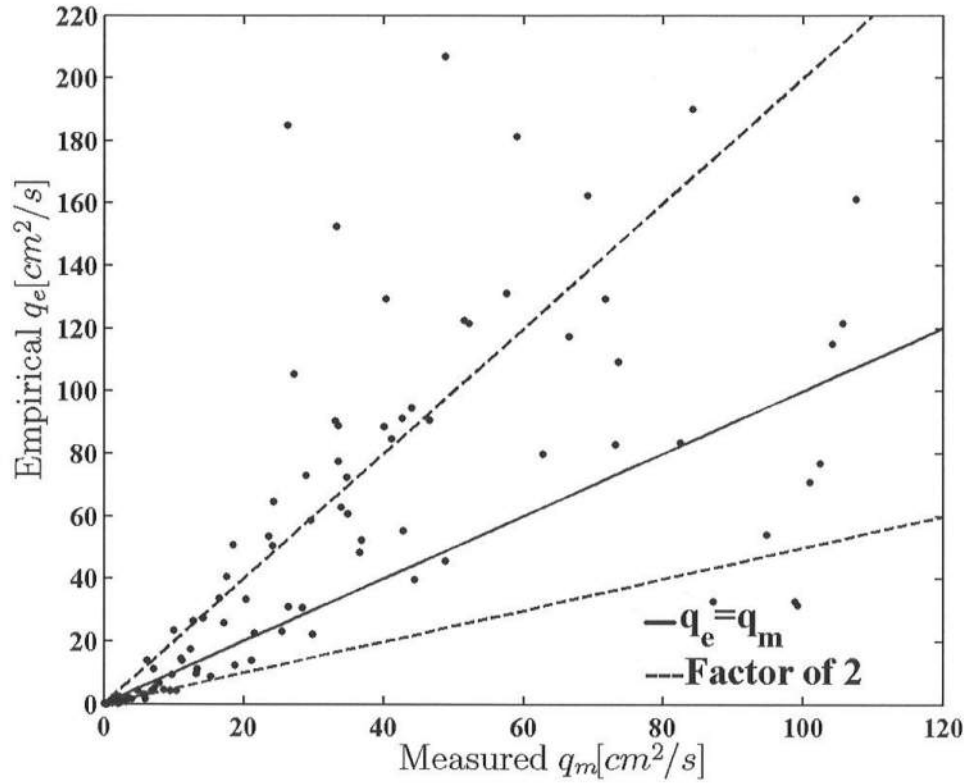

Fig. 4-5. Empirical wave overtopping and overflow rates versus measured rates

4.3 COMPARISONS FOR CROSS-SHORE WAVE TRANSFORMATION

The computed cross-shore variations of $\overline{\eta}$, σ_η, $\overline{U}$ and σ_U along with the measured values of η and σ_η at gages G1-G6 are plotted for all the 107 tests in Appendix B. As examples, wave overtopping tests 2 and 41 and overflow tests 94 and 103 are shown in Figs. 4-6, 4-7, 4-8 and 4-9. The bottom elevation z_b is plotted with the mean water level, $\left(\overline{\eta}+S\right)$ above $z=0$ in the same panel. The agreement between the computed and

measured $\left(\overline{\eta}+S\right)$ and σ_η for gages G1-G3 is excellent since the measured values at $x=0$ are specified as input to the numerical model.

The landward limits in Figs. 4-6 and 4-7 are the landward ends of computation where the mean water depth h=0.14 cm and h=0.56 cm. The computed q_o=3 cm^2/s for test 2 and q_o=26 cm^2/s for test 41. The mean water level $\left(\overline{\eta}+S\right)$ increases landward due to the onshore increase of wave setup. The standard deviation of the free surface oscillation, σ_η, does not change much in the onshore direction until the 1/5 slope. The decrease of the wave height represented by σ_η occurs mostly on the 1/5 due to wave breaking on the slope where $H_{mo}=4\sigma_\eta=9.8$ cm and $H_{mo}/h=0.79$ for test 2 and $H_{mo}=11.7$ cm and $H_{mo}/h=0.6$ for test 41 at the toe of the 1/5 slope.

The mean velocity $\overline{U}$ and the standard deviation σ_U of the oscillatory wave velocity are computed using Eqs. (2-10) and (2-16). The offshore (negative) return current $\overline{U}$ is small on the beach and increases on the 1/5 slope before $\overline{U}$ becomes onshore due to wave overtopping flow. The standard deviation σ_U increases gradually on the beach and rapidly on the 1/5 slope mostly due to the landward decrease of the water depth. The rapid decrease of $\sigma_U=C(\sigma_\eta/h)$ near the shoreline occurs because of the decrease of the phase velocity C while the ratio of σ_η/h stays approximately constant in very shallow water (Kobayashi et al. 1998).

The landward limits in Figs. 4-8 and 4-9 are the landward ends of the levee crest where the mean water depth $h=1.3$ cm and $h=2.1$ cm and the computed

q_o=57 cm^2/s for test 94 and q_o=100 cm^2/s for test 103. The computed mean water level $\left(\overline{\eta}+S\right)$ exhibits little wave setup due to the water level decrease associated with the overflow. The standard deviation σ_η increases on the 1/5 slope due to the shoaling where $H_{mo}=8.2\ cm$ and $H_{mo}/h=0.28$ for test 94 and $H_{mo}=3\ cm$ and $H_{mo}/h=0.1$ for test 103 at the toe of the 1/5 slope. The computed values of σ_η remain approximately constant on the submerged levee crest because some waves forced to break on the seaward slope cease breaking as explained by Kobayashi et al. (2007). The computed mean velocity $\overline{U}$ is almost zero except in the region of very small water depth near the levee crest. In this region, $\overline{U}$ becomes as large as σ_U and wave and current interactions included in the present numerical model become important.

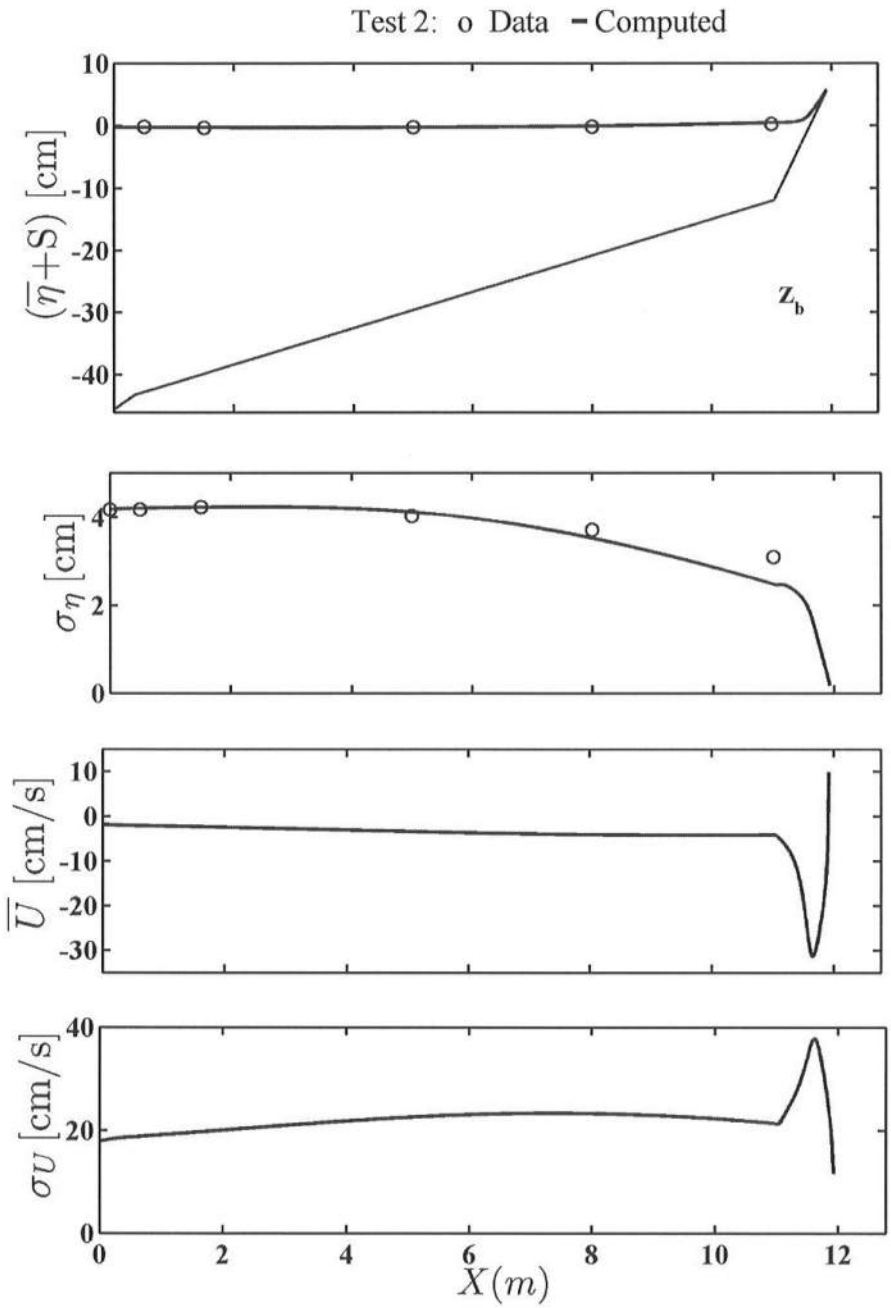

Fig. 4-6. Computed cross-shore variations of $\overline{\eta}$, σ_η, $\overline{U}$ and σ_U and measured $\overline{\eta}$ and σ_η for Test 2

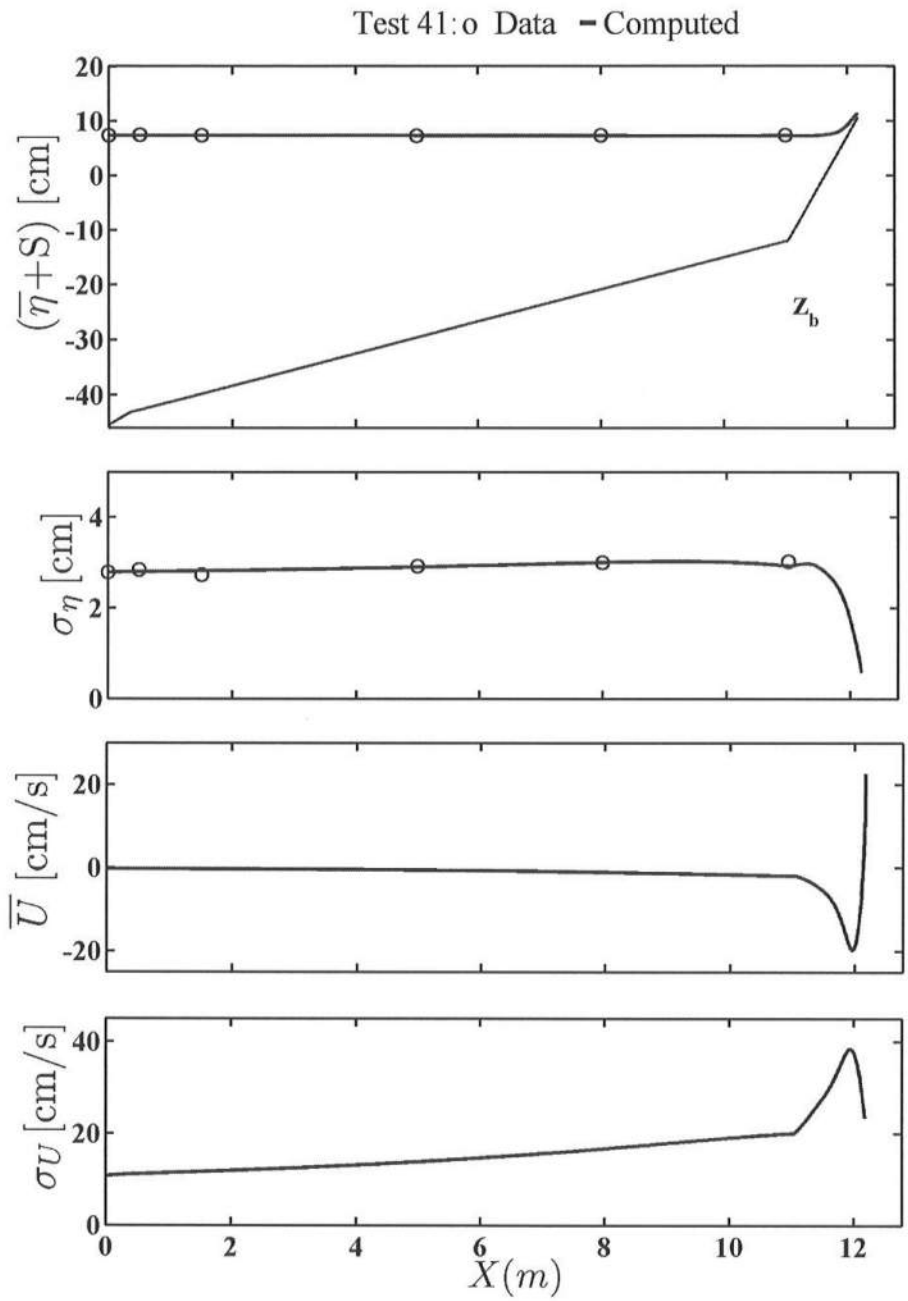

Fig. 4-7. Computed cross-shore variations of $\overline{\eta}$, σ_η, $\overline{U}$ and σ_U and measured $\overline{\eta}$ and σ_η for Test 41

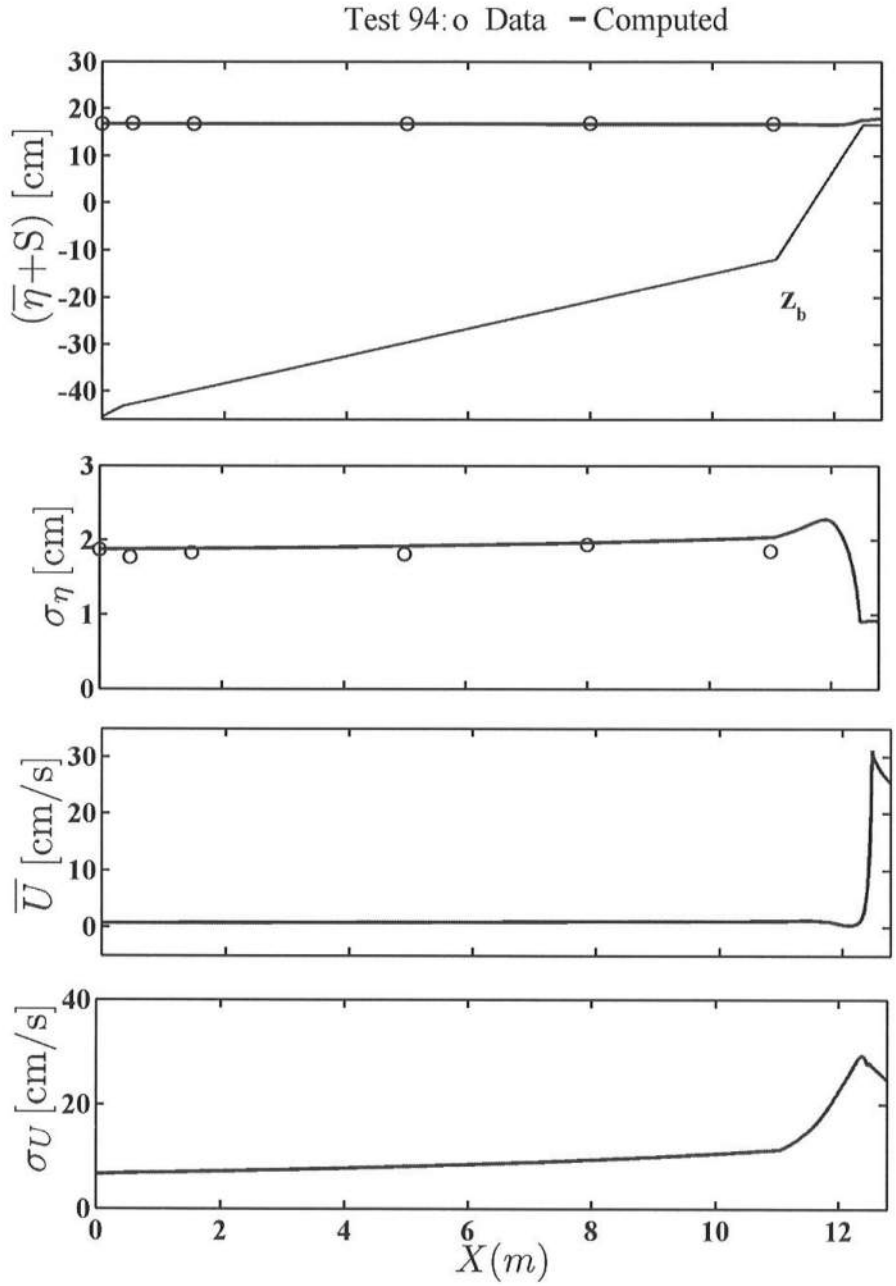

Fig. 4-8. Computed cross-shore variations of $\overline{\eta}$, σ_η, $\overline{U}$ and σ_U and measured $\overline{\eta}$ and σ_η for Test 94

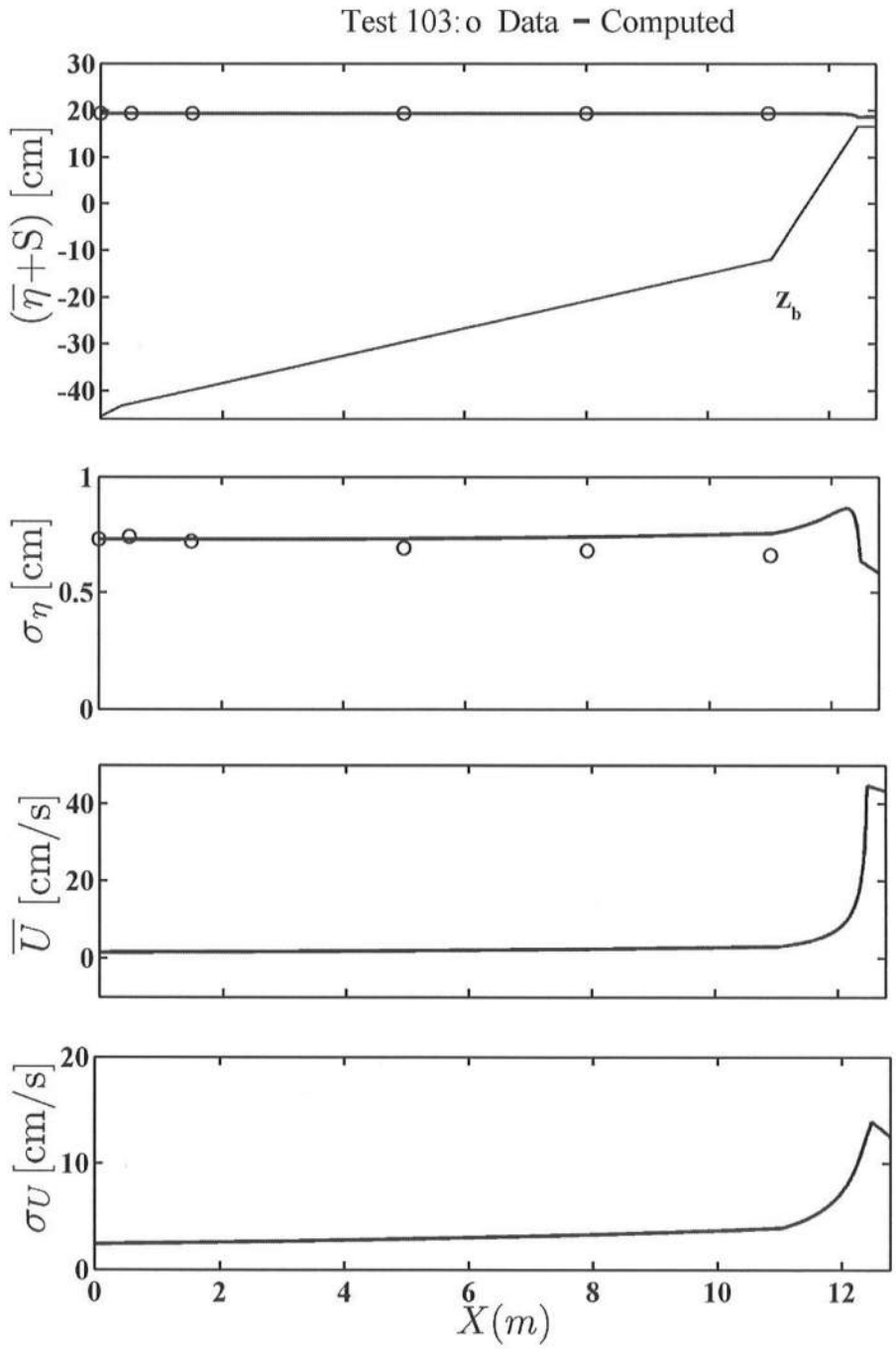

Fig. 4-9. Computed cross-shore variations of $\overline{\eta}$, σ_η, $\overline{U}$ and σ_U and measured $\overline{\eta}$ and σ_η for Test 103

CHAPTER 5

FIELD APPLICATION

As an application of the numerical model developed for combined wave overtopping and overflow conditions, the model is applied to an earthen levee in Louisiana. The levee called Jefferson Parish Lakefront levee shown in Fig. 5-1 is composed of 5 segments with different slopes which is obviously a more complicated than the idealized levee in the present experiments. Therefore, finding an equivalent uniform slope required in the Dutch formula (van der Meer 2002) is really difficult. The bottom elevation $z_b(x)$ for $0 \le x \le 56$ m is specified as input to the numerical model. The still water level S above $z = 0$ due to storm surge and tide is increased from $S = 0$ to $S = 2.6$ m by an increment of 0.2 m where the levee crest height $R_c = 1.8$ m. Four wave conditions at $x = 0$ are used for the following computation as listed in Table 5-1. The RMS wave height $H_{rms} = \sqrt{8}\sigma_\eta$ is 0.8 m for waves 1 and 2 and 1.6 m for waves 3 and 4. The spectral peak period $T_p = 5$ s for waves 1 and 3 and $T_p = 8$ s for waves 2 and 4. The computed q_o is expected to increase with the increase of H_{rms} and T_p. The wave setdown or setup $\overline{\eta}$ at $x = 0$ is neglected.

The empirical parameters in the numerical model are kept the same except that a typical runup wire height δ_r above 1/4.4 slope is increased to δ_r=10 cm to account for grass. Fig. 5-2 shows the computed wave overtopping and overflow rate q_o as a function of the still water level S for waves 1-4 where the crest is at SWL when $S = 1.8\ m$.

Table 5-1: Four wave Conditions at x=0

Waves	1	2	3	4
$H_{rms}\ (m)$	0.8	0.8	1.6	1.6
$T_p\ (s)$	5.0	8.0	5.0	8.0

The rate q_o increases with the increase of S and the increase becomes more rapid once the levee crest is submerged. The effects of the wave height and period on the rate q_o are reduced with the increase of S in terms of the percentage changes of q_o among waves 1-4 where the computed values of q_o are tabulated in Table 5-2.

Table 5-1 and Fig. 5-2 show that wave 4 with the larger wave period and height produces the highest wave overtopping and overflow rate. The increase of the wave period with the same height increases q_o by comparing q_o for waves 1 and 2 and for waves 3 and 4. By comparing the computed q_o of waves 1 and 3 and also the computed q_o for waves 2 with 4, the wave height is also important as expected.

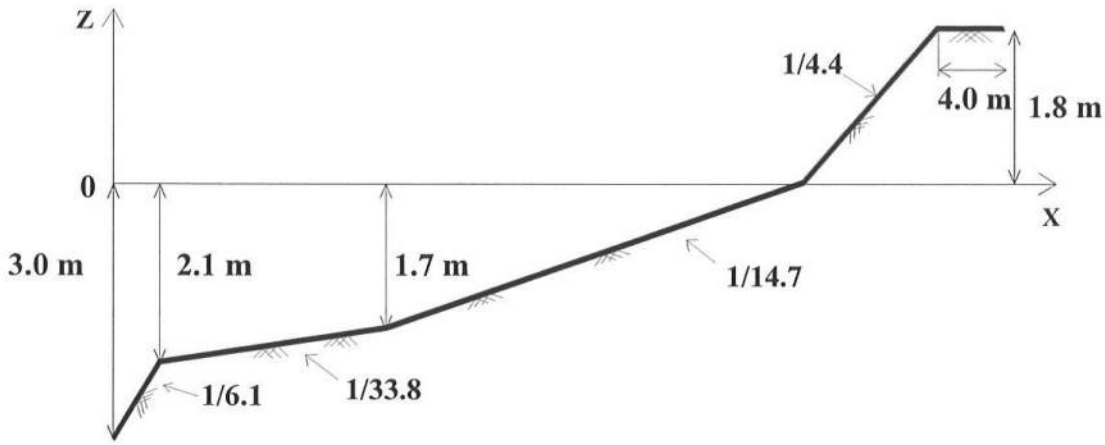

Fig. 5-1. Jefferson Parish Lakefront levee's geometry

van der Meer (2002) suggested that erosion of the inner (landward) slope of clayey soil with a reasonably good grass cover might occur for the wave overtopping rate exceeding 0.001 m^2/s . Fig. 5-3 shows the computed q_o plotted to distinguish the small overtopping rates. This allowable rate is too crude and perhaps conservative. Efforts are being made to quantify the resistance or strength of a dike against wave overtopping (van der Meer et al. 2006). The computed q_o for waves 1 and 3 exceeds 0.001 m^2/s when S=0.6 m and 0.4 m, respectively. The effect of the wave period on the computed q_o is significant for q_o on the order of 0.001 m^2/s but becomes small for q_o on the order of 0.1 m^2/s or larger. However, no data is available to verify the computed results.

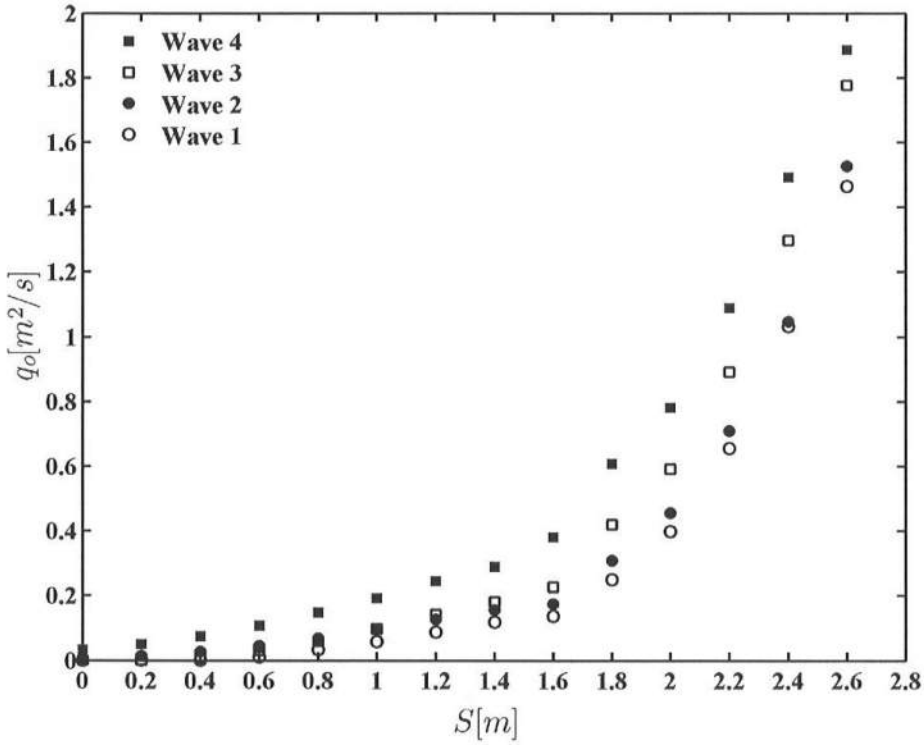

Fig. 5-2. Wave overtopping/overflow rate versus surge for waves 1,2,3 and 4

Table 5-2: Wave overtopping/overflow rates for different surge levels and waves 1-4

$S\ (m)$	$q_o\ (m^2/s)$			
	Wave 1	**Wave 2**	**Wave 3**	**Wave 4**
0	0.0000	0.0053	0.0000	0.0336
0.2	0.0000	0.0131	0.0002	0.0504
0.4	0.0006	0.0263	0.0066	0.0752
0.6	0.0102	0.0445	0.0302	0.1072
0.8	0.0332	0.0676	0.0595	0.1477
1.0	0.0588	0.0964	0.0972	0.1918
1.2	0.0874	0.1267	0.1411	0.2451
1.4	0.1181	0.1558	0.1815	0.2890
1.6	0.1369	0.1737	0.2262	0.3810
1.8	0.2500	0.3077	0.4206	0.6083
2	0.3989	0.4558	0.5920	0.7816
2.2	0.6559	0.7097	0.8918	1.0886
2.4	1.0320	1.0464	1.2972	1.4925
2.6	1.4639	1.5261	1.7761	1.8859

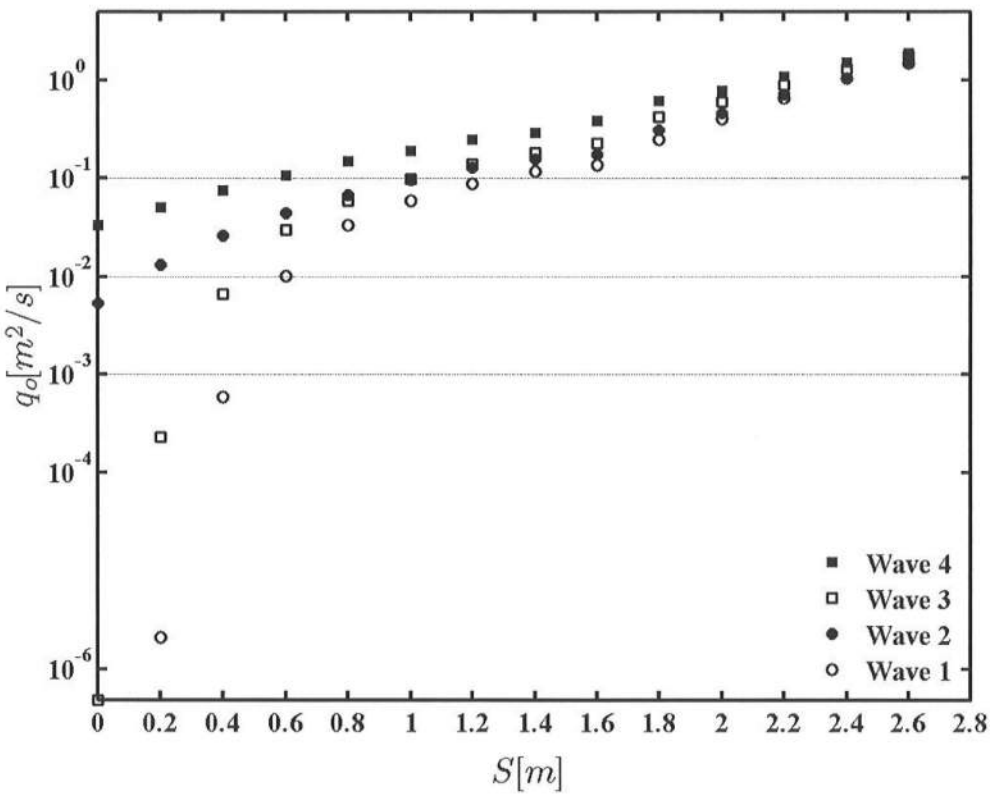

Fig. 5-3. Computed rate q in comparison with allowable overtopping of 0.001 m^2/s

CHAPTER 6

CONCLUSIONS

Experiments consisting of 107 tests were conducted in a wave flume to examine the transition from little wave overtopping to excessive wave overtopping and overflow on an impermeable smooth levee. A numerical model based on time-averaged continuity, momentum and wave action equations is developed to predict the cross-shore variations of the mean and standard deviation of the free surface elevation and depth-averaged fluid velocity. Wave and current interactions are included so that the governing equations reduce to those used in hydraulic engineering in the absence of waves. An empirical formula is proposed to express the wave overtopping and overflow rate in terms of the computed variables on the seaward slope of the levee. The measured and computed mean water levels indicate that the excessive wave overtopping and overflow rate induces the large onshore mean velocity and reduces wave setup on the seaward slope of the levee. The empirical formula is shown to predict the wave overtopping and overflow rates within a factor of 2. The numerical model will need to be verified in a large-scale experiment on an earthen levee covered with a layer of grass.

The numerical model is applied to an earthen levee in Louisiana. The numerical model allows one to compute the irregular wave transformation, breaking, overtopping

and overflow on the levee of complicated geometry. The numerical model is very efficient computationally and can easily be used to predict the temporal change of wave overtopping and overflow rate during an entire storm. The numerical model will need to be extended to the landward slope of the levee and coupled with an erosion model. The extended model may then be used to assess the performance of an earthen levee under a number of storms in manners similar to the performance computation by Kobayashi e al. (2003) for rubble mound structures. Finally, large-scale data with detailed and extensive measurements will be needed to calibrate and verify numerical models because existing levee erosion models are highly empirical.

REFRENCES

Battjes, J.A., and Stive, M.J.F (1985). "Calibration and verification of a dissipation model for random breaking waves" J. Geophys. Res., 90(C5), 9159-9167.

Besley, P. (1999). Overtopping of seawalls: design and assessment manual HR Wallingford, Report W178.

Besley, P., Stewart, T. and Allsop, N. W. H. (1998). "Overtopping of vertical structures: new prediction methods to account for shallow water conditions." Proc. Conference on Coastlines, Sructures and Beakwaters, Institute of Civil Engineers, U.K.

Burchartch, H. F. and Hughes, S. A. (2003). Coastal Engineering Manual, Fundamentals of design. Chapter 5, Part VI, Design of coastal project elements, Engineer Research and Development Centre, US Army Corps of Engineering, Vicksburg, USA.

Dean, R.G., and Dalrymple, R.A., (1991). Water wave mechanics for engineers and scientists. World Scientific, Singapore.

D'Eliso, C., Omeraci, H., and Kortenhaus, A. (2006). "Breaking of coastal dikes induced by wave overtopping." Coastal Engineering 2006, Proc. 30th Coastal Engineering Conf., World Scientific, Singapore, 2844-2856.

Goda, Y. (2000). Random seas and design of maritime structures. World Scientific, Singapore.

Hedges, T. S., and Reis M. T. (1999). "Wave overtopping models and seawall freeboards." Coastal engineering and marina developments (C.A. Brebbia and P. Anagnostopoulos (Eds.)), Computational Mechanics Publications: 567-576.

Henderson, F.M.(1966). Open channel flow. Macmillan, New York, N.Y.

Herbert D.M. (1996). "Overtopping of seawalls: a comparison between prototype and physical model data" HR Wallingford, Report TR 22.

Kobayashi, N., and de los Santos, F. J (2007). "Irregular wave seepage and overtopping of permeable slopes" J. Waterway, Port, Coastal and Ocean Eng., 133(4), 296-304.

Kobayashi, N., and Raichle, A. W (1994). "Irregular wave overtopping of revetments in surf zones" J. Waterway, Port, Coastal and Ocean Eng., 120(1), 56-73.

Kobayashi, N., and Wurjanto, A. (1989). "Wave overtopping on coastal structures" Journal of Waterway, Port, Coastal and Ocean Engineering, ASCE, 115(2), 235-251.

Kobayashi, N., Cox, D. T. and Wurjanto, A. (1990). "Irregular wave reflection and runup on rough impermeable slopes" Journal of Waterway, Port, Coastal and Ocean Engineering, ASCE, 116(6), 708-726.

Kobayashi, N., Farhadzadeh, A., and Melby, J.A. (2007). "Wave overtopping and overflow on levees" J. Waterway, Port, Coastal and Ocean Eng., (submitted in August 2007).

Kobayashi, N., Pozueta, B., and Melby, J.A. (2003). "Performance of coastal structures against sequences of hurricanes" J. Waterway, Port, Coastal and Ocean Eng., 129(5), 219-228.

Kobayashi, N., Herrman, M.N., Johnson, B.D., and Orzech, M.D. (1998). "Probability distribution of surface elevation in surf and swash zones" J. Waterway, Port, Coastal and Ocean Eng., 124(3), 99-107.

Kobayashi, N., Meigs, L.E., Ota, T., and Melby, J. A. (2007). "Irregular breaking wave transmission over submerged porous breakwater." J. Waterway, Port, Coastal and Ocean Eng., 133(2), 104-116.

Mei, C.C. (1989). The applied dynamics of ocean surface waves. World Scientific, Singapore.

Phillips, O.M. (1977). The dynamics of the upper ocean. Cambridge Univ. Press, Cambridge, U.K.

Sakai, S., and Kobayashi, N. (1990). "Breaking condition of shoaling waves on opposing current." J. Waterway, Port, Coastal and Ocean Eng., 116(2), 303-306.

Schüttrumpf, H., and Oumeraci, H. (2005). "Layer thickness and velocities of the wave overtopping flow at sea dikes." Coastal Engineering, 52, 473-495.

Shankar, N.J., and Jayaratne, M.P.R. (2003). "Wave run-up and overtopping on smooth and rough slopes of coastal structures.", Ocean Engineering , 30, 221–238.

Stanczak, G., Oumeraci, H., and Kortenhaus, A. (2006). "Breaching of sea dikes initiated by breaking wave impact on seaward slope." Coastal Engineering 2006, Proc. 30th Coastal Engineering Conf., World Scientific, Singapore, 2880-2892.

van der Meer, J. (2002). Wave run-up and wave overtopping at dikes. Technical Advisory Committee for Flood Defense in the Netherlands (TAW), Delft, The Netherlands.

van der Meer, J.W., and Janssen J.P.F.M. (1995). "Wave run-up and wave overtopping at dikes.", Wave forces on inclined and vertical wall structures , pp 1- 26, ed. Kobayashi N. & Demirbilek Z., ASCE, New York, N.Y.

van der Meer, J. W., Bernardini, P., Snijders, W., and Regeling, E. (2006). "The wave overtopping simulator." Coastal Engineering 2006, Proc. 30th Coastal Engineering Conf., World Scientific, Singapore, 4654-4666.

van Gent, M.R. A. (2001). "Wave runup on dikes with shallow foreshores." J. Waterway, Port, Coastal and Ocean Eng., 127(5), 254-262.

Waal J., and van der Meer, J. (1992). "Wave runup and overtopping on coastal structures."Coastal Engineering 1992, Proc. 23rd Coastal Engineering Conf., World Scientific, Singapore, 1758-1771.

Wang, Z., and Bowles, D. S. (2006). "Dam breach simulations with multiple breach locations under wind and wave actions.", Advances in Water Resources, 29, 1222–1237.

APPENDIX A

SENSITIVITIES TO INPUT EMPIRICAL PARAMETERS

Tables A.1-A.4 present the comparisons of the numerical model with the 107 tests using the following input values:

Table	Breaker ratio parameter γ	Runup wire elevation δ_r (m)	Levee friction factor f_b
A.1	0.7	0.02	0.0
A.2	0.8	0.02	0.0
A.3	0.8	0.01	0.0
A.4	0.8	0.02	0.01

It is noted that Table A.2 is the same as Table 4-1 in Chapter 4.

Figs. A.1-A.4 show the computed wave overtopping and overflow rates in comparison with the measured rates where Fig. A.2 corresponds to Fig. 4-4 in Chapter 4. These figures show that the overall agreement for the 107 tests is the best for γ=0.8, δ_r=0.02 m and f_b=0.0.

Table A.1a: $\gamma = 0.7$; $\delta_r = 0.02$ m; $f_b = 0$

Test No.	Numerical Model							Measured				
	H_{SWL} cm	q_{SWL} cm^2/s	P_o	q_o cm^2/s	q_o (empirical) cm^2/s	$S+\overline{\eta_r}$ cm	σ_r cm	H_1 cm	P_o	q_m cm^2/s	$S+\overline{\eta_r}$ cm	σ_m cm
1	0.00	34.98	0.0000	0.00	0.01	0.64	1.95	-16.57	0.12	0.26	1.09	3.14
2	0.00	52.38	0.0000	0.00	0.47	1.37	2.61	-16.76	0.46	2.20	1.29	5.27
3	0.00	59.45	0.0000	0.00	1.66	1.66	2.87	-16.85	0.46	1.96	1.37	5.57
4	0.00	32.59	0.0000	0.00	0.01	0.48	1.90	-16.54	0.08	0.11	0.90	2.13
5	0.00	50.19	0.0000	0.00	0.59	1.19	2.60	-16.65	0.24	1.27	1.47	3.58
6	0.00	56.83	0.0000	0.00	1.77	1.47	2.83	-16.68	0.22	2.13	1.63	4.34
7	0.00	26.50	0.0000	0.00	0.00	0.26	1.62	-16.53	0.00	0.00	0.17	1.62
8	0.00	42.30	0.0000	0.00	0.34	0.76	2.39	-16.61	0.13	0.89	0.91	3.15
9	0.00	50.81	0.0000	0.00	1.51	1.11	2.71	-16.65	0.19	1.40	1.11	3.57
10	0.00	36.99	0.0000	0.00	0.06	2.67	2.23	-14.57	0.12	0.64	2.91	2.59
11	0.00	54.62	0.0002	0.01	1.76	3.30	2.97	-14.89	0.32	3.29	3.70	4.12
12	0.00	58.38	0.0005	0.03	3.11	3.44	3.12	-15.13	0.22	6.84	3.67	5.19
13	0.00	33.82	0.0000	0.00	0.05	2.52	2.12	-14.56	0.07	0.27	2.53	2.18
14	0.00	47.44	0.0000	0.00	1.20	2.91	2.80	-14.84	0.34	3.95	3.14	3.94
15	0.00	54.29	0.0002	0.01	2.17	3.25	3.00	-14.91	0.39	5.59	3.38	4.63
16	0.00	25.25	0.0000	0.00	0.01	2.26	1.67	-14.53	0.02	0.03	2.22	1.60
17	0.00	40.82	0.0000	0.00	1.00	2.61	2.59	-14.76	0.29	2.30	2.66	3.21
18	0.00	50.26	0.0001	0.01	3.36	2.97	2.97	-14.83	0.37	4.71	3.04	4.14

q_{SWL}=wave-induced flux at SWL; q_m=measured rate of overtopping/overflow; σ_m=measured standard deviation of free surface oscillation along the runup wire

Table A.1b: $\gamma = 0.7$; $\delta_r = 0.02$ m; $f_b = 0$

Test	Numerical Model							Measured				
No.	H_{SWL}	q_{SWL}	P_o	q_o	q_o (empirical)	$S+\overline{\eta_r}$	σ_r	H_1	P_o	q_m	$S+\overline{\eta_r}$	σ_m
	cm	cm^2/s		cm^2/s	cm^2/s	cm	cm	cm		cm^2/s	cm	cm
19	0.00	36.49	0.0000	0.00	0.12	4.59	2.24	-12.63	NM	2.06	5.18	2.67
20	0.00	53.59	0.0030	0.16	3.13	5.03	3.16	-13.19	NM	10.40	5.61	4.34
21	0.00	61.44	0.0093	0.57	7.16	5.36	3.43	-13.34	NM	13.19	5.84	5.34
22	0.00	30.85	0.0000	0.00	0.06	4.39	1.98	-12.58	NM	0.65	5.02	2.05
23	0.00	48.13	0.0017	0.08	3.53	4.67	3.10	-13.29	NM	8.57	5.10	3.97
24	0.00	59.70	0.0092	0.55	11.20	5.19	3.47	-13.17	NM	11.08	5.44	4.85
25	0.00	23.57	0.0000	0.00	0.03	4.20	1.57	-12.53	NM	0.02	4.33	1.53
26	0.00	43.95	0.0004	0.02	2.71	4.60	2.83	-12.90	0.85	5.77	4.70	3.24
27	0.00	48.65	0.0021	0.10	9.57	4.66	3.17	-13.14	0.81	6.98	4.69	3.88
28	0.00	39.84	0.0009	0.04	0.65	6.59	2.48	-10.74	0.26	3.16	6.82	2.42
29	0.00	60.80	0.0455	2.77	9.53	7.20	3.51	-11.24	0.74	18.75	7.90	4.34
30	0.00	70.28	0.0941	6.61	17.96	7.65	3.77	-11.29	0.66	25.40	8.37	5.34
31	0.00	34.29	0.0001	0.00	0.36	6.46	2.17	-10.61	0.17	1.23	6.54	2.06
32	0.00	55.15	0.0264	1.45	7.16	6.96	3.33	-11.10	0.69	15.17	7.58	4.03
33	0.00	64.46	0.0693	4.47	21.20	7.28	3.72	-11.24	0.67	17.06	7.72	4.89
34	0.00	23.05	0.0000	0.00	0.07	6.16	1.54	-10.56	0.07	0.29	6.44	1.63
35	0.00	39.51	0.0029	0.12	4.89	6.24	2.82	-11.20	0.50	7.13	6.46	3.35
36	0.00	50.99	0.0190	0.97	12.26	6.71	3.27	-11.14	0.51	11.17	6.97	4.08
37	0.00	37.33	0.0082	0.31	1.60	8.38	2.47	-8.92	0.45	5.85	8.94	2.56
38	0.00	63.80	0.2093	13.36	18.19	9.35	3.58	-9.13	0.82	29.78	10.28	4.38
39	0.00	70.19	0.3130	21.97	43.21	9.57	3.82	-9.31	0.85	36.76	10.22	5.19
40	0.00	30.15	0.0008	0.02	0.84	8.21	2.05	-8.78	0.27	2.62	8.54	2.05
41	0.00	53.97	0.1041	5.62	12.15	8.83	3.33	-9.15	0.65	21.05	9.60	3.99
42	0.00	63.89	0.2200	14.05	25.92	9.29	3.65	-9.14	0.68	28.42	9.56	4.47
43	0.00	20.74	0.0000	0.00	0.18	8.09	1.40	-8.57	0.09	0.51	8.41	1.42
44	0.00	42.06	0.0291	1.22	9.22	8.35	2.88	-9.14	0.54	9.74	8.40	3.12
45	0.00	54.03	0.1049	5.67	25.97	8.83	3.33	-9.04	0.63	14.12	8.82	3.69

Table A.1c: $\gamma = 0.7$; $\delta_r = 0.02$ m; $f_b = 0$

Test No.	Numerical Model							Measured				
	H_{SWL} cm	q_{SWL} cm^2/s	P_o	q_o cm^2/s	q_o (empirical) cm^2/s	$S+\overline{\eta_r}$ cm	σ_r cm	H_1 cm	P_o	q_m cm^2/s	$S+\overline{\eta_r}$ cm	σ_m cm
46	0.00	36.76	0.0592	2.18	4.23	10.33	2.43	-6.94	0.54	9.40	10.84	2.35
47	0.00	59.57	0.5199	30.97	42.05	11.25	3.35	-7.08	0.78	36.60	11.51	3.80
48	0.00	60.14	0.5293	31.83	38.22	11.28	3.35	-7.22	0.93	48.71	11.48	4.61
49	0.00	25.91	0.0057	0.15	1.86	9.96	1.92	-6.96	0.30	3.72	10.22	1.86
50	0.00	52.95	0.3751	19.86	28.58	10.90	3.24	-7.08	0.79	26.32	11.13	3.45
51	0.00	59.80	0.5358	32.04	65.47	11.17	3.43	-7.15	0.82	34.63	11.17	4.31
52	0.00	19.77	0.0001	0.00	0.52	10.04	1.36	-6.61	0.16	1.09	10.22	1.41
53	0.00	42.42	0.1355	5.75	17.49	10.45	2.77	-6.98	0.56	12.39	10.52	2.85
54	0.00	49.58	0.2878	14.27	39.80	10.74	3.12	-7.01	0.60	17.46	10.61	3.46
55	0.00	18.29	0.0057	0.10	2.50	11.86	1.36	-4.79	0.36	3.32	12.09	1.46
56	0.00	36.07	0.4129	14.89	33.79	12.43	2.43	-4.84	0.69	16.42	12.48	2.60
57	0.00	39.11	0.6007	23.49	53.31	12.48	2.70	-5.04	0.74	23.53	12.47	3.17
58	0.00	27.65	0.1004	2.78	6.67	12.07	1.92	-4.86	0.58	7.81	12.38	1.91
59	0.00	43.19	0.7555	32.63	58.65	12.60	2.88	-5.17	0.80	34.80	12.66	3.21
60	0.00	48.97	0.8767	42.93	79.52	12.86	2.95	-5.09	0.81	41.10	12.74	3.67
61	0.00	33.59	0.2858	9.60	11.22	12.27	2.29	-4.96	0.64	13.33	12.65	2.34
62	0.00	14.08	0.0881	1.24	13.93	13.50	1.27	-3.11	0.54	6.10	13.52	1.40
63	0.00	23.64	0.8905	21.05	50.61	14.12	1.97	-2.90	0.81	24.02	14.29	2.46
64	0.00	26.88	0.9774	26.28	72.96	14.20	2.16	-2.96	0.89	28.91	14.16	2.84
65	0.00	20.82	0.6098	12.70	26.69	13.97	1.72	-2.89	0.72	12.86	14.15	1.88
66	0.00	34.32	0.9999	34.32	88.59	14.49	2.41	-2.89	0.90	40.03	14.48	2.89
67	0.00	22.05	0.7793	17.18	22.67	14.13	1.79	-2.81	0.79	21.56	14.49	2.10

Table A.1d: $\gamma = 0.7$; $\delta_r = 0.02$ m; $f_b = 0$

Test No.	Numerical Model							Measured				
	H_{SWL} cm	q_{SWL} cm^2/s	P_o	q_o cm^2/s	q_o (empirical) cm^2/s	$S+\overline{\eta_r}$ cm	σ_r cm	H_1 cm	P_o	q_m cm^2/s	$S+\overline{\eta_r}$ cm	σ_m cm
68	0.00	8.39	0.6637	5.57	23.60	14.92	1.11	-1.66	0.77	10.00	14.99	1.26
69	0.01	18.44	1.0000	18.48	88.89	15.29	1.92	-1.69	0.88	33.46	15.06	2.04
70	0.00	12.94	0.9992	12.93	50.76	15.13	1.54	-1.64	0.81	18.50	15.12	1.53
71	0.38	28.87	1.0000	36.31	131.39	15.85	2.27	-1.44	0.96	57.44	15.53	2.42
72	0.14	21.50	1.0000	23.12	77.60	15.59	1.95	-1.44	0.88	33.51	15.60	1.79
73	0.35	6.24	1.0000	12.62	33.34	16.32	0.98	-0.25	0.98	20.35	16.11	1.08
74	0.60	14.40	1.0000	28.89	94.76	16.33	1.56	-0.48	1.00	43.87	15.99	1.89
75	0.71	17.72	1.0000	36.53	122.76	16.59	1.65	-0.36	1.00	51.40	16.07	2.15
76	0.55	11.80	1.0000	24.58	63.01	16.45	1.27	-0.22	0.98	33.82	16.31	1.41
77	0.66	16.24	1.0000	33.00	91.35	16.44	1.65	-0.48	0.93	42.56	16.09	1.60
78	0.87	23.04	1.0000	48.41	129.43	16.80	1.86	-0.34	0.97	71.64	16.03	2.04
79	0.53	12.49	1.0000	24.52	152.52	15.79	1.97	-1.21	1.00	33.13	15.57	2.05
80	0.54	12.43	1.0000	24.85	105.59	16.24	1.55	-0.54	1.00	27.15	16.04	1.46
81	0.57	16.12	1.0000	29.47	185.02	15.56	2.42	-1.79	1.00	26.27	15.61	2.80
82	0.55	9.68	1.0000	22.49	64.84	16.77	1.02	0.24	1.00	24.20	16.69	1.02
83	0.59	14.32	1.0000	28.65	129.48	16.26	1.69	-0.60	1.00	40.32	16.07	1.78
84	0.60	12.76	1.0000	27.41	90.45	16.62	1.32	-0.03	1.00	33.08	16.55	1.32
85	0.67	17.77	1.0000	34.95	206.61	15.76	2.49	-1.68	1.00	48.79	15.44	2.60
86	0.67	9.64	1.0000	26.97	58.57	17.09	0.88	0.61	1.00	29.61	17.20	0.86
87	1.04	10.49	1.0000	43.77	55.23	17.55	0.70	1.22	1.00	42.66	17.68	0.75
88	0.92	15.46	1.0000	43.27	90.90	17.31	1.08	0.80	1.00	46.46	17.34	1.08
89	0.78	21.33	1.0000	42.71	181.44	16.38	2.06	-0.76	1.00	58.89	16.26	2.21
90	0.87	18.10	1.0000	43.34	121.67	17.06	1.34	0.41	1.00	52.10	17.01	1.52
91	1.12	11.06	1.0000	48.42	39.81	17.64	0.71	1.33	1.00	44.30	17.79	0.75

Table A.1e: $\gamma = 0.7$; $\delta_r = 0.02$ m; $f_b = 0$

Test No.	Numerical Model							Measured				
	H_{SWL} cm	q_{SWL} cm^2/s	P_o	q_o cm^2/s	q_o (empirical) cm^2/s	$S+\overline{\eta_r}$ cm	σ_r cm	H_1 cm	P_o	q_m cm^2/s	$S+\overline{\eta_r}$ cm	σ_m cm
92	1.21	19.05	1.0000	60.58	117.61	17.66	1.03	1.26	1.00	66.37	18.03	1.26
93	1.29	15.36	1.0000	61.36	80.07	17.83	0.83	1.55	1.00	62.74	18.11	0.90
94	0.98	24.04	1.0000	54.52	162.59	17.05	1.60	0.24	1.00	69.06	17.22	1.88
95	1.54	16.12	1.0000	75.93	83.71	18.11	0.81	1.91	1.00	82.36	18.50	0.90
96	1.50	19.23	1.0000	76.85	109.35	18.01	0.97	1.72	1.00	73.54	18.10	1.05
97	1.64	16.05	1.0000	81.82	82.94	18.17	0.85	2.00	1.00	73.17	18.72	0.81
98	1.28	31.14	1.0000	76.46	190.03	17.53	1.55	0.80	1.00	84.18	17.71	1.83
99	1.85	9.26	1.0000	88.34	54.14	18.47	0.54	2.56	1.00	94.70	19.11	0.50
100	1.84	20.57	1.0000	98.79	121.73	18.42	0.93	2.33	1.00	105.63	18.86	1.11
101	1.89	8.46	1.0000	89.68	32.89	18.51	0.51	2.62	1.00	87.07	19.21	0.51
102	1.91	23.89	1.0000	106.37	115.16	18.43	1.07	2.22	1.00	104.11	18.97	1.09
103	2.05	8.31	1.0000	100.47	32.87	18.65	0.53	2.86	1.00	98.76	19.53	0.51
104	2.02	18.06	1.0000	107.69	71.01	18.57	0.91	2.55	1.00	100.89	19.25	0.97
105	2.09	14.82	1.0000	109.27	77.07	18.65	0.81	2.72	1.00	102.41	19.39	0.79
106	1.69	28.11	1.0000	96.99	161.39	18.21	1.20	1.87	1.00	107.48	18.61	1.62
107	2.05	8.03	1.0000	99.68	31.77	18.64	0.52	2.85	1.00	99.18	19.53	0.51

Table A.2a: $\gamma = 0.8$; $\delta_r = 0.02$ m; $f_b = 0$

Test No.	Numerical Model							Measured				
	H_{SWL} cm	q_{SWL} cm^2/s	P_o	q_o cm^2/s	q_o (empirical) cm^2/s	$S+\overline{\eta_r}$ cm	σ_r cm	H_1 cm	P_o	q_m cm^2/s	$S+\overline{\eta_r}$ cm	σ_m cm
1	0.00	40.83	0.0025	0.10	0.01	0.77	2.27	-16.57	0.12	0.26	1.09	3.14
2	0.00	61.60	0.0486	2.99	0.74	1.65	3.02	-16.76	0.46	2.20	1.29	5.27
3	0.00	69.18	0.0872	6.03	2.48	2.00	3.29	-16.85	0.46	1.96	1.37	5.57
4	0.00	37.21	0.0012	0.05	0.01	0.57	2.18	-16.54	0.08	0.11	0.90	2.13
5	0.00	58.59	0.0420	2.46	0.89	1.42	3.00	-16.65	0.24	1.27	1.47	3.58
6	0.00	65.88	0.0748	4.93	2.58	1.75	3.25	-16.68	0.22	2.13	1.63	4.34
7	0.00	28.94	0.0000	0.00	0.00	0.29	1.79	-16.53	0.00	0.00	0.17	1.62
8	0.00	48.50	0.0165	0.80	0.48	0.90	2.73	-16.61	0.13	0.89	0.91	3.15
9	0.00	58.62	0.0486	2.85	2.14	1.32	3.09	-16.65	0.19	1.40	1.11	3.57
10	0.00	42.55	0.0253	1.08	0.09	2.79	2.53	-14.57	0.12	0.64	2.91	2.59
11	0.00	62.75	0.1521	9.55	2.54	3.59	3.33	-14.89	0.32	3.29	3.70	4.12
12	0.00	66.81	0.1858	12.42	4.44	3.77	3.48	-15.13	0.22	6.84	3.67	5.19
13	0.00	37.92	0.0129	0.49	0.07	2.60	2.36	-14.56	0.07	0.27	2.53	2.18
14	0.00	54.76	0.1047	5.73	1.70	3.13	3.15	-14.84	0.34	3.95	3.14	3.94
15	0.00	62.34	0.1541	9.61	3.10	3.53	3.36	-14.91	0.39	5.59	3.38	4.63
16	0.00	27.01	0.0004	0.01	0.01	2.28	1.79	-14.53	0.02	0.03	2.22	1.60
17	0.00	45.93	0.0542	2.49	1.27	2.73	2.86	-14.76	0.29	2.30	2.66	3.21
18	0.00	57.06	0.1278	7.29	4.43	3.17	3.29	-14.83	0.37	4.71	3.04	4.14

q_{SWL} =wave-induced flux at SWL; q_m =measured rate of overtopping/overflow; σ_m =measured standard deviation of free surface oscillation along the runup wire

Table A.2b: $\gamma = 0.8$; $\delta_r = 0.02$ m; f_b=0

Test	Numerical Model							Measured				
No.	H_{SWL}	q_{SWL}	P_o	q_o	q_o (empirical)	$S+\overline{\eta_r}$	σ_r	H_1	P_o	q_m	$S+\overline{\eta_r}$	σ_m
	cm	cm^2/s		cm^2/s	cm^2/s	cm	cm	cm		cm^2/s	cm	cm
19	0.00	41.45	0.0619	2.57	0.16	4.70	2.51	-12.63	NM	2.06	5.18	2.67
20	0.00	59.84	0.2585	15.47	4.34	5.28	3.42	-13.19	NM	10.40	5.61	4.34
21	0.00	67.06	0.3196	21.43	9.74	5.62	3.61	-13.34	NM	13.19	5.84	5.34
22	0.00	33.58	0.0191	0.64	0.07	4.44	2.15	-12.58	NM	0.65	5.02	2.05
23	0.00	54.47	0.2274	12.38	4.70	4.89	3.38	-13.29	NM	8.57	5.10	3.97
24	0.00	64.47	0.3118	20.10	14.41	5.39	3.65	-13.17	NM	11.08	5.44	4.85
25	0.00	24.90	0.0011	0.03	0.03	4.21	1.66	-12.53	NM	0.02	4.33	1.53
26	0.00	48.14	0.1489	7.17	3.20	4.72	3.03	-12.90	0.85	5.77	4.70	3.24
27	0.00	53.03	0.2177	11.54	11.35	4.80	3.36	-13.14	0.81	6.98	4.69	3.88
28	0.00	43.32	0.1825	7.90	0.79	6.70	2.67	-10.74	0.26	3.16	6.82	2.42
29	0.00	62.63	0.4277	26.79	12.39	7.34	3.53	-11.24	0.74	18.75	7.90	4.34
30	0.00	71.14	0.4820	34.29	23.17	7.74	3.64	-11.29	0.66	25.40	8.37	5.34
31	0.00	36.60	0.0926	3.39	0.39	6.50	2.30	-10.61	0.17	1.23	6.54	2.06
32	0.00	56.85	0.3793	21.56	8.96	7.08	3.39	-11.10	0.69	15.17	7.58	4.03
33	0.00	64.76	0.4529	29.33	26.10	7.34	3.65	-11.24	0.67	17.06	7.72	4.89
34	0.00	24.36	0.0066	0.16	0.07	6.17	1.63	-10.56	0.07	0.29	6.44	1.63
35	0.00	41.83	0.2155	9.01	5.29	6.32	2.91	-11.20	0.50	7.13	6.46	3.35
36	0.00	52.04	0.3403	17.71	13.93	6.79	3.32	-11.14	0.51	11.17	6.97	4.08
37	0.00	38.59	0.2873	11.09	1.78	8.45	2.56	-8.92	0.45	5.85	8.94	2.56
38	0.00	62.83	0.5789	36.37	22.49	9.36	3.43	-9.13	0.82	29.78	10.28	4.38
39	0.00	70.78	0.6318	44.72	52.31	9.55	3.64	-9.31	0.85	36.76	10.22	5.19
40	0.00	31.50	0.1486	4.68	0.85	8.23	2.12	-8.78	0.27	2.62	8.54	2.05
41	0.00	51.82	0.4977	25.79	14.09	8.85	3.25	-9.15	0.65	21.05	9.60	3.99
42	0.00	62.19	0.5806	36.11	30.81	9.27	3.48	-9.14	0.68	28.42	9.56	4.47
43	0.00	21.86	0.0174	0.38	0.18	8.10	1.48	-8.57	0.09	0.51	8.41	1.42
44	0.00	41.02	0.3608	14.80	9.56	8.38	2.86	-9.14	0.54	9.74	8.40	3.12
45	0.00	50.32	0.4804	24.18	27.55	8.81	3.19	-9.04	0.63	14.12	8.82	3.69

Table A.2c: $\gamma = 0.8$; $\delta_r = 0.02$ m; $f_b = 0$

Test No.	Numerical Model							Measured				
	H_{SWL} cm	q_{SWL} cm^2/s	P_o	q_o cm^2/s	q_o (empirical) cm^2/s	$S+\overline{\eta_r}$ cm	σ_r cm	H_1 cm	P_o	q_m cm^2/s	$S+\overline{\eta_r}$ cm	σ_m cm
46	0.00	34.67	0.4446	15.41	4.40	10.36	2.42	-6.94	0.54	9.40	10.84	2.35
47	0.00	61.62	0.7310	45.04	48.50	11.26	3.33	-7.08	0.78	36.60	11.51	3.80
48	0.00	63.81	0.7417	47.33	45.70	11.34	3.36	-7.22	0.93	48.71	11.48	4.61
49	0.00	26.37	0.2443	6.44	1.85	9.97	1.95	-6.96	0.30	3.72	10.22	1.86
50	0.00	50.79	0.6649	33.77	31.18	10.87	3.13	-7.08	0.79	26.32	11.13	3.45
51	0.00	61.02	0.7322	44.68	72.55	11.17	3.40	-7.15	0.82	34.63	11.17	4.31
52	0.00	20.74	0.0739	1.53	0.52	10.04	1.42	-6.61	0.16	1.09	10.22	1.41
53	0.00	37.94	0.5148	19.53	17.57	10.42	2.65	-6.98	0.56	12.39	10.52	2.85
54	0.00	45.05	0.6118	27.56	40.62	10.67	2.95	-7.01	0.60	17.46	10.61	3.46
55	0.00	18.31	0.2479	4.54	2.49	11.86	1.40	-4.79	0.36	3.32	12.09	1.46
56	0.00	33.24	0.6867	22.83	33.71	12.40	2.38	-4.84	0.69	16.42	12.48	2.60
57	0.00	38.58	0.7549	29.12	53.59	12.47	2.71	-5.04	0.74	23.53	12.47	3.17
58	0.00	24.64	0.5009	12.34	6.63	12.07	1.90	-4.86	0.58	7.81	12.38	1.91
59	0.00	45.67	0.8094	36.96	60.87	12.65	2.99	-5.17	0.80	34.80	12.66	3.21
60	0.00	54.42	0.8519	46.36	84.72	12.97	3.14	-5.09	0.81	41.10	12.74	3.67
61	0.00	30.59	0.6471	19.80	11.35	12.27	2.28	-4.96	0.64	13.33	12.65	2.34
62	0.00	12.64	0.5052	6.39	13.90	13.50	1.30	-3.11	0.54	6.10	13.52	1.40
63	0.00	25.47	0.8467	21.57	50.60	14.14	2.07	-2.90	0.81	24.02	14.29	2.46
64	0.00	29.55	0.8833	26.10	72.97	14.24	2.30	-2.96	0.89	28.91	14.16	2.84
65	0.00	20.42	0.7700	15.72	26.67	13.97	1.77	-2.89	0.72	12.86	14.15	1.88
66	0.00	37.38	0.9270	34.65	88.83	14.54	2.55	-2.89	0.90	40.03	14.48	2.89
67	0.00	23.09	0.8178	18.88	22.66	14.14	1.88	-2.81	0.79	21.56	14.49	2.10

Table A.2d: $\gamma = 0.8$; $\delta_r = 0.02$ m; $f_b = 0$

Test No.	Numerical Model							Measured				
	H_{SWL} cm	q_{SWL} cm^2/s	P_o	q_o cm^2/s	q_o (empirical) cm^2/s	$S+\overline{\eta_r}$ cm	σ_r cm	H_1 cm	P_o	q_m cm^2/s	$S+\overline{\eta_r}$ cm	σ_m cm
68	0.00	8.38	0.7860	6.58	23.59	14.92	1.16	-1.66	0.77	10.00	14.99	1.26
69	0.05	19.87	0.9550	19.37	88.88	15.31	2.02	-1.69	0.88	33.46	15.06	2.04
70	0.00	14.34	0.9115	13.07	50.76	15.13	1.62	-1.64	0.81	18.50	15.12	1.53
71	0.42	30.32	0.9901	38.62	131.45	15.87	2.35	-1.44	0.96	57.44	15.53	2.42
72	0.18	22.86	0.9748	24.66	77.57	15.61	2.04	-1.44	0.88	33.51	15.60	1.79
73	0.36	6.59	0.9942	13.22	33.33	16.31	1.02	-0.25	0.98	20.35	16.11	1.08
74	0.63	15.24	0.9983	30.81	94.73	16.34	1.63	-0.48	1.00	43.87	15.99	1.89
75	0.71	21.13	1.0000	39.81	122.70	16.59	1.72	-0.36	1.00	51.40	16.07	2.15
76	0.56	12.45	0.9993	25.62	63.00	16.43	1.32	-0.22	0.98	33.82	16.31	1.41
77	0.68	17.20	0.9997	34.66	91.32	16.45	1.71	-0.48	0.93	42.56	16.09	1.60
78	0.88	26.92	1.0000	52.61	129.37	16.77	1.91	-0.34	0.97	71.64	16.03	2.04
79	0.56	13.43	0.9841	26.25	152.48	15.80	2.05	-1.21	1.00	33.13	15.57	2.05
80	0.56	13.15	0.9959	26.21	105.56	16.24	1.62	-0.54	1.00	27.15	16.04	1.46
81	0.63	16.16	0.9828	31.47	185.16	15.59	2.53	-1.79	1.00	26.27	15.61	2.80
82	0.57	10.19	1.0000	23.49	64.82	16.75	1.06	0.24	1.00	24.20	16.69	1.02
83	0.61	15.14	0.9970	30.19	129.44	16.26	1.76	-0.60	1.00	40.32	16.07	1.78
84	0.62	13.45	1.0000	28.77	90.43	16.61	1.37	-0.03	1.00	33.08	16.55	1.32
85	0.70	19.07	0.9894	37.28	206.96	15.78	2.58	-1.68	1.00	48.79	15.44	2.60
86	0.69	10.19	1.0000	28.05	58.57	17.08	0.92	0.61	1.00	29.61	17.20	0.86
87	0.99	10.47	1.0000	41.28	55.25	17.56	0.76	1.22	1.00	42.66	17.68	0.75
88	0.93	16.29	1.0000	44.29	90.88	17.29	1.12	0.80	1.00	46.46	17.34	1.08
89	0.81	22.67	0.9994	45.49	181.46	16.39	2.13	-0.76	1.00	58.89	16.26	2.21
90	0.88	19.03	1.0000	44.69	121.63	17.04	1.39	0.41	1.00	52.10	17.01	1.52
91	1.06	11.09	1.0000	45.47	39.83	17.64	0.75	1.33	1.00	44.30	17.79	0.75

Table A.2e: $\gamma = 0.8$; $\delta_r = 0.02$ m; $f_b = 0$

Test No.	Numerical Model							Measured				
	H_{SWL} cm	q_{SWL} cm^2/s	P_o	q_o cm^2/s	q_o (empirical) cm^2/s	$S+\overline{\eta_r}$ cm	σ_r cm	H_1 cm	P_o	q_m cm^2/s	$S+\overline{\eta_r}$ cm	σ_m cm
92	1.25	21.42	1.0000	65.01	117.53	17.66	1.12	1.26	1.00	66.37	18.03	1.26
93	1.34	17.23	1.0000	66.09	80.01	17.84	0.93	1.55	1.00	62.74	18.11	0.90
94	1.01	25.37	1.0000	57.37	162.53	17.05	1.66	0.24	1.00	69.06	17.22	1.88
95	1.53	17.20	1.0000	76.60	83.71	18.10	0.85	1.91	1.00	82.36	18.50	0.90
96	1.50	20.49	1.0000	78.12	109.34	17.99	1.02	1.72	1.00	73.54	18.10	1.05
97	1.57	16.49	1.0000	78.19	82.97	18.15	0.82	2.00	1.00	73.17	18.72	0.81
98	1.28	30.71	1.0000	75.90	190.04	17.51	1.58	0.80	1.00	84.18	17.71	1.83
99	1.84	9.89	1.0000	87.78	54.13	18.46	0.56	2.56	1.00	94.70	19.11	0.50
100	1.91	22.87	1.0000	105.34	121.62	18.44	1.04	2.33	1.00	105.63	18.86	1.11
101	1.87	9.02	1.0000	89.15	32.88	18.49	0.53	2.62	1.00	87.07	19.21	0.51
102	1.89	25.46	1.0000	107.00	115.13	18.41	1.12	2.22	1.00	104.11	18.97	1.09
103	2.04	8.85	1.0000	99.95	32.87	18.64	0.54	2.86	1.00	98.76	19.53	0.51
104	2.00	19.31	1.0000	108.08	71.00	18.55	0.94	2.55	1.00	100.89	19.25	0.97
105	2.07	15.87	1.0000	109.31	77.07	18.63	0.84	2.72	1.00	102.41	19.39	0.79
106	1.76	31.55	1.0000	104.76	161.24	18.21	1.32	1.87	1.00	107.48	18.61	1.62
107	2.03	8.54	1.0000	99.19	31.77	18.63	0.53	2.85	1.00	99.18	19.53	0.51

Table A.3a: $\gamma = 0.8$; $\delta_r = 0.01$ m; $f_b = 0$

Test No.	Numerical Model							Measured				
	H_{SWL} cm	q_{SWL} cm^2/s	P_o	q_o cm^2/s	q_o (empirical) cm^2/s	$S+\overline{\eta_r}$ cm	σ_r cm	H_1 cm	P_o	q_m cm^2/s	$S+\overline{\eta_r}$ cm	σ_m cm
1	0.00	40.77	0.0130	0.53	0.01	1.64	2.53	-16.57	0.12	0.26	1.09	3.14
2	0.00	60.63	0.0976	5.91	0.74	2.75	3.19	-16.76	0.46	2.20	1.29	5.27
3	0.00	67.92	0.1357	9.21	2.48	3.11	3.36	-16.85	0.46	1.96	1.37	5.57
4	0.00	37.18	0.0081	0.30	0.01	1.40	2.44	-16.54	0.08	0.11	0.90	2.13
5	0.00	57.84	0.0889	5.14	0.89	2.51	3.19	-16.65	0.24	1.27	1.47	3.58
6	0.00	64.76	0.1252	8.11	2.58	2.87	3.35	-16.68	0.22	2.13	1.63	4.34
7	0.00	28.94	0.0008	0.02	0.00	0.97	2.07	-16.53	0.00	0.00	0.17	1.62
8	0.00	48.28	0.0468	2.26	0.48	1.92	2.95	-16.61	0.13	0.89	0.91	3.15
9	0.00	57.93	0.0975	5.65	2.14	2.43	3.27	-16.65	0.19	1.40	1.11	3.57
10	0.00	42.29	0.0683	2.89	0.09	3.75	2.76	-14.57	0.12	0.64	2.91	2.59
11	0.00	61.66	0.1974	12.17	2.54	4.65	3.30	-14.89	0.32	3.29	3.70	4.12
12	0.00	65.90	0.2186	14.40	4.44	4.82	3.36	-15.13	0.22	6.84	3.67	5.19
13	0.00	37.81	0.0436	1.65	0.07	3.50	2.60	-14.56	0.07	0.27	2.53	2.18
14	0.00	53.86	0.1644	8.85	1.70	4.21	3.24	-14.84	0.34	3.95	3.14	3.94
15	0.00	61.30	0.1995	12.23	3.10	4.59	3.32	-14.91	0.39	5.59	3.38	4.63
16	0.00	27.01	0.0048	0.13	0.01	2.96	2.08	-14.53	0.02	0.03	2.22	1.60
17	0.00	45.48	0.1122	5.10	1.26	3.78	3.05	-14.76	0.29	2.30	2.66	3.21
18	0.00	56.12	0.1830	10.27	4.43	4.26	3.33	-14.83	0.37	4.71	3.04	4.14

q_{SWL} =wave-induced flux at SWL; q_m =measured rate of overtopping/overflow; σ_m =measured standard deviation of free surface oscillation along the runup wire

Table A.3b: $\gamma = 0.8$; $\delta_r = 0.01$ m; f_b=0

Test No.	Numerical Model							Measured				
	H_{SWL} cm	q_{SWL} cm^2/s	P_o	q_o cm^2/s	q_o (empirical) cm^2/s	$S+\overline{\eta_r}$ cm	σ_r cm	H_1 cm	P_o	q_m cm^2/s	$S+\overline{\eta_r}$ cm	σ_m cm
19	0.00	40.80	0.1314	5.36	0.16	5.64	2.70	-12.63	NM	2.06	5.18	2.67
20	0.00	59.16	0.2865	16.95	4.34	6.28	3.24	-13.19	NM	10.40	5.61	4.34
21	0.00	66.86	0.3252	21.74	9.74	6.58	3.32	-13.34	NM	13.19	5.84	5.34
22	0.00	33.41	0.0630	2.10	0.07	5.25	2.40	-12.58	NM	0.65	5.02	2.05
23	0.00	53.55	0.2685	14.38	4.70	5.92	3.27	-13.29	NM	8.57	5.10	3.97
24	0.00	64.06	0.3233	20.71	14.41	6.38	3.38	-13.17	NM	11.08	5.44	4.85
25	0.00	24.89	0.0112	0.28	0.03	4.84	1.95	-12.53	NM	0.02	4.33	1.53
26	0.00	47.09	0.2153	10.14	3.20	5.74	3.08	-12.90	0.85	5.77	4.70	3.24
27	0.00	52.09	0.2631	13.70	11.34	5.84	3.27	-13.14	0.81	6.98	4.69	3.88
28	0.00	42.03	0.2559	10.75	0.79	7.60	2.70	-10.74	0.26	3.16	6.82	2.42
29	0.00	62.72	0.4219	26.46	12.39	8.22	3.16	-11.24	0.74	18.75	7.90	4.34
30	0.00	71.84	0.4637	33.32	23.17	8.55	3.22	-11.29	0.66	25.40	8.37	5.34
31	0.00	35.64	0.1807	6.44	0.39	7.35	2.48	-10.61	0.17	1.23	6.54	2.06
32	0.00	56.82	0.3821	21.71	8.96	7.98	3.08	-11.10	0.69	15.17	7.58	4.03
33	0.00	65.19	0.4445	28.98	26.10	8.21	3.27	-11.24	0.67	17.06	7.72	4.89
34	0.00	24.30	0.0389	0.95	0.07	6.78	1.91	-10.56	0.07	0.29	6.44	1.63
35	0.00	40.62	0.2852	11.59	5.28	7.28	2.92	-11.20	0.50	7.13	6.46	3.35
36	0.00	51.40	0.3609	18.55	13.92	7.72	3.08	-11.14	0.51	11.17	6.97	4.08
37	0.00	37.35	0.3541	13.23	1.78	9.27	2.52	-8.92	0.45	5.85	8.94	2.56
38	0.00	63.11	0.5665	35.75	22.49	10.11	3.01	-9.13	0.82	29.78	10.28	4.38
39	0.00	71.49	0.6132	43.84	52.31	10.26	3.17	-9.31	0.85	36.76	10.22	5.19
40	0.00	30.25	0.2560	7.74	0.84	8.99	2.28	-8.78	0.27	2.62	8.54	2.05
41	0.00	51.91	0.4958	25.73	14.09	9.67	2.90	-9.15	0.65	21.05	9.60	3.99
42	0.00	62.49	0.5693	35.58	30.81	10.03	3.06	-9.14	0.68	28.42	9.56	4.47
43	0.00	21.69	0.0786	1.71	0.18	8.63	1.75	-8.57	0.09	0.51	8.41	1.42
44	0.00	40.09	0.4054	16.25	9.55	9.24	2.71	-9.14	0.54	9.74	8.40	3.12
45	0.00	49.95	0.4897	24.46	27.55	9.64	2.88	-9.04	0.63	14.12	8.82	3.69

Table A.3c: $\gamma = 0.8$; $\delta_r = 0.01$ m; f_b=0

Test No.	Numerical Model							Measured				
	H_{SWL} cm	q_{SWL} cm^2/s	P_o	q_o cm^2/s	q_o (empirical) cm^2/s	$S+\overline{\eta_r}$ cm	σ_r cm	H_1 cm	P_o	q_m cm^2/s	$S+\overline{\eta_r}$ cm	σ_m cm
46	0.00	33.76	0.4949	16.71	4.40	11.08	2.30	-6.94	0.54	9.40	10.84	2.35
47	0.00	62.09	0.7242	44.97	48.50	11.92	2.87	-7.08	0.78	36.60	11.51	3.80
48	0.00	64.23	0.7353	47.23	45.70	11.99	2.89	-7.22	0.93	48.71	11.48	4.61
49	0.00	24.89	0.3664	9.12	1.84	10.65	2.08	-6.96	0.30	3.72	10.22	1.86
50	0.00	50.87	0.6638	33.77	31.19	11.58	2.74	-7.08	0.79	26.32	11.13	3.45
51	0.00	61.32	0.7206	44.19	72.56	11.81	2.91	-7.15	0.82	34.63	11.17	4.31
52	0.00	20.00	0.1951	3.90	0.52	10.55	1.65	-6.61	0.16	1.09	10.22	1.41
53	0.00	37.28	0.5473	20.40	17.56	11.17	2.44	-6.98	0.56	12.39	10.52	2.85
54	0.00	45.05	0.6200	27.93	40.62	11.41	2.62	-7.01	0.60	17.46	10.61	3.46
55	0.00	16.85	0.4071	6.86	2.49	12.33	1.56	-4.79	0.36	3.32	12.09	1.46
56	0.00	32.64	0.7111	23.21	33.70	13.02	2.13	-4.84	0.69	16.42	12.48	2.60
57	0.00	38.45	0.7593	29.19	53.59	13.09	2.32	-5.04	0.74	23.53	12.47	3.17
58	0.00	23.63	0.5847	13.82	6.63	12.65	1.87	-4.86	0.58	7.81	12.38	1.91
59	0.00	45.69	0.8173	37.35	60.87	13.28	2.56	-5.17	0.80	34.80	12.66	3.21
60	0.00	54.46	0.8529	46.45	84.72	13.55	2.65	-5.09	0.81	41.10	12.74	3.67
61	0.00	30.01	0.6802	20.41	11.35	12.89	2.07	-4.96	0.64	13.33	12.65	2.34
62	0.00	11.52	0.6619	7.62	13.89	13.92	1.44	-3.11	0.54	6.10	13.52	1.40
63	0.00	25.13	0.8810	22.14	50.60	14.67	1.85	-2.90	0.81	24.02	14.29	2.46
64	0.00	29.25	0.9126	26.69	72.96	14.80	2.02	-2.96	0.89	28.91	14.16	2.84
65	0.00	19.88	0.8295	16.49	26.66	14.47	1.69	-2.89	0.72	12.86	14.15	1.88
66	0.00	37.06	0.9458	35.05	88.81	15.09	2.16	-2.89	0.90	40.03	14.48	2.89
67	0.00	22.79	0.8558	19.51	22.65	14.63	1.70	-2.81	0.79	21.56	14.49	2.10

Table A.3d: $\gamma = 0.8$; $\delta_r = 0.01$ m; $f_b = 0$

Test No.	Numerical Model							Measured				
	H_{SWL} cm	q_{SWL} cm^2/s	P_o	q_o cm^2/s	q_o (empirical) cm^2/s	$S+\overline{\eta_r}$ cm	σ_r cm	H_1 cm	P_o	q_m cm^2/s	$S+\overline{\eta_r}$ cm	σ_m cm
68	0.00	7.95	0.8890	7.07	23.59	15.27	1.29	-1.66	0.77	10.00	14.99	1.26
69	0.05	19.69	0.9842	19.74	88.87	15.86	1.87	-1.69	0.88	33.46	15.06	2.04
70	0.00	13.97	0.9609	13.43	50.75	15.62	1.62	-1.64	0.81	18.50	15.12	1.53
71	0.42	30.29	0.9989	38.82	131.45	16.35	1.97	-1.44	0.96	57.44	15.53	2.42
72	0.18	22.68	0.9934	24.82	77.57	16.11	1.81	-1.44	0.88	33.51	15.60	1.79
73	0.36	6.59	1.0000	13.25	33.33	16.54	0.91	-0.25	0.98	20.35	16.11	1.08
74	0.63	15.24	1.0000	30.83	94.73	16.71	1.43	-0.48	1.00	43.87	15.99	1.89
75	0.71	21.13	1.0000	39.81	122.70	16.83	1.44	-0.36	1.00	51.40	16.07	2.15
76	0.56	12.45	1.0000	25.63	63.00	16.74	1.18	-0.22	0.98	33.82	16.31	1.41
77	0.68	17.20	1.0000	34.66	91.32	16.78	1.49	-0.48	0.93	42.56	16.09	1.60
78	0.88	26.92	1.0000	52.61	129.37	17.01	1.56	-0.34	0.97	71.64	16.03	2.04
79	0.56	13.39	0.9977	26.31	152.48	16.29	1.79	-1.21	1.00	33.13	15.57	2.05
80	0.56	13.13	1.0000	26.21	105.56	16.55	1.34	-0.54	1.00	27.15	16.04	1.46
81	0.60	17.34	0.9958	31.71	185.14	16.14	2.14	-1.79	1.00	26.27	15.61	2.80
82	0.57	10.19	1.0000	23.49	64.82	16.88	0.83	0.24	1.00	24.20	16.69	1.02
83	0.61	15.13	1.0000	30.21	129.44	16.61	1.47	-0.60	1.00	40.32	16.07	1.78
84	0.62	13.45	1.0000	28.77	90.43	16.83	1.10	-0.03	1.00	33.08	16.55	1.32
85	0.71	19.16	0.9997	37.71	206.96	16.41	2.32	-1.68	1.00	48.79	15.44	2.60
86	0.69	10.19	1.0000	28.05	58.57	17.13	0.70	0.61	1.00	29.61	17.20	0.86
87	0.99	10.47	1.0000	41.28	55.25	17.53	0.60	1.22	1.00	42.66	17.68	0.75
88	0.93	16.29	1.0000	44.29	90.88	17.38	0.88	0.80	1.00	46.46	17.34	1.08
89	0.81	22.67	1.0000	45.50	181.46	16.78	1.75	-0.76	1.00	58.89	16.26	2.21
90	0.88	19.03	1.0000	44.69	121.63	17.22	1.11	0.41	1.00	52.10	17.01	1.52
91	1.06	11.09	1.0000	45.47	39.83	17.61	0.61	1.33	1.00	44.30	17.79	0.75

Table A.3e: $\gamma = 0.8$; $\delta_r = 0.01$ m; $f_b = 0$

Test No.	Numerical Model							Measured				
	H_{SWL} cm	q_{SWL} cm^2/s	P_o	q_o cm^2/s	q_o (empirical) cm^2/s	$S+\overline{\eta_r}$ cm	σ_r cm	H_1 cm	P_o	q_m cm^2/s	$S+\overline{\eta_r}$ cm	σ_m cm
92	1.25	21.42	1.0000	65.01	117.53	17.75	0.96	1.26	1.00	66.37	18.03	1.26
93	1.34	17.23	1.0000	66.09	80.01	17.87	0.84	1.55	1.00	62.74	18.11	0.90
94	1.01	25.37	1.0000	57.37	162.53	17.31	1.35	0.24	1.00	69.06	17.22	1.88
95	1.53	17.20	1.0000	76.60	83.71	18.10	0.83	1.91	1.00	82.36	18.50	0.90
96	1.50	20.49	1.0000	78.12	109.34	18.03	0.94	1.72	1.00	73.54	18.10	1.05
97	1.57	16.49	1.0000	78.19	82.97	18.11	0.81	2.00	1.00	73.17	18.72	0.81
98	1.28	30.71	1.0000	75.90	190.04	17.72	1.30	0.80	1.00	84.18	17.71	1.83
99	1.84	9.89	1.0000	87.78	54.13	18.38	0.66	2.56	1.00	94.70	19.11	0.50
100	1.91	22.87	1.0000	105.34	121.62	18.44	1.04	2.33	1.00	105.63	18.86	1.11
101	1.87	9.02	1.0000	89.15	32.88	18.42	0.63	2.62	1.00	87.07	19.21	0.51
102	1.89	25.46	1.0000	107.00	115.13	18.42	1.10	2.22	1.00	104.11	18.97	1.09
103	2.04	8.85	1.0000	99.95	32.87	18.58	0.64	2.86	1.00	98.76	19.53	0.51
104	2.00	19.31	1.0000	108.08	71.00	18.53	0.97	2.55	1.00	100.89	19.25	0.97
105	2.07	15.87	1.0000	109.31	77.07	18.60	0.88	2.72	1.00	102.41	19.39	0.79
106	1.76	31.55	1.0000	104.76	161.24	18.29	1.21	1.87	1.00	107.48	18.61	1.62
107	2.03	8.54	1.0000	99.19	31.77	18.58	0.63	2.85	1.00	99.18	19.53	0.51

Table A.4a: $\gamma = 0.8$; $\delta_r = 0.02$ m; f_b =0.01

Test No.	Numerical Model							Measured				
	H_{SWL} cm	q_{SWL} cm^2/s	P_o	q_o cm^2/s	q_o (empirical) cm^2/s	$S+\overline{\eta_r}$ cm	σ_r cm	H_1 cm	P_o	q_m cm^2/s	$S+\overline{\eta_r}$ cm	σ_m cm
1	0.00	37.20	0.0022	0.08	0.01	0.81	2.25	-16.57	0.12	0.26	1.09	3.14
2	0.00	56.84	0.0442	2.51	0.74	1.72	2.96	-16.76	0.46	2.20	1.29	5.27
3	0.00	64.31	0.0804	5.17	2.47	2.07	3.22	-16.85	0.46	1.96	1.37	5.57
4	0.00	33.79	0.0011	0.04	0.01	0.61	2.15	-16.54	0.08	0.11	0.90	2.13
5	0.00	53.78	0.0380	2.04	0.89	1.48	2.94	-16.65	0.24	1.27	1.47	3.58
6	0.00	60.88	0.0686	4.18	2.58	1.82	3.18	-16.68	0.22	2.13	1.63	4.34
7	0.00	26.23	0.0000	0.00	0.00	0.32	1.78	-16.53	0.00	0.00	0.17	1.62
8	0.00	44.13	0.0146	0.65	0.48	0.95	2.68	-16.61	0.13	0.89	0.91	3.15
9	0.00	53.68	0.0441	2.37	2.14	1.39	3.03	-16.65	0.19	1.40	1.11	3.57
10	0.00	38.58	0.0231	0.89	0.09	2.84	2.49	-14.57	0.12	0.64	2.91	2.59
11	0.00	58.11	0.1439	8.36	2.54	3.66	3.27	-14.89	0.32	3.29	3.70	4.12
12	0.00	62.26	0.1774	11.04	4.44	3.84	3.41	-15.13	0.22	6.84	3.67	5.19
13	0.00	34.28	0.0117	0.40	0.07	2.64	2.33	-14.56	0.07	0.27	2.53	2.18
14	0.00	50.05	0.0978	4.89	1.70	3.19	3.09	-14.84	0.34	3.95	3.14	3.94
15	0.00	57.65	0.1457	8.40	3.10	3.60	3.29	-14.91	0.39	5.59	3.38	4.63
16	0.00	24.36	0.0004	0.01	0.01	2.31	1.79	-14.53	0.02	0.03	2.22	1.60
17	0.00	41.57	0.0498	2.07	1.27	2.79	2.81	-14.76	0.29	2.30	2.66	3.21
18	0.00	52.27	0.1201	6.28	4.43	3.24	3.23	-14.83	0.37	4.71	3.04	4.14

q_{SWL} =wave-induced flux at SWL; q_m =measured rate of overtopping/overflow; σ_m =measured standard deviation of free surface oscillation along the runup wire

Table A.4b: $\gamma = 0.8$; $\delta_r = 0.02$ m; f_b=0.01

Test	Numerical Model							Measured				
No.	H_{SWL}	q_{SWL}	P_o	q_o	q_o (empirical)	$S+\overline{\eta_r}$	σ_r	H_1	P_o	q_m	$S+\overline{\eta_r}$	σ_m
	cm	cm^2/s		cm^2/s	cm^2/s	cm	cm	cm		cm^2/s	cm	cm
19	0.00	37.65	0.0582	2.19	0.16	4.75	2.47	-12.63	NM	2.06	5.18	2.67
20	0.00	55.86	0.2507	14.00	4.33	5.35	3.36	-13.19	NM	10.40	5.61	4.34
21	0.00	63.29	0.3144	19.90	9.73	5.69	3.56	-13.34	NM	13.19	5.84	5.34
22	0.00	30.33	0.0180	0.55	0.07	4.47	2.13	-12.58	NM	0.65	5.02	2.05
23	0.00	50.27	0.2187	11.00	4.70	4.96	3.32	-13.29	NM	8.57	5.10	3.97
24	0.00	60.51	0.3048	18.44	14.42	5.47	3.59	-13.17	NM	11.08	5.44	4.85
25	0.00	22.45	0.0011	0.02	0.03	4.24	1.66	-12.53	NM	0.02	4.33	1.53
26	0.00	43.96	0.1419	6.23	3.21	4.78	2.97	-12.90	0.85	5.77	4.70	3.24
27	0.00	48.84	0.2097	10.24	11.36	4.87	3.30	-13.14	0.81	6.98	4.69	3.88
28	0.00	39.89	0.1767	7.05	0.79	6.75	2.63	-10.74	0.26	3.16	6.82	2.42
29	0.00	59.54	0.4241	25.25	12.38	7.41	3.48	-11.24	0.74	18.75	7.90	4.34
30	0.00	68.27	0.4822	32.92	23.17	7.82	3.61	-11.29	0.66	25.40	8.37	5.34
31	0.00	33.30	0.0897	2.99	0.39	6.54	2.27	-10.61	0.17	1.23	6.54	2.06
32	0.00	53.71	0.3743	20.10	8.96	7.15	3.35	-11.10	0.69	15.17	7.58	4.03
33	0.00	61.71	0.4503	27.79	26.10	7.42	3.61	-11.24	0.67	17.06	7.72	4.89
34	0.00	21.96	0.0067	0.15	0.07	6.20	1.63	-10.56	0.07	0.29	6.44	1.63
35	0.00	38.27	0.2088	7.99	5.30	6.37	2.87	-11.20	0.50	7.13	6.46	3.35
36	0.00	48.73	0.3338	16.27	13.93	6.85	3.27	-11.14	0.51	11.17	6.97	4.08
37	0.00	35.96	0.2832	10.18	1.78	8.49	2.53	-8.92	0.45	5.85	8.94	2.56
38	0.00	60.36	0.5769	34.82	22.49	9.43	3.39	-9.13	0.82	29.78	10.28	4.38
39	0.00	68.17	0.6300	42.95	52.31	9.62	3.59	-9.31	0.85	36.76	10.22	5.19
40	0.00	28.73	0.1472	4.23	0.85	8.27	2.11	-8.78	0.27	2.62	8.54	2.05
41	0.00	49.43	0.4952	24.48	14.09	8.92	3.21	-9.15	0.65	21.05	9.60	3.99
42	0.00	59.71	0.5788	34.56	30.81	9.33	3.44	-9.14	0.68	28.42	9.56	4.47
43	0.00	19.72	0.0181	0.36	0.18	8.12	1.48	-8.57	0.09	0.51	8.41	1.42
44	0.00	38.45	0.3564	13.71	9.56	8.43	2.82	-9.14	0.54	9.74	8.40	3.12
45	0.00	47.91	0.4775	22.87	27.57	8.87	3.15	-9.04	0.63	14.12	8.82	3.69

Table A.4c: $\gamma = 0.8$; $\delta_r = 0.02$ m; f_b=0.01

Test No.	Numerical Model							Measured				
	H_{SWL} cm	q_{SWL} cm^2/s	P_o	q_o cm^2/s	q_o (empirical) cm^2/s	$S+\overline{\eta_r}$ cm	σ_r cm	H_1 cm	P_o	q_m cm^2/s	$S+\overline{\eta_r}$ cm	σ_m cm
46	0.00	32.94	0.4427	14.59	4.40	10.40	2.40	-6.94	0.54	9.40	10.84	2.35
47	0.00	59.86	0.7333	43.89	48.51	11.33	3.30	-7.08	0.78	36.60	11.51	3.80
48	0.00	62.00	0.7442	46.14	45.70	11.41	3.33	-7.22	0.93	48.71	11.48	4.61
49	0.00	24.23	0.2445	5.92	1.85	10.00	1.94	-6.96	0.30	3.72	10.22	1.86
50	0.00	48.95	0.6642	32.51	31.20	10.92	3.10	-7.08	0.79	26.32	11.13	3.45
51	0.00	59.29	0.7345	43.55	72.58	11.24	3.37	-7.15	0.82	34.63	11.17	4.31
52	0.00	18.78	0.0760	1.43	0.52	10.06	1.42	-6.61	0.16	1.09	10.22	1.41
53	0.00	36.30	0.5140	18.66	17.58	10.47	2.63	-6.98	0.56	12.39	10.52	2.85
54	0.00	43.29	0.6106	26.43	40.63	10.72	2.92	-7.01	0.60	17.46	10.61	3.46
55	0.00	16.86	0.2513	4.24	2.49	11.88	1.40	-4.79	0.36	3.32	12.09	1.46
56	0.00	32.03	0.6861	21.98	33.72	12.43	2.36	-4.84	0.69	16.42	12.48	2.60
57	0.00	37.30	0.7552	28.16	53.61	12.51	2.68	-5.04	0.74	23.53	12.47	3.17
58	0.00	23.50	0.5016	11.79	6.63	12.09	1.89	-4.86	0.58	7.81	12.38	1.91
59	0.00	44.25	0.8103	35.86	60.89	12.70	2.95	-5.17	0.80	34.80	12.66	3.21
60	0.00	52.80	0.8527	45.02	84.74	13.02	3.11	-5.09	0.81	41.10	12.74	3.67
61	0.00	29.41	0.6462	19.01	11.35	12.30	2.26	-4.96	0.64	13.33	12.65	2.34
62	0.00	11.91	0.5086	6.06	13.90	13.52	1.30	-3.11	0.54	6.10	13.52	1.40
63	0.00	24.72	0.8477	20.95	50.61	14.16	2.06	-2.90	0.81	24.02	14.29	2.46
64	0.00	28.69	0.8844	25.38	72.98	14.27	2.28	-2.96	0.89	28.91	14.16	2.84
65	0.00	19.74	0.7710	15.22	26.67	13.99	1.76	-2.89	0.72	12.86	14.15	1.88
66	0.00	36.32	0.9282	33.71	88.84	14.58	2.53	-2.89	0.90	40.03	14.48	2.89
67	0.00	22.50	0.8193	18.44	22.66	14.17	1.87	-2.81	0.79	21.56	14.49	2.10

Table A.4d: $\gamma = 0.8$; $\delta_r = 0.02$ m; f_b=0.01

Test No.	Numerical Model							Measured				
	H_{SWL} cm	q_{SWL} cm^2/s	P_o	q_o cm^2/s	q_o (empirical) cm^2/s	$S+\overline{\eta_r}$ cm	σ_r cm	H_1 cm	P_o	q_m cm^2/s	$S+\overline{\eta_r}$ cm	σ_m cm
68	0.00	8.03	0.7882	6.33	23.60	14.93	1.16	-1.66	0.77	10.00	14.99	1.26
69	0.06	19.28	0.9560	18.92	88.88	15.33	2.00	-1.69	0.88	33.46	15.06	2.04
70	0.00	13.85	0.9129	12.64	50.76	15.15	1.62	-1.64	0.81	18.50	15.12	1.53
71	0.43	29.57	0.9908	38.25	131.47	15.90	2.33	-1.44	0.96	57.44	15.53	2.42
72	0.19	22.17	0.9756	24.17	77.58	15.63	2.03	-1.44	0.88	33.51	15.60	1.79
73	0.36	6.32	0.9943	12.95	33.33	16.31	1.02	-0.25	0.98	20.35	16.11	1.08
74	0.63	14.65	0.9985	30.34	94.74	16.36	1.61	-0.48	1.00	43.87	15.99	1.89
75	0.74	17.98	1.0000	37.82	122.73	16.61	1.70	-0.36	1.00	51.40	16.07	2.15
76	0.57	11.99	0.9995	25.63	63.00	16.44	1.31	-0.22	0.98	33.82	16.31	1.41
77	0.69	16.56	0.9999	34.58	91.33	16.47	1.70	-0.48	0.93	42.56	16.09	1.60
78	0.88	26.15	1.0000	52.08	129.38	16.79	1.89	-0.34	0.97	71.64	16.03	2.04
79	0.55	13.09	0.9847	25.83	152.49	15.82	2.03	-1.21	1.00	33.13	15.57	2.05
80	0.57	12.66	0.9961	25.99	105.56	16.25	1.60	-0.54	1.00	27.15	16.04	1.46
81	0.62	15.73	0.9835	30.94	185.17	15.62	2.49	-1.79	1.00	26.27	15.61	2.80
82	0.57	9.81	1.0000	23.15	64.83	16.76	1.05	0.24	1.00	24.20	16.69	1.02
83	0.62	14.57	0.9973	29.73	129.44	16.27	1.74	-0.60	1.00	40.32	16.07	1.78
84	0.63	12.95	1.0000	28.50	90.44	16.62	1.36	-0.03	1.00	33.08	16.55	1.32
85	0.70	18.72	0.9900	37.05	206.98	15.81	2.54	-1.68	1.00	48.79	15.44	2.60
86	0.68	9.81	1.0000	27.50	58.57	17.08	0.92	0.61	1.00	29.61	17.20	0.86
87	0.99	10.11	1.0000	40.99	55.25	17.56	0.76	1.22	1.00	42.66	17.68	0.75
88	0.93	15.74	1.0000	43.92	90.89	17.29	1.11	0.80	1.00	46.46	17.34	1.08
89	0.81	21.77	0.9996	44.40	181.48	16.40	2.11	-0.76	1.00	58.89	16.26	2.21
90	0.87	20.43	1.0000	46.06	121.60	17.03	1.35	0.41	1.00	52.10	17.01	1.52
91	1.07	10.71	1.0000	45.17	39.83	17.64	0.75	1.33	1.00	44.30	17.79	0.75

Table A.4e: $\gamma = 0.8$; $\delta_r = 0.02$ m; f_b =0.01

Test No.	Numerical Model							Measured				
	H_{SWL} cm	q_{SWL} cm^2/s	P_o	q_o cm^2/s	q_o (empirical) cm^2/s	$S+\overline{\eta_r}$ cm	σ_r cm	H_1 cm	P_o	q_m cm^2/s	$S+\overline{\eta_r}$ cm	σ_m cm
92	1.21	19.46	1.0000	61.29	117.60	17.64	1.06	1.26	1.00	66.37	18.03	1.26
93	1.29	15.77	1.0000	61.61	80.06	17.81	0.86	1.55	1.00	62.74	18.11	0.90
94	1.01	26.94	1.0000	58.88	162.49	17.06	1.66	0.24	1.00	69.06	17.22	1.88
95	1.58	17.42	1.0000	79.90	83.67	18.11	0.90	1.91	1.00	82.36	18.50	0.90
96	1.44	18.85	1.0000	73.03	109.40	17.97	0.94	1.72	1.00	73.54	18.10	1.05
97	1.53	15.66	1.0000	74.91	82.99	18.13	0.78	2.00	1.00	73.17	18.72	0.81
98	1.30	31.89	1.0000	78.16	189.99	17.53	1.60	0.80	1.00	84.18	17.71	1.83
99	1.93	9.79	1.0000	93.46	54.08	18.48	0.64	2.56	1.00	94.70	19.11	0.50
100	1.90	22.19	1.0000	103.90	121.63	18.43	1.02	2.33	1.00	105.63	18.86	1.11
101	1.98	8.92	1.0000	96.05	32.85	18.53	0.62	2.62	1.00	87.07	19.21	0.51
102	1.82	23.49	1.0000	100.22	115.24	18.37	1.02	2.22	1.00	104.11	18.97	1.09
103	2.12	8.59	1.0000	105.59	32.83	18.68	0.62	2.86	1.00	98.76	19.53	0.51
104	1.91	17.91	1.0000	100.49	71.10	18.50	0.83	2.55	1.00	100.89	19.25	0.97
105	2.07	15.37	1.0000	108.37	77.08	18.63	0.82	2.72	1.00	102.41	19.39	0.79
106	1.75	30.63	1.0000	103.07	161.26	18.20	1.30	1.87	1.00	107.48	18.61	1.62
107	2.12	8.28	1.0000	104.92	31.73	18.67	0.61	2.85	1.00	99.18	19.53	0.51

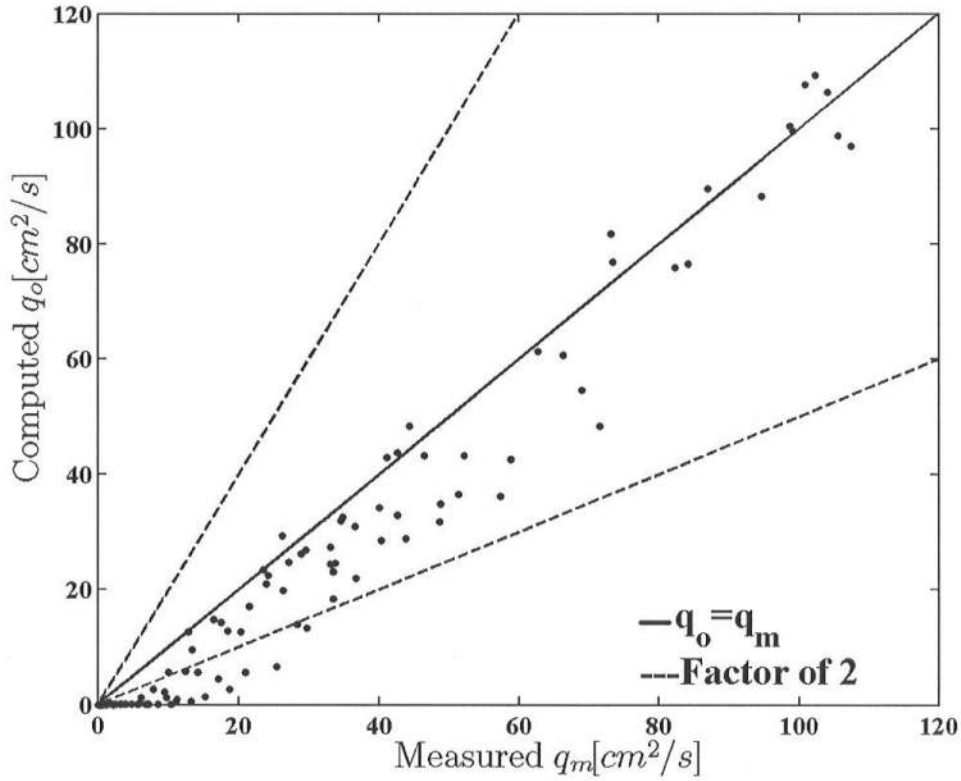

Fig. A1: γ=0.7; δ_r=0.02 m; f_b=0.0

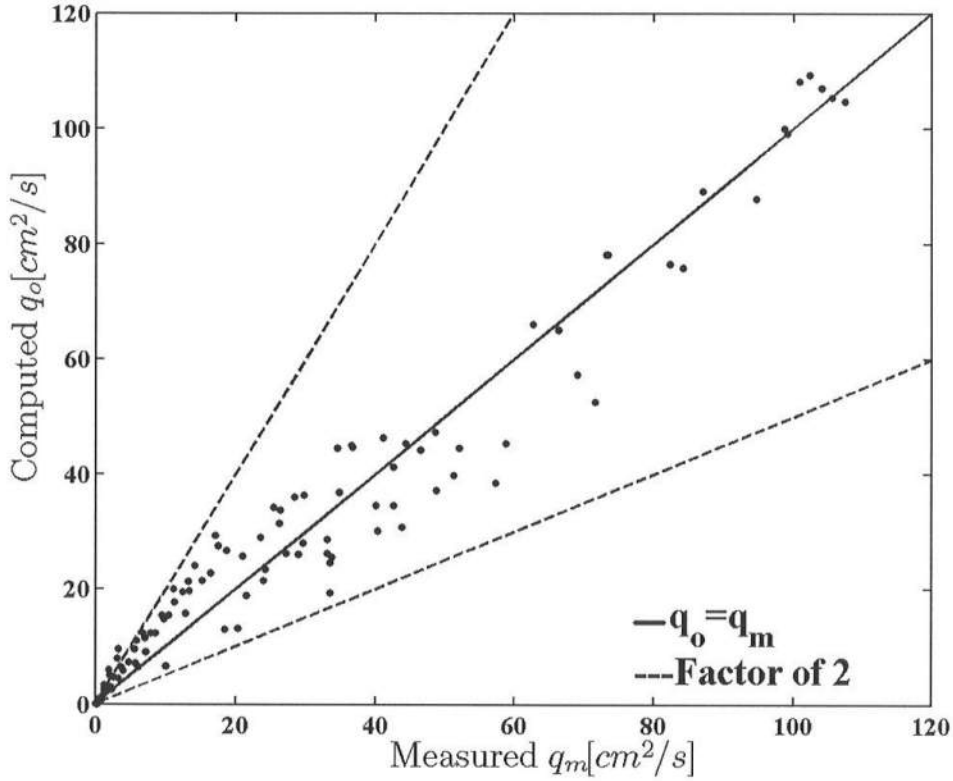

Fig. A.2: γ=0.8; δ_r=0.02 m; f_b=0.0

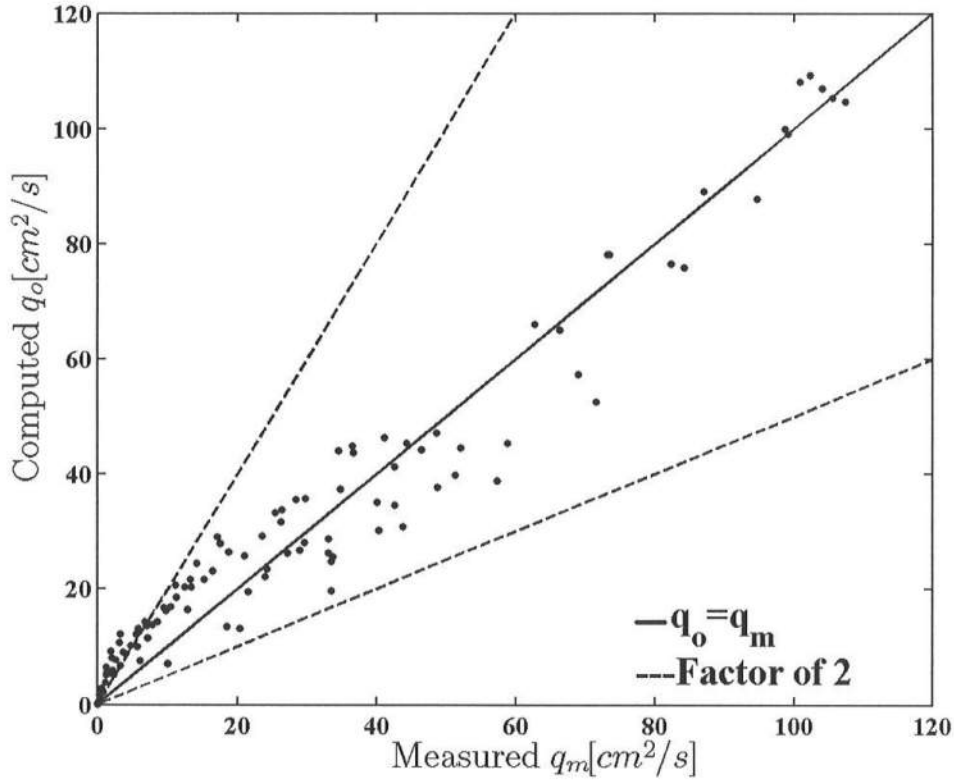

Fig. A.3: γ=0.8; δ_r=0.01 m; f_b=0.0

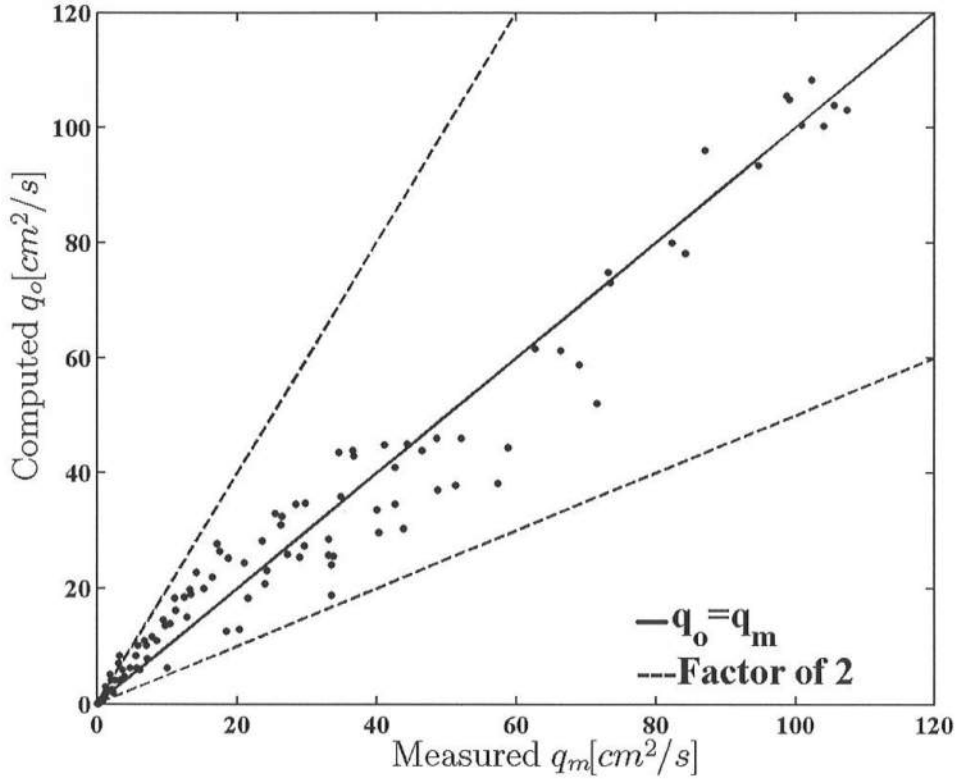

Fig. A.4: γ=0.8; δ_r=0.02 m; f_b=0.01

APPENDIX B

COMPUTED AND MEASURED CROSS-SHORE VARIATIONS

Figs. B.1-B.107 show the computed and measured cross-shore variations of the mean and standard deviation of the free surface elevation η and horizontal velocity U for each of the 107 tests in the same way as in Figs. 4-6 to 4-9 in Chapter 4.

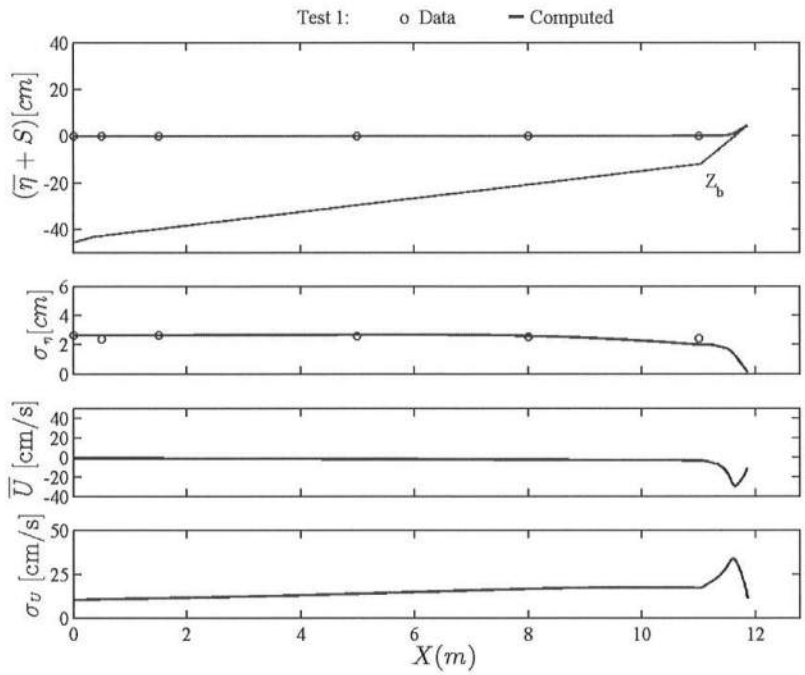

Fig. B.1: Test 1

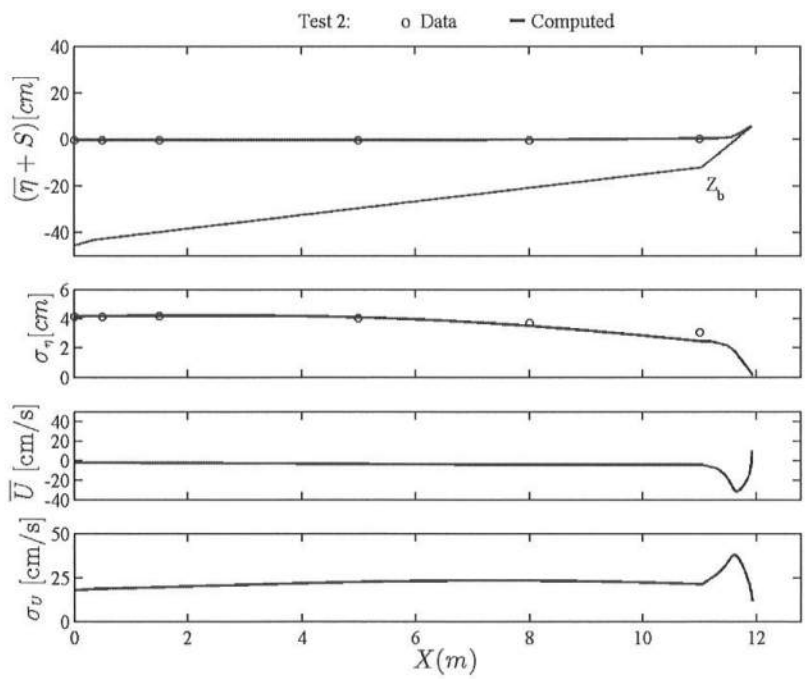

Fig. B.2: Test 2

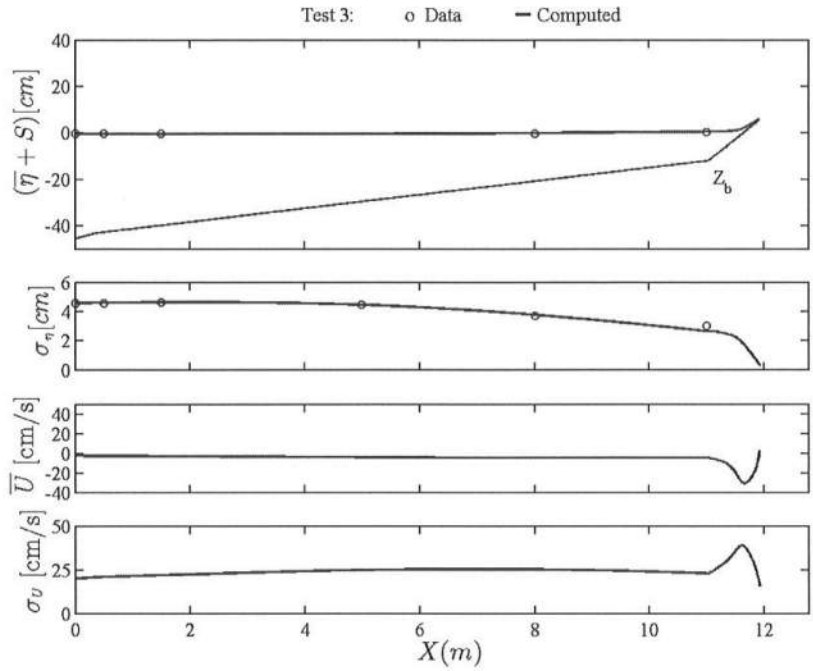

Fig. B.3: Test 3

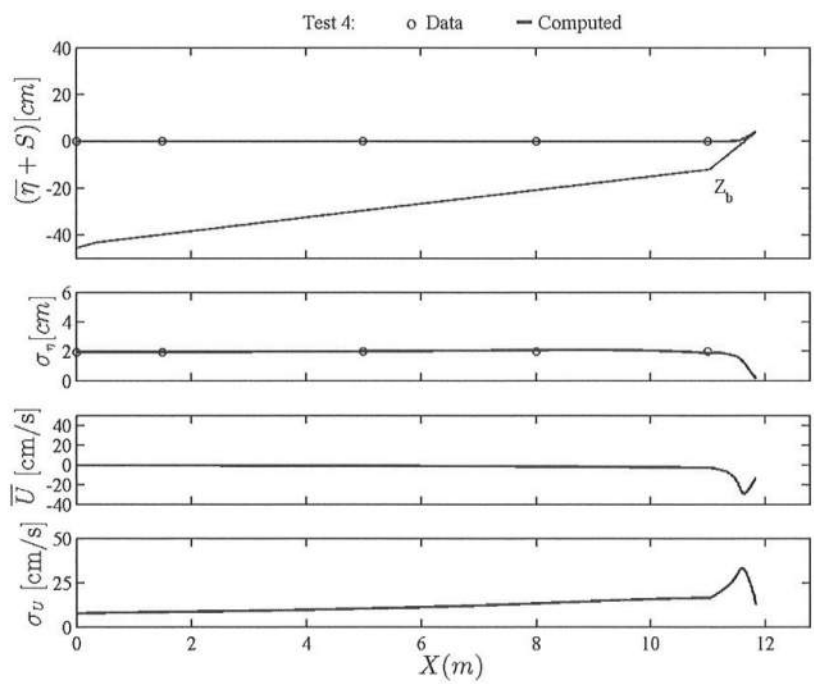

Fig. B.4: Test 4

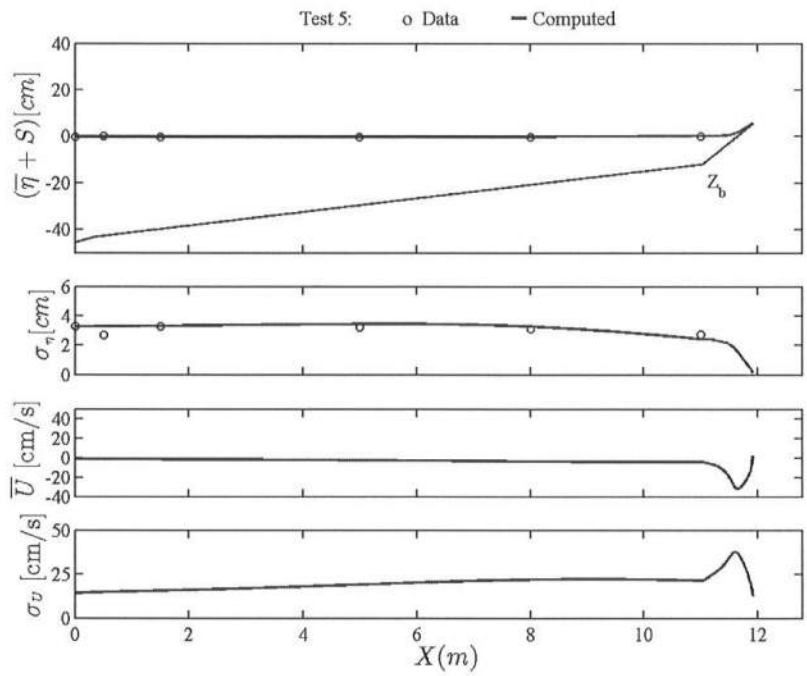

Fig. B.5: Test 5

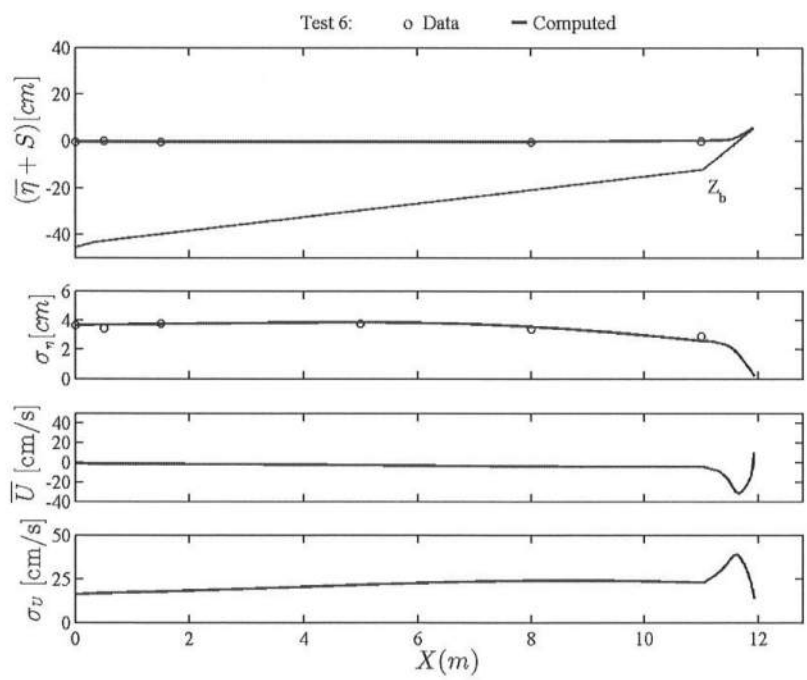

Fig. B.6: Test 6

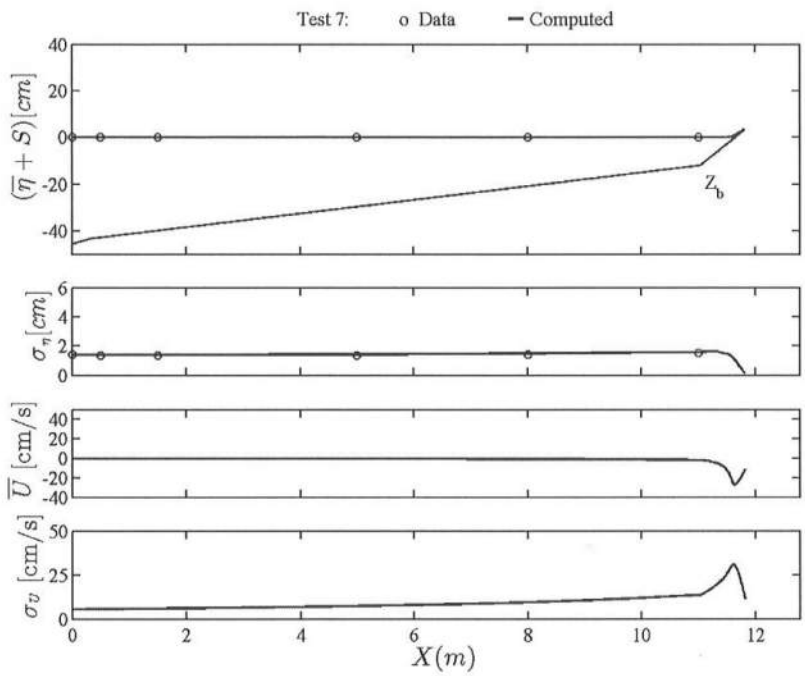

Fig. B.7: Test 7

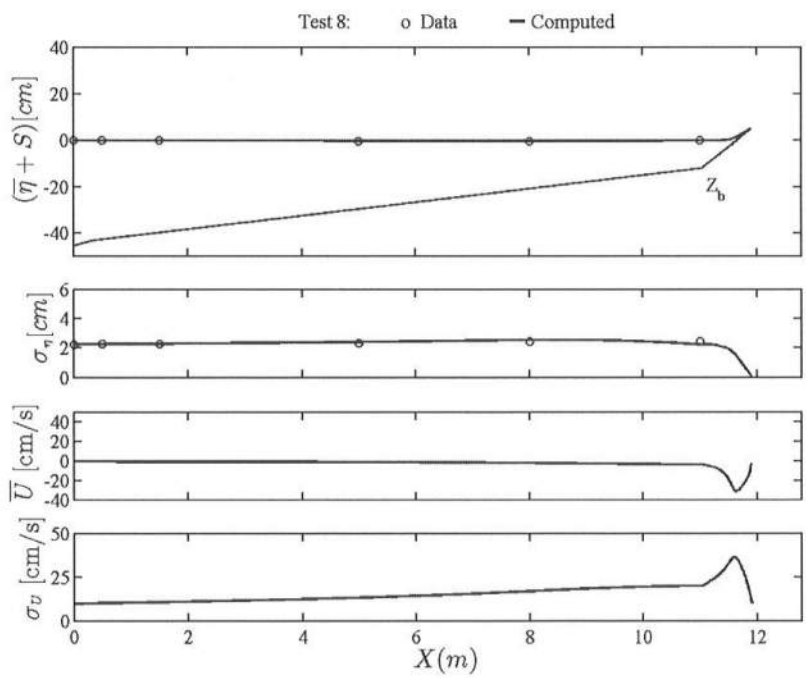

Fig. B.8: Test 8

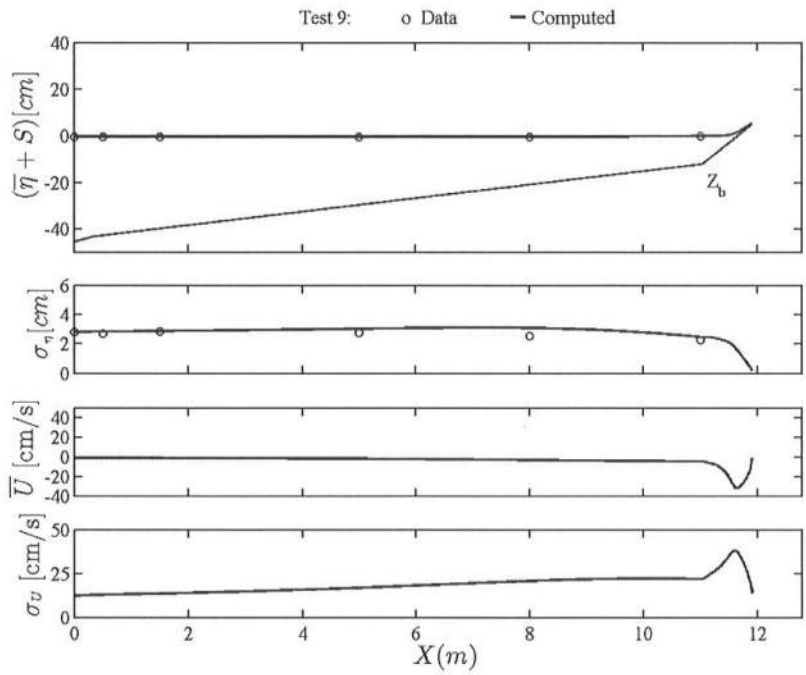

Fig. B.9: Test 9

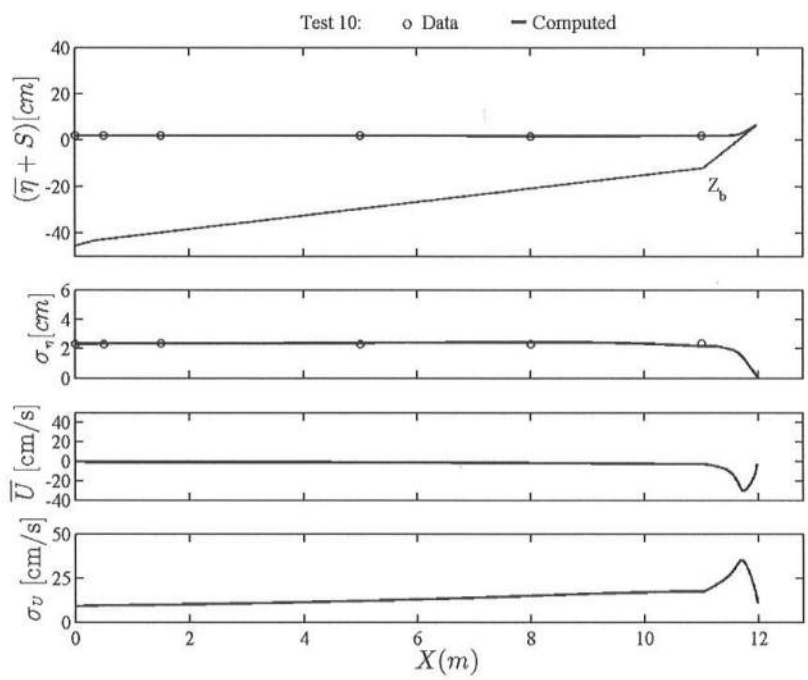

Fig. B.10: Test 10

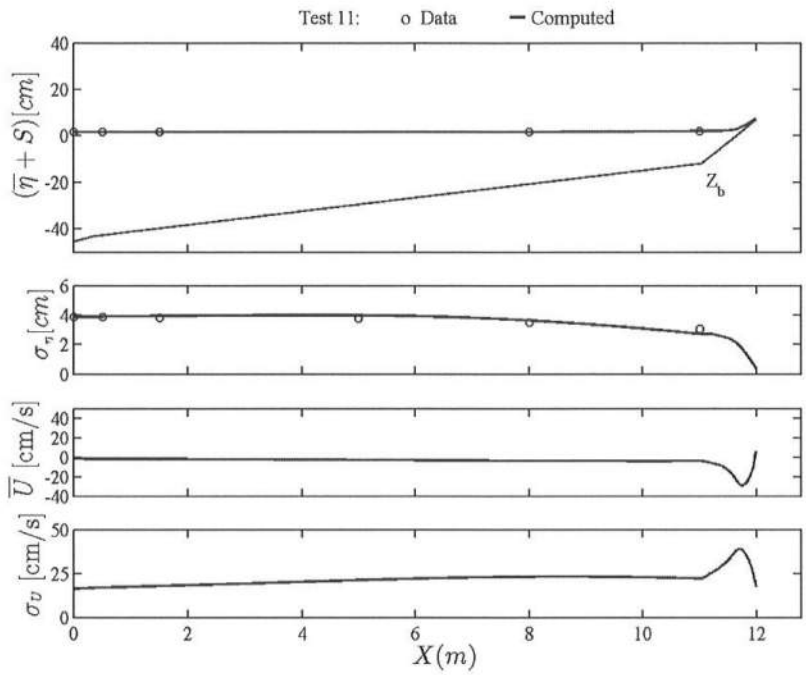

Fig. B.11: Test 11

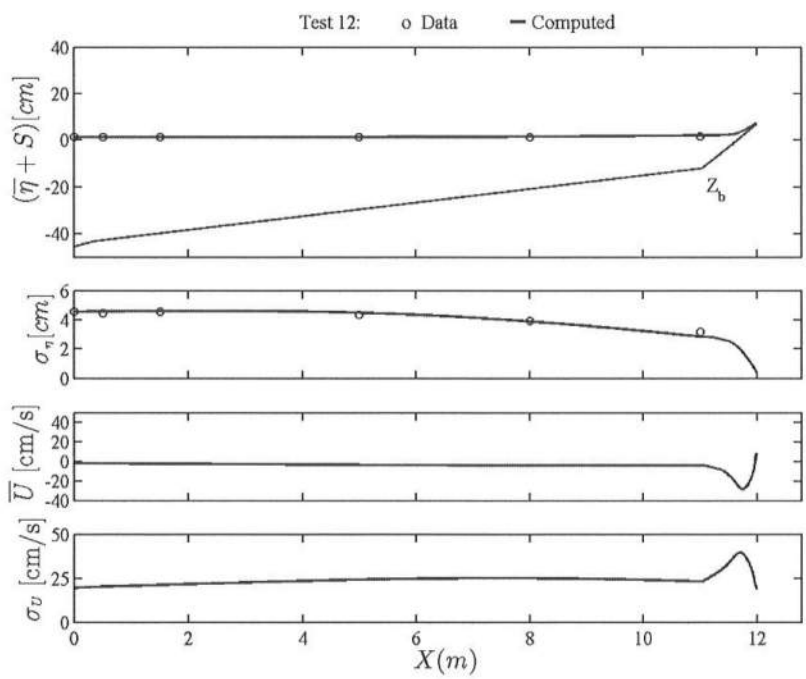

Fig. B.12: Test 12

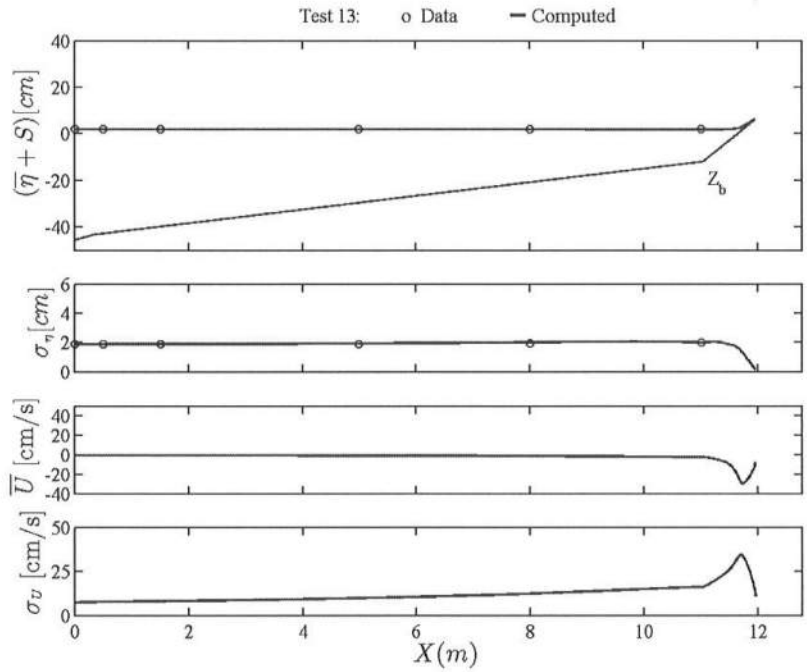

Fig. B.13: Test 13

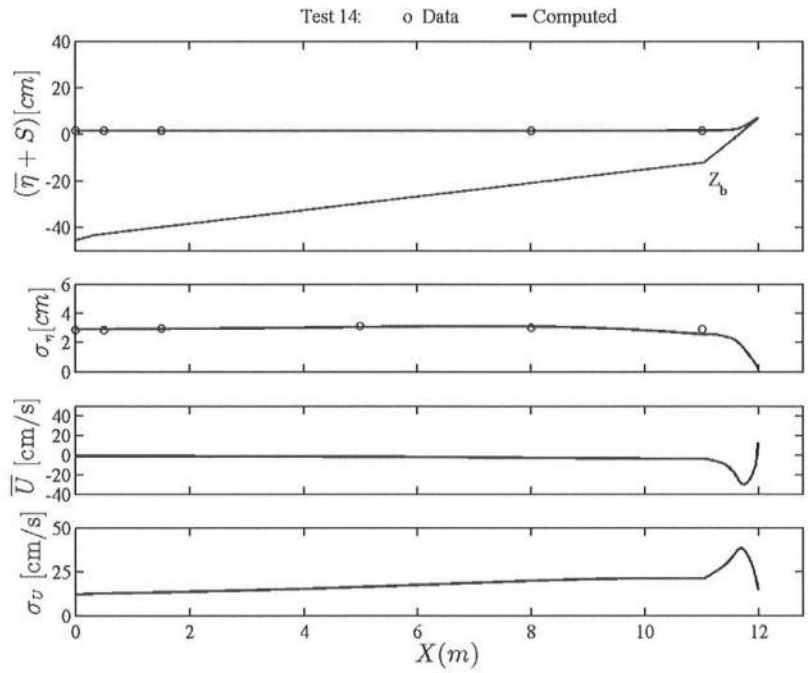

Fig. B.14: Test 14

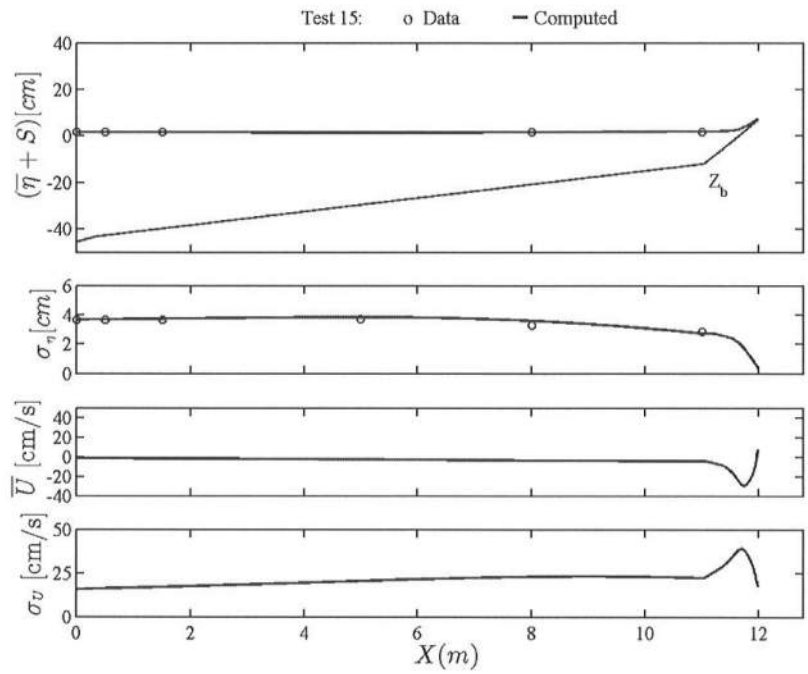

Fig. B.15: Test 15

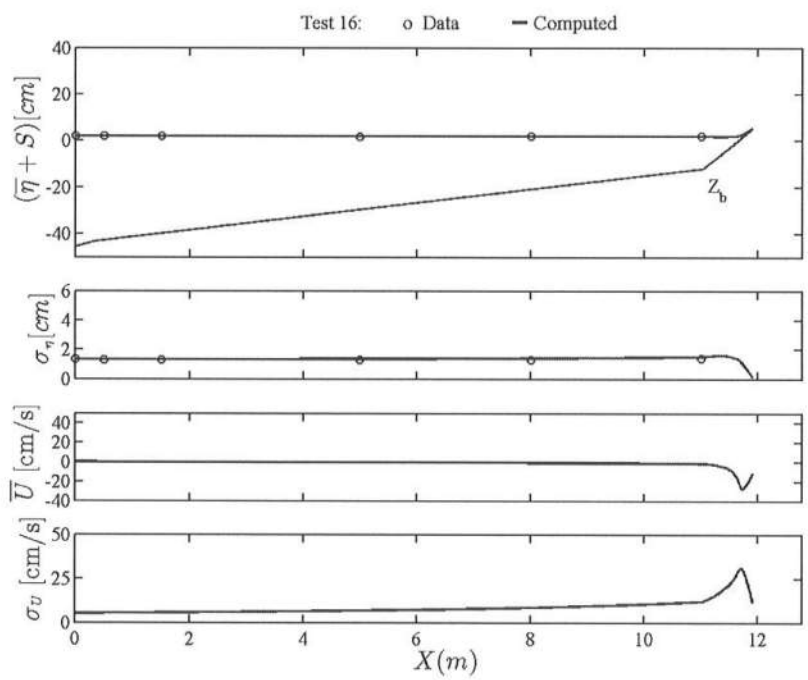

Fig. B.16: Test 16

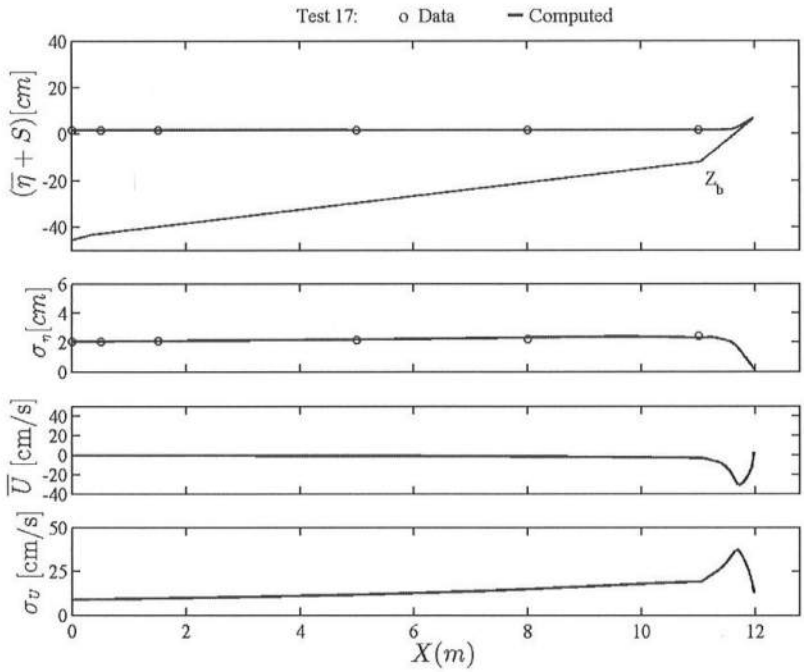

Fig. B.17: Test 17

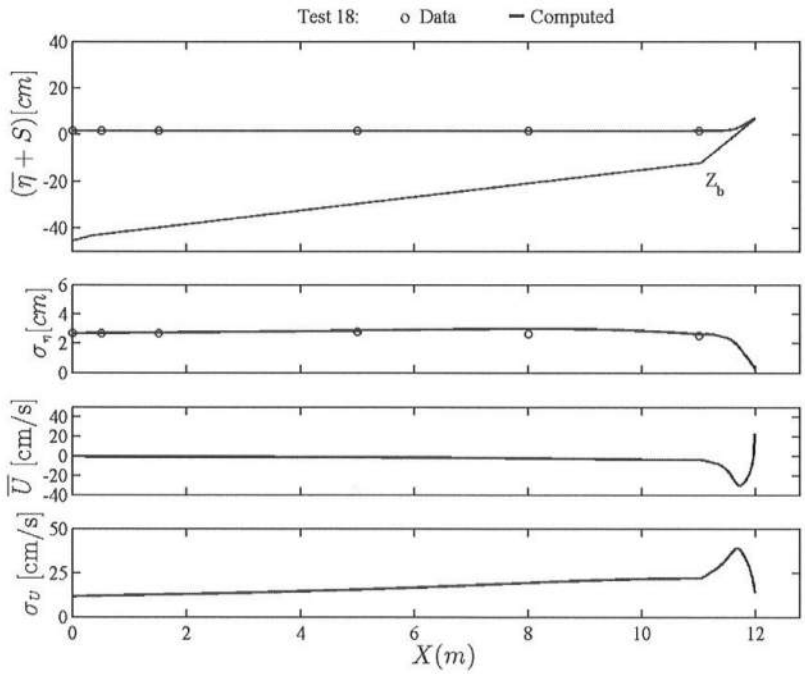

Fig. B.18: Test 18

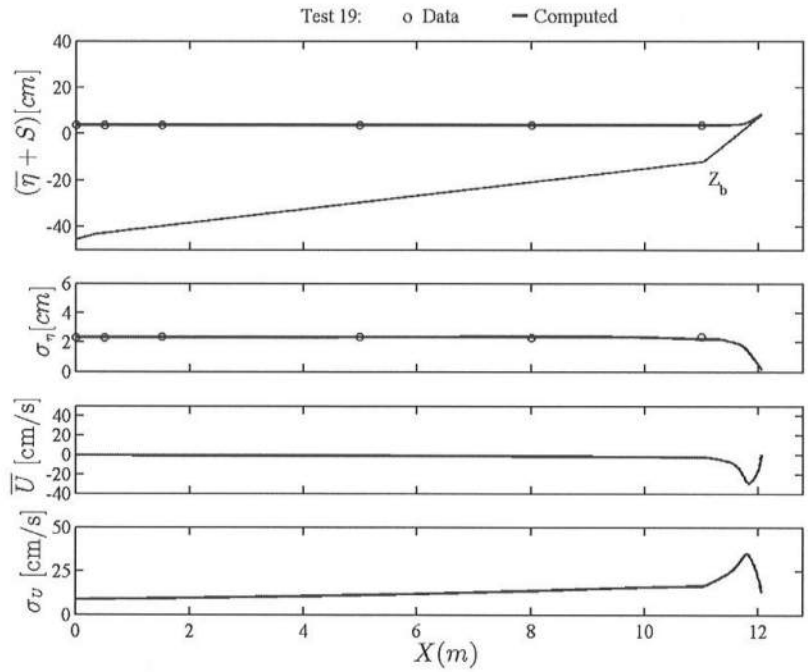

Fig. B.19: Test 19

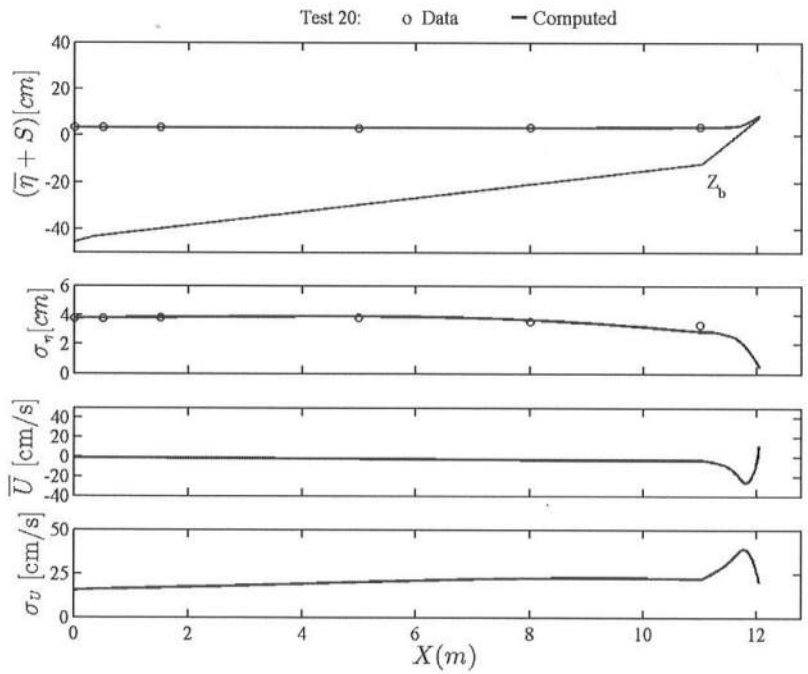

Fig. B.20: Test 20

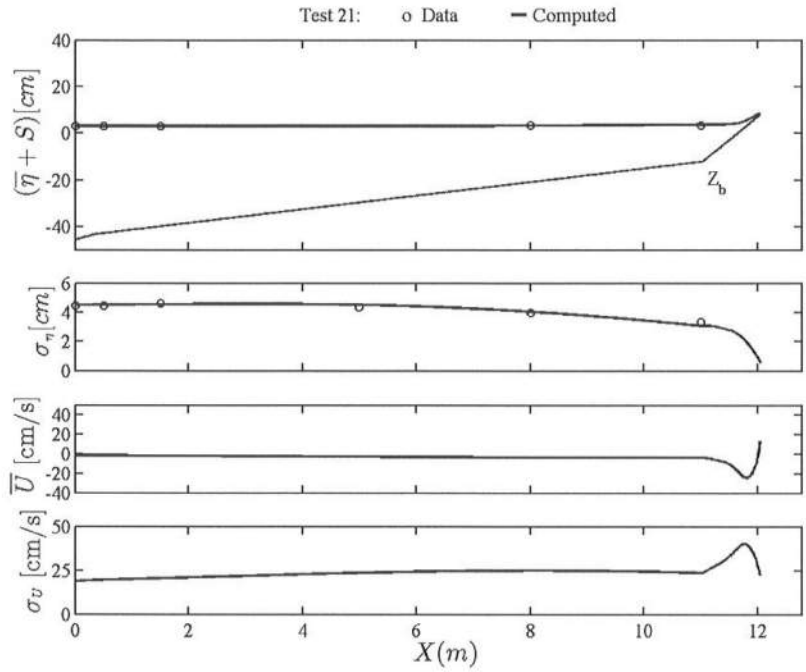

Fig. B.21: Test 21

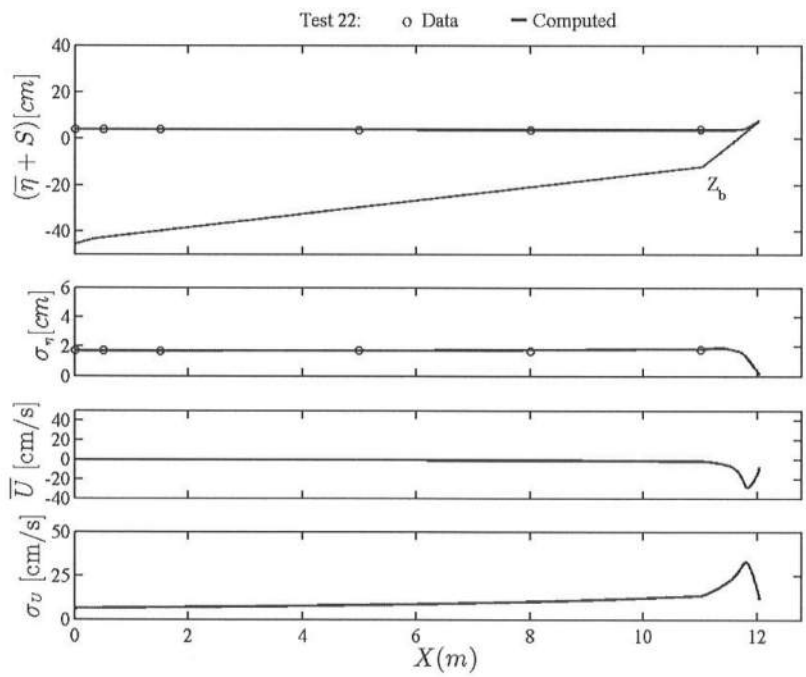

Fig. B.22: Test 22

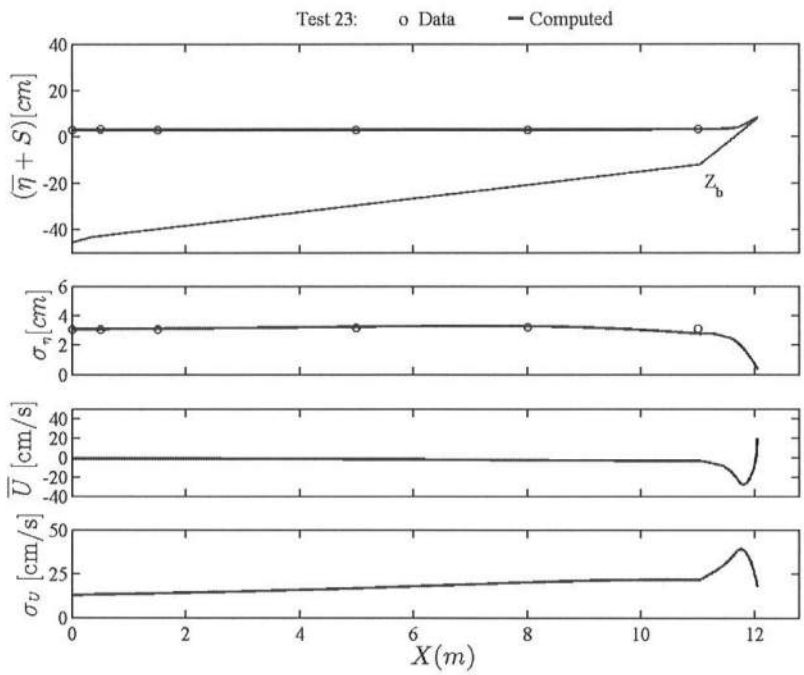

Fig. B.23 Test 23

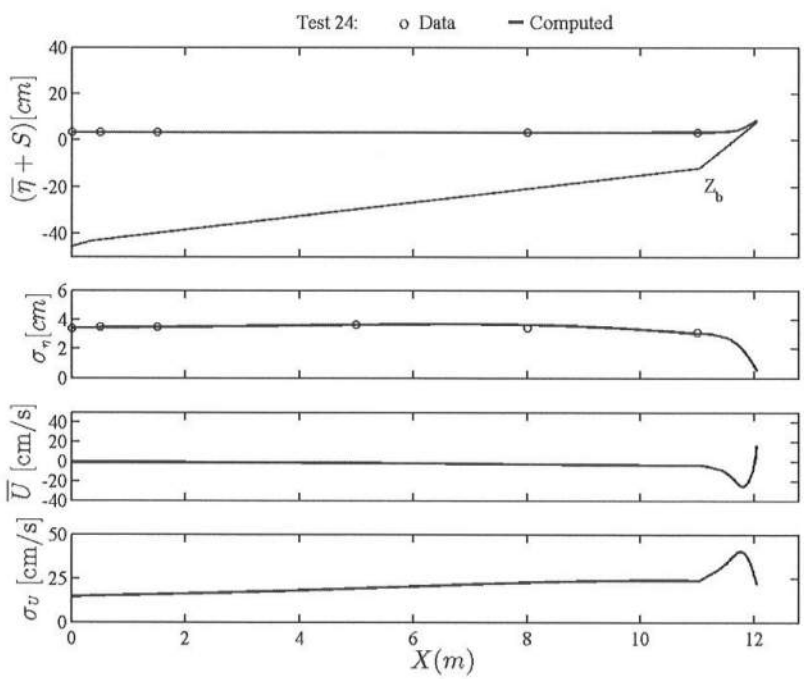

Fig. B.24 Test 24

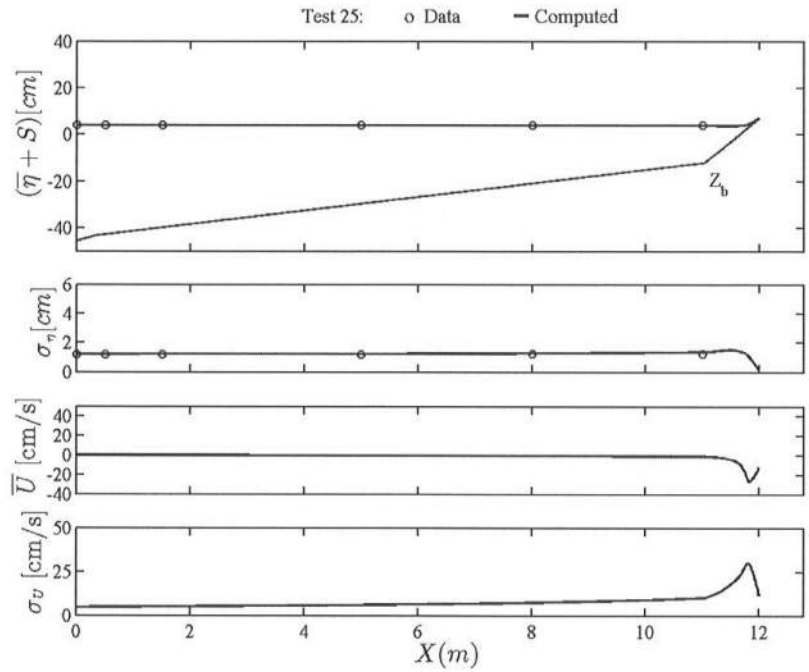

Fig. B.25 Test 25

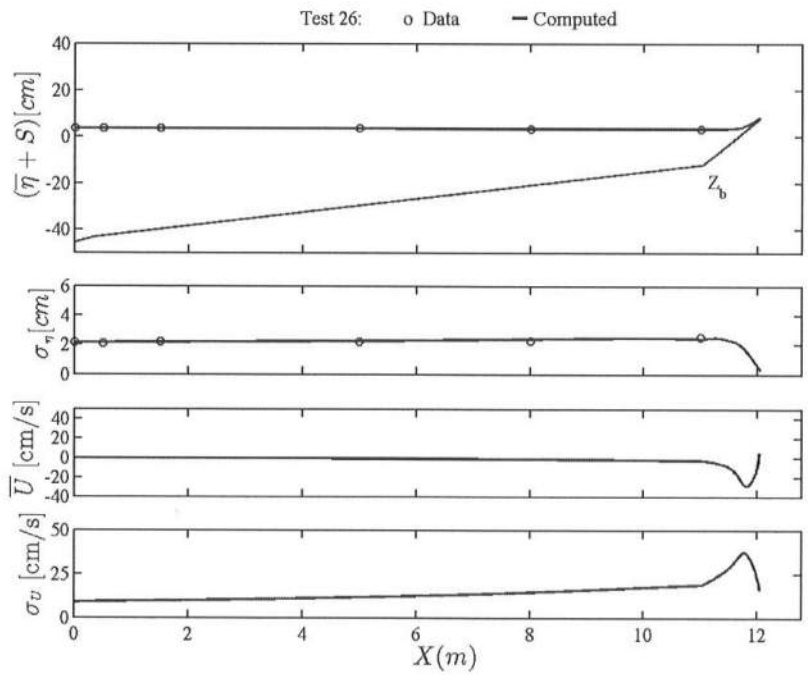

Fig. B.26 Test 26

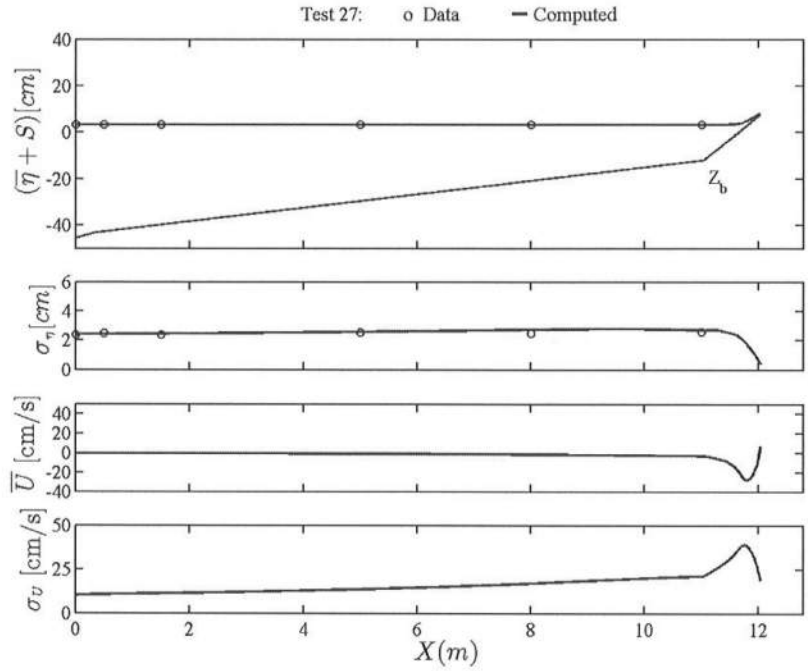

Fig. B.27: Test 27

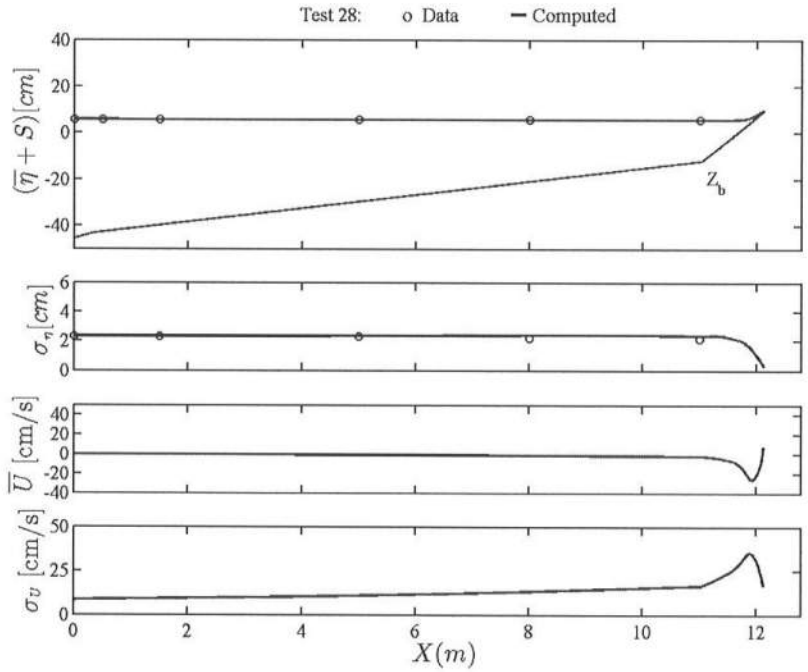

Fig. B.28: Test 28

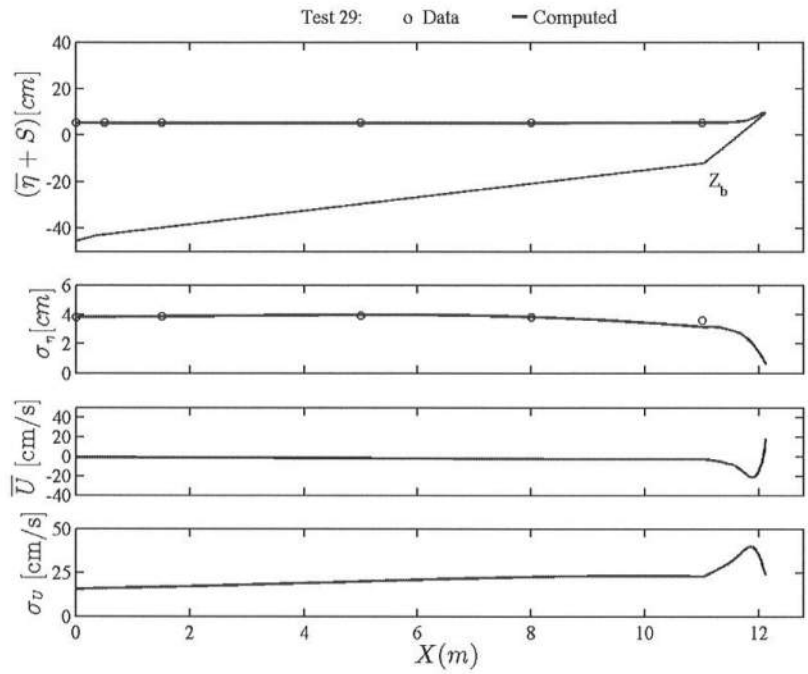

Fig. B.29: Test 29

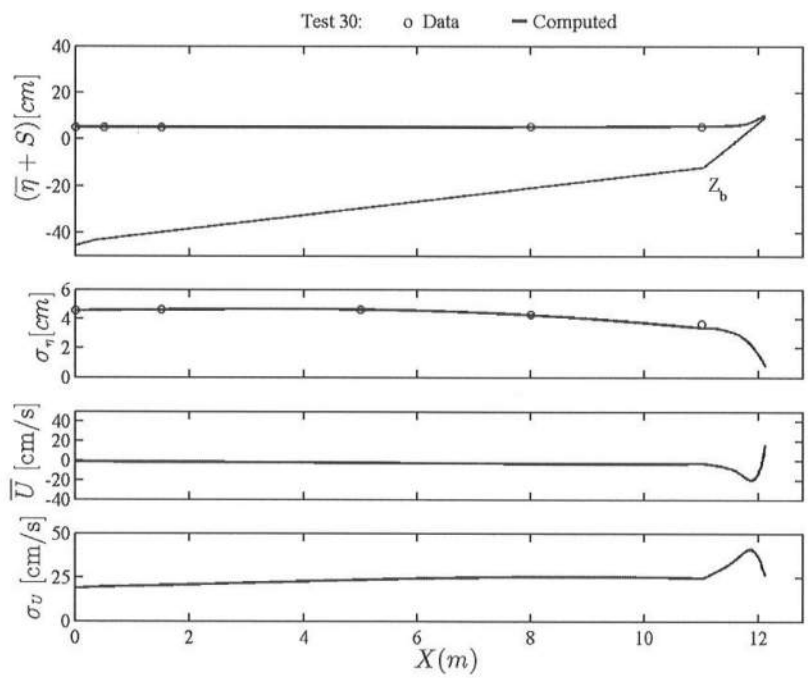

Fig. B.30: Test 30

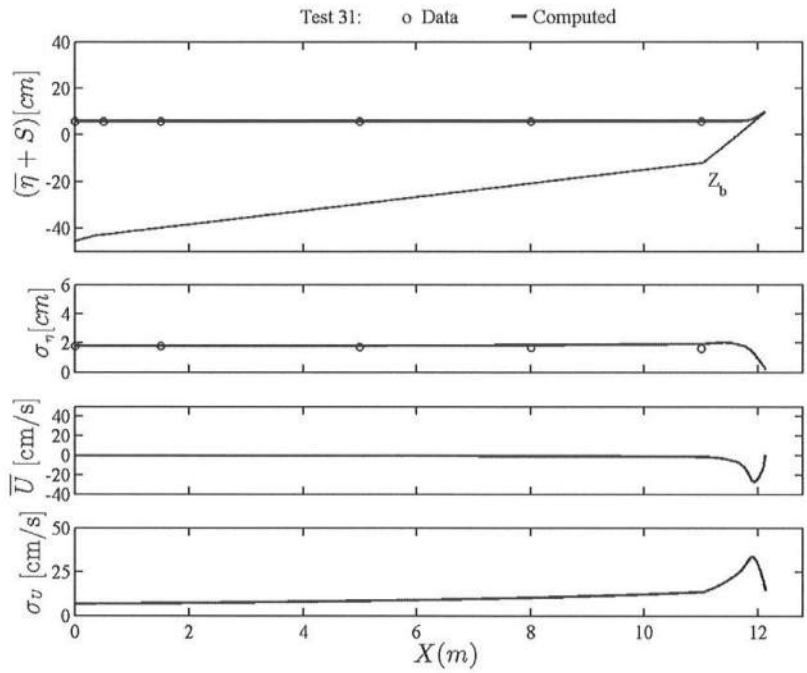

Fig. B.31: Test 31

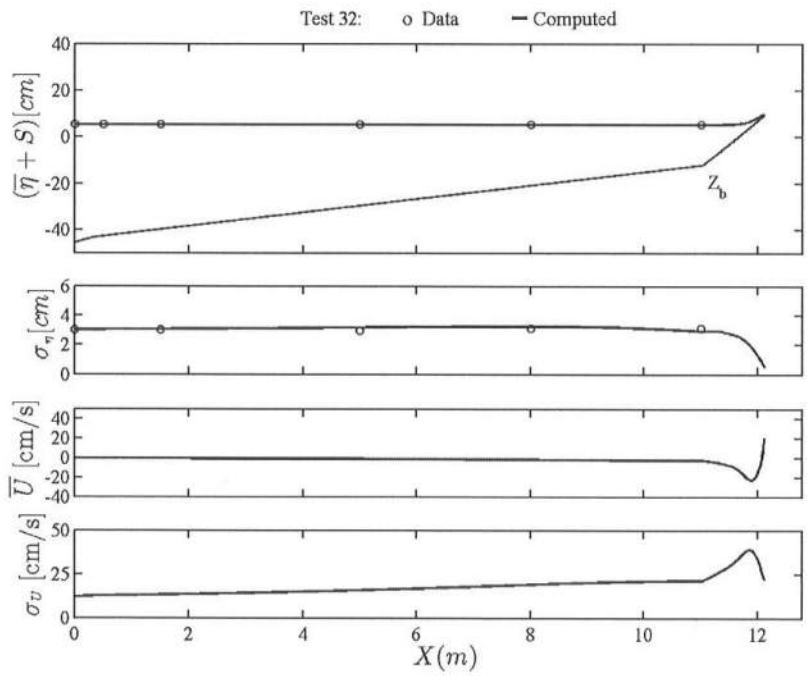

Fig. B.32: Test 32

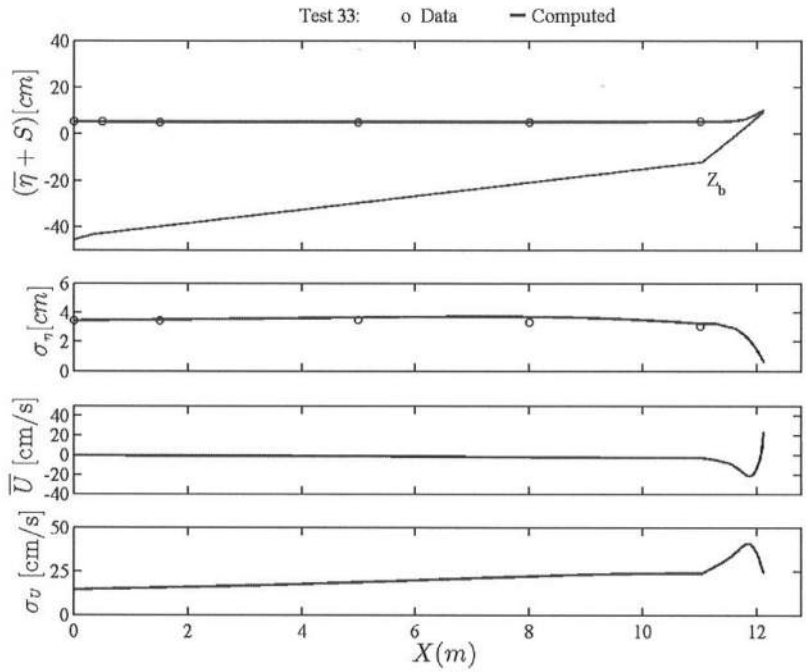

Fig. B.33: Test 33

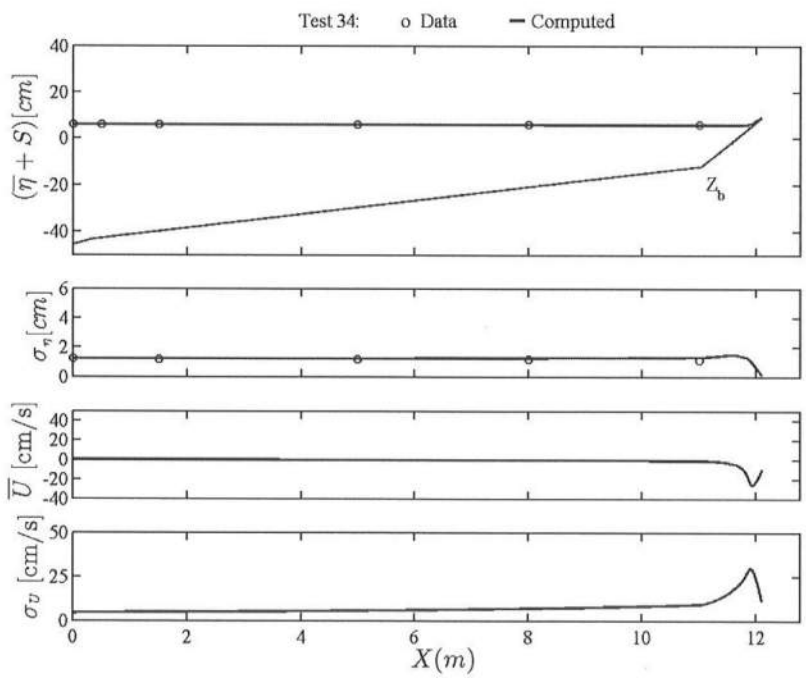

Fig. B.34: Test 34

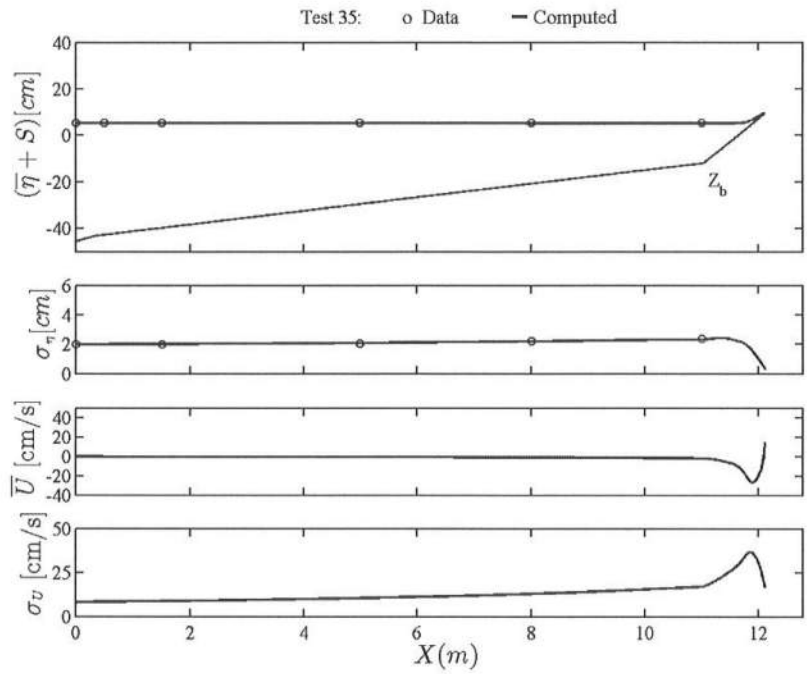

Fig. B.35: Test 35

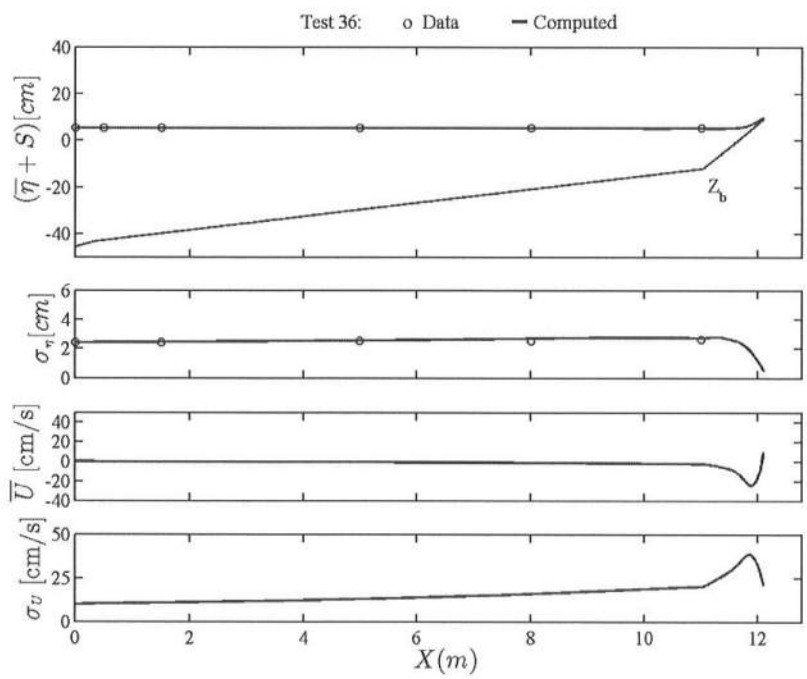

Fig. B.36: Test 36

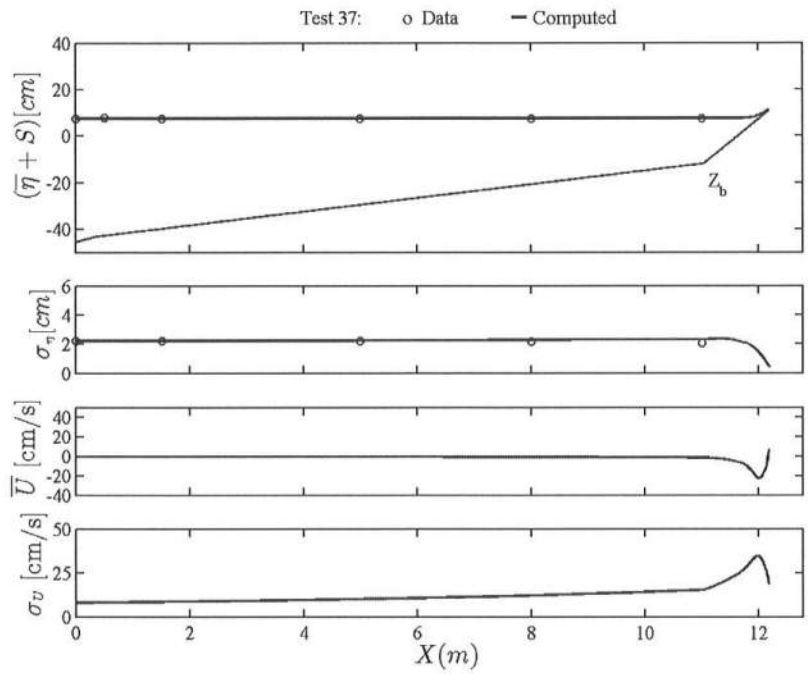

Fig. B.37: Test 37

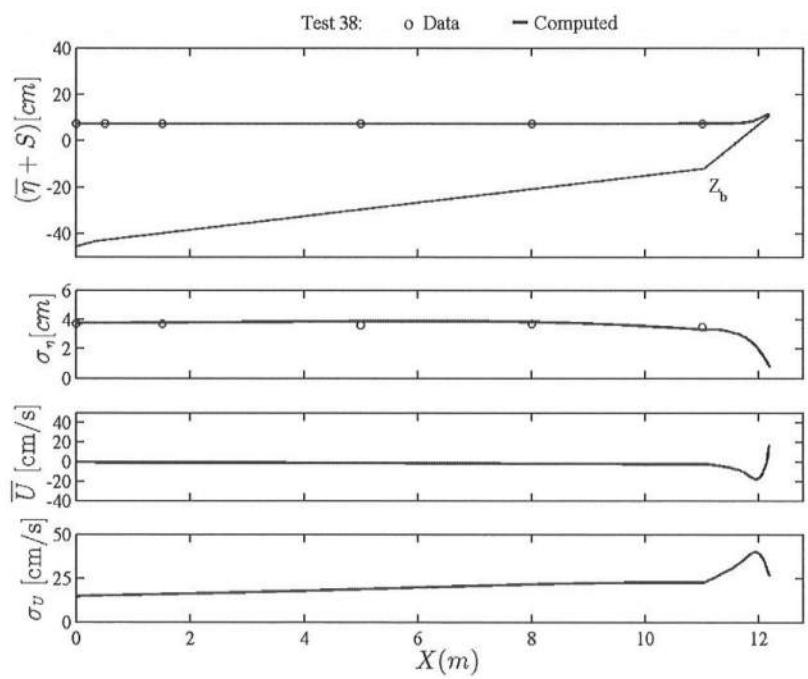

Fig. B.38: Test 38

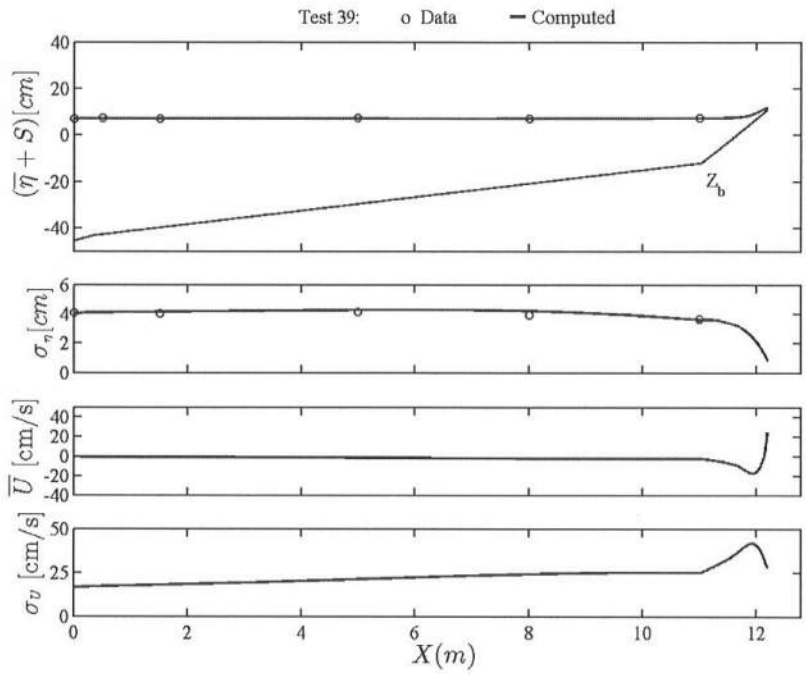

Fig. B.39: Test 39

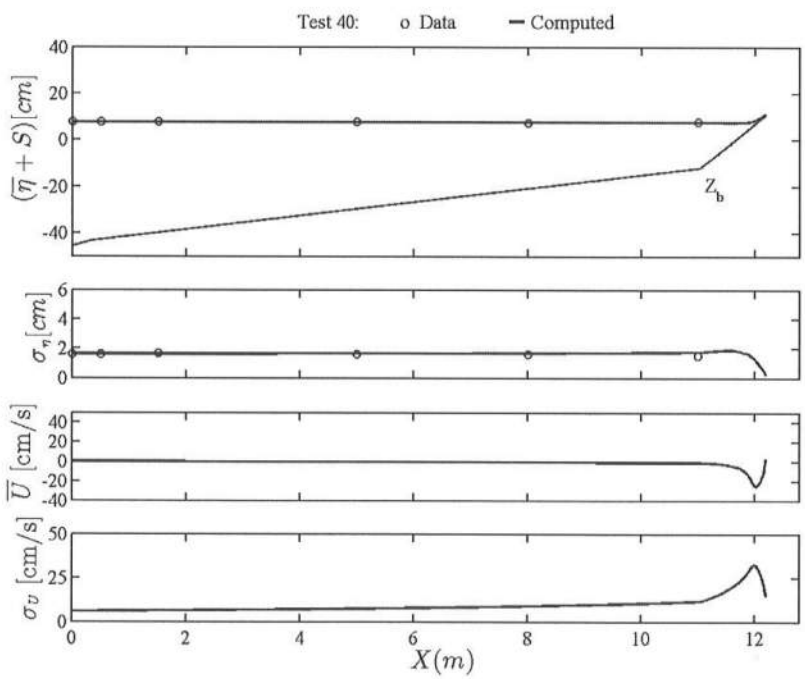

Fig. B.40: Test 40

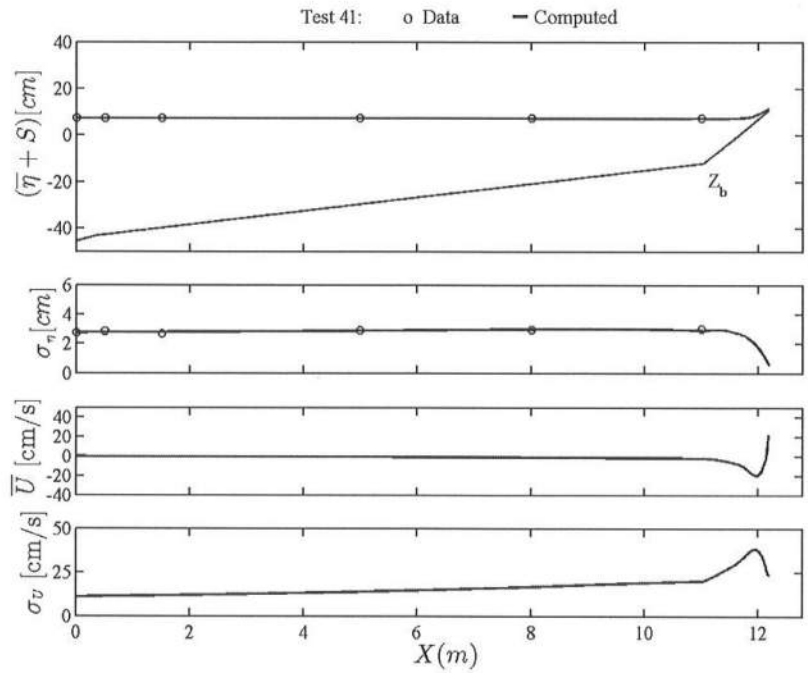

Fig. B.41: Test 41

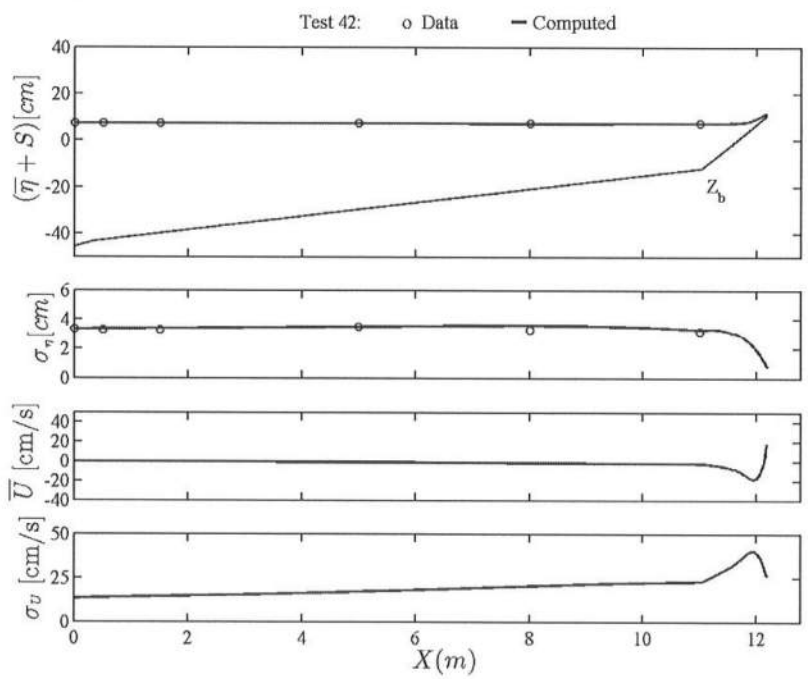

Fig. B.42: Test 42

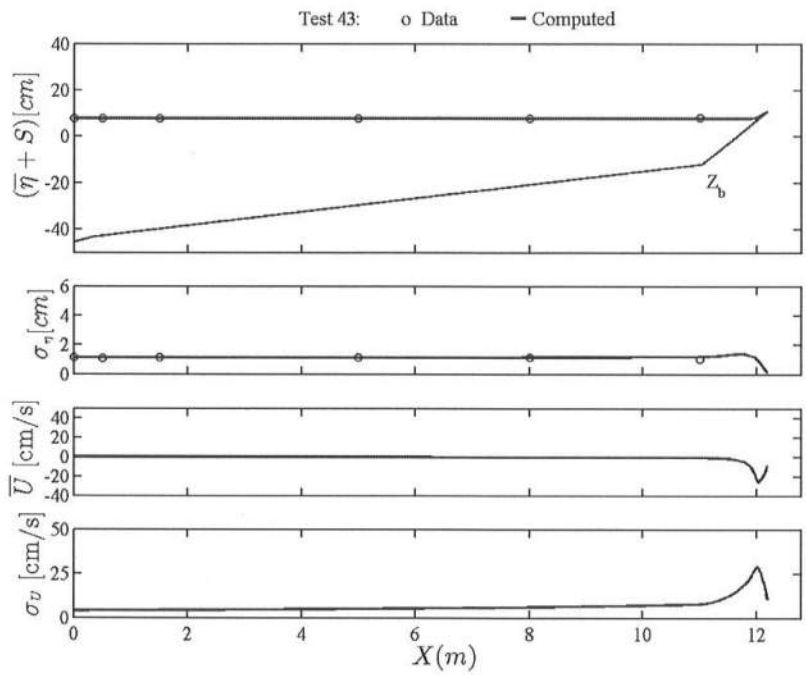

Fig. B.43: Test 43

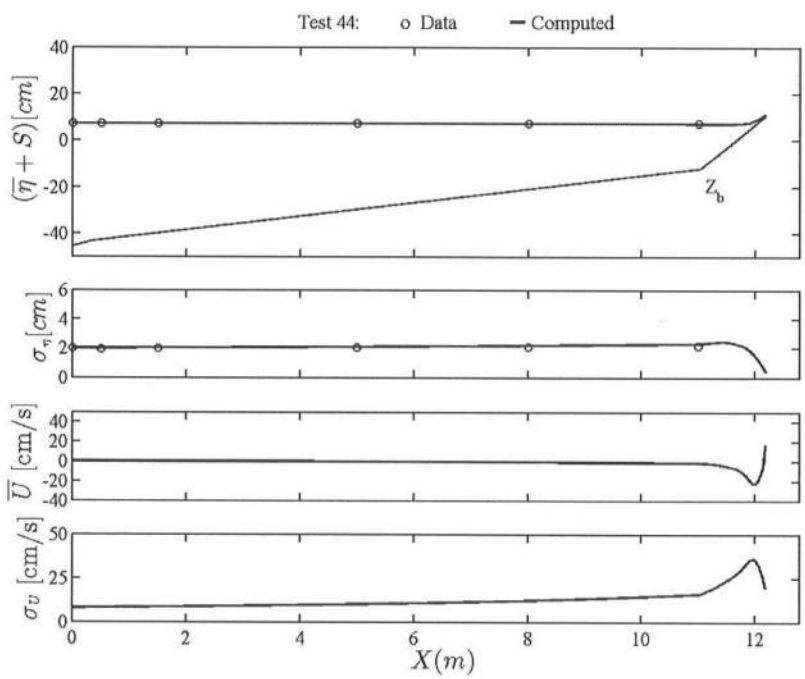

Fig. B.44: Test 44

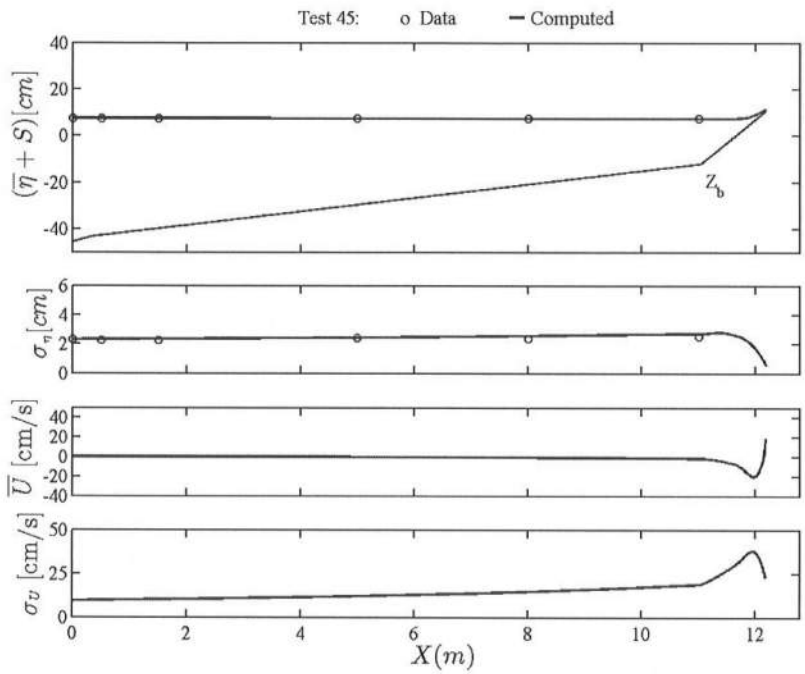

Fig. B.45: Test 45

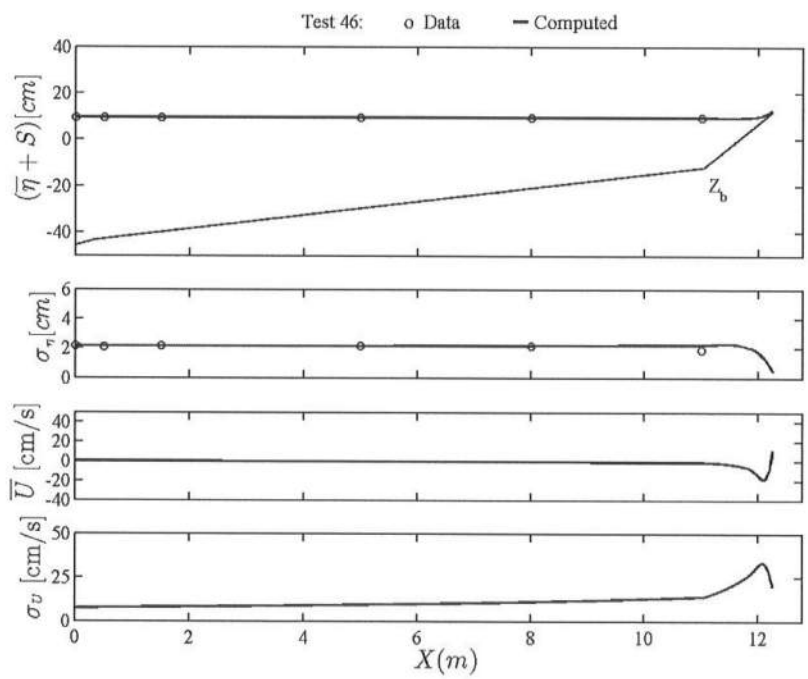

Fig. B.46: Test 46

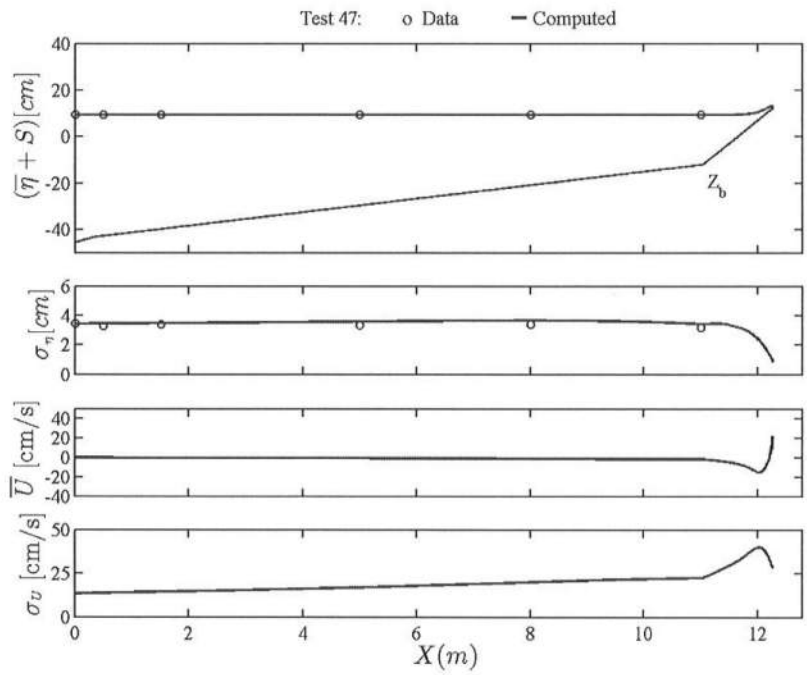

Fig. B.47: Test 47

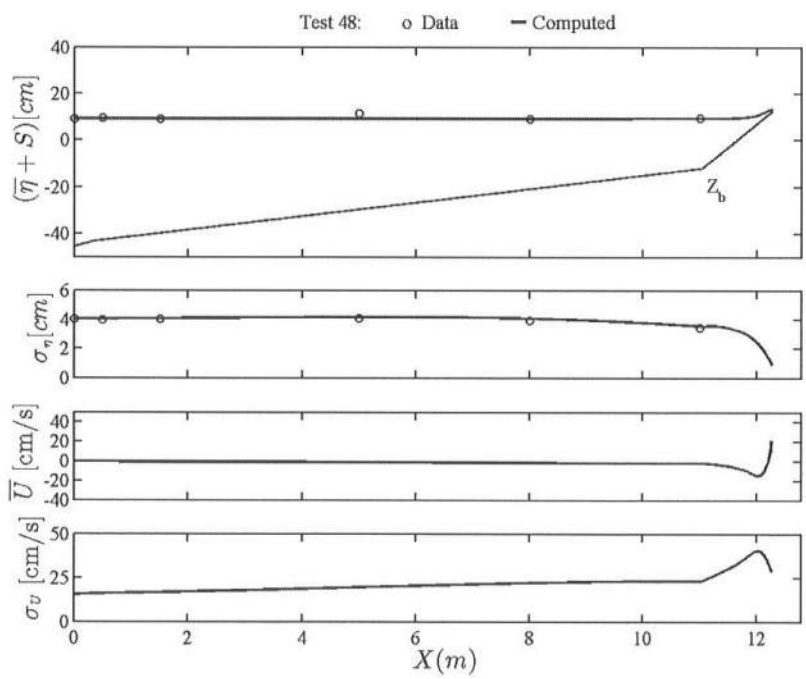

Fig. B.48: Test 48

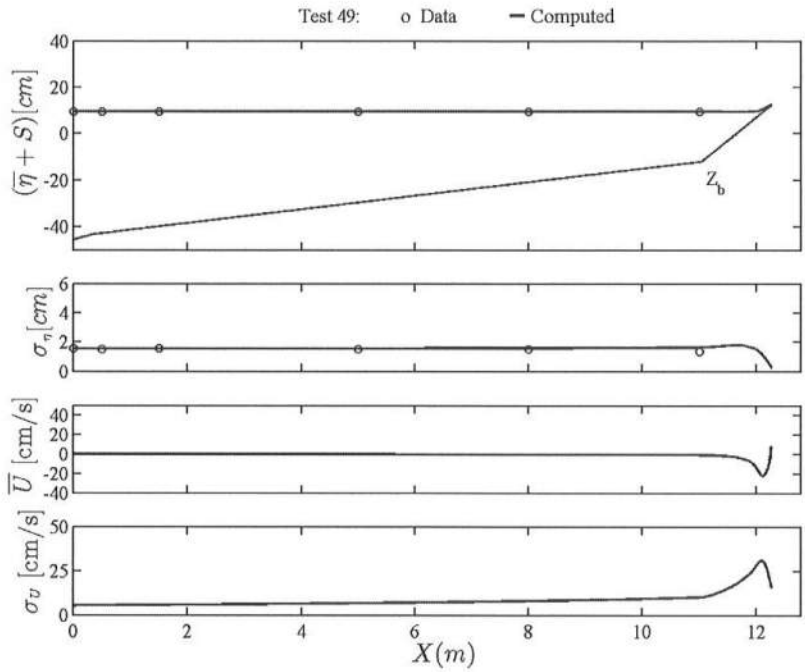

Fig. B.49: Test 49

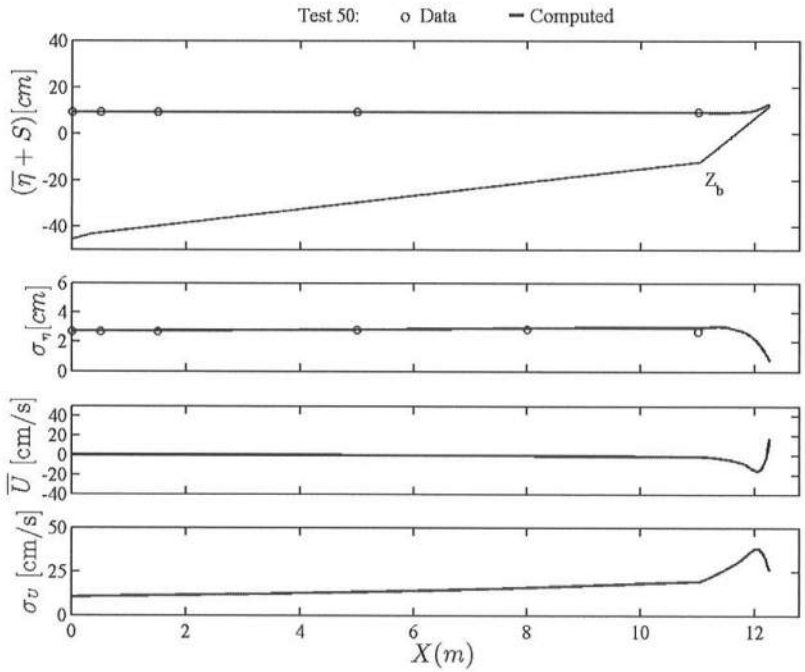

Fig. B.50: Test 50

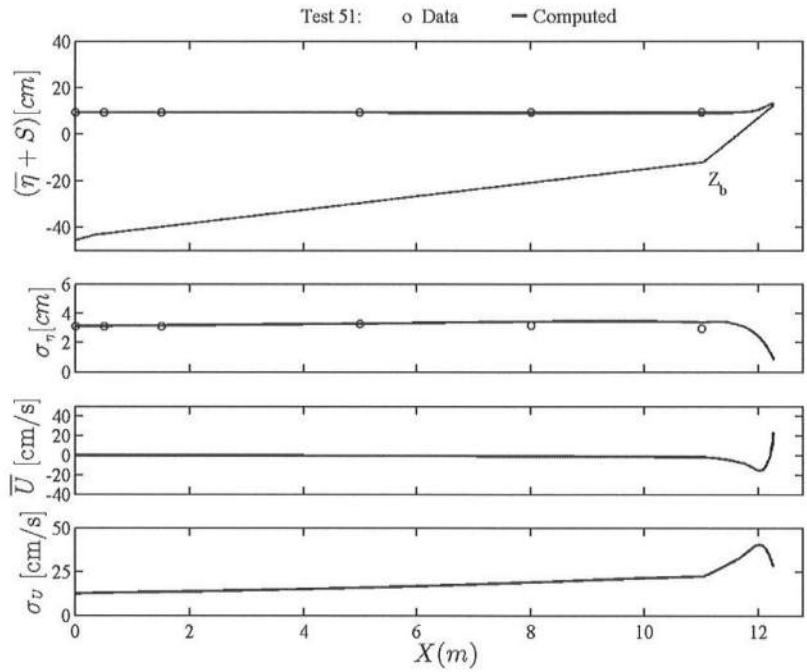

Fig. B.51: Test 51

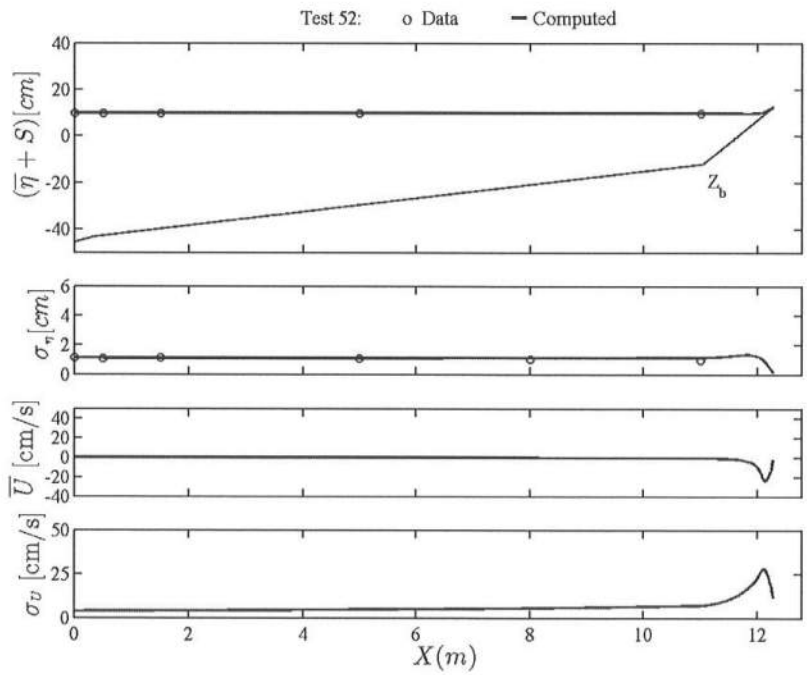

Fig. B.52: Test 52

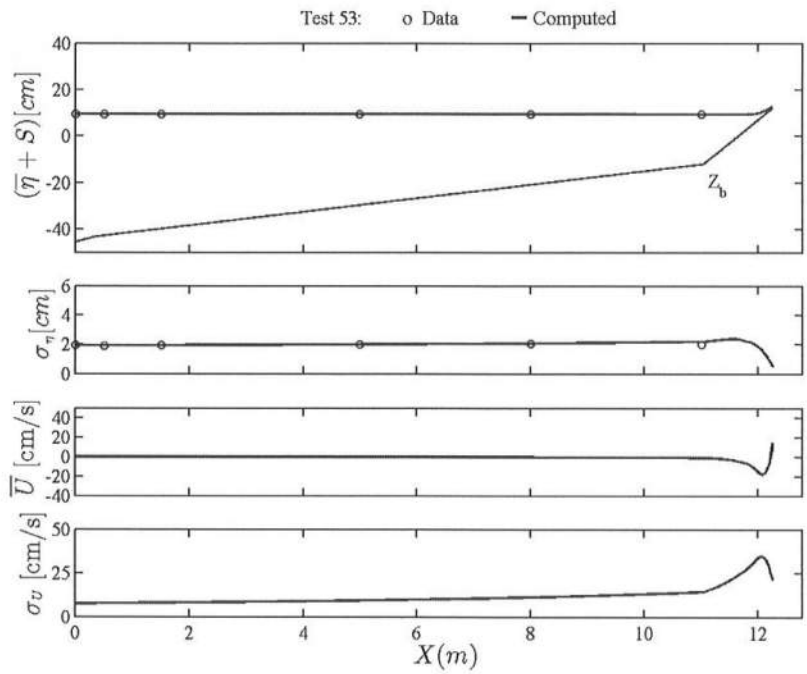

Fig. B.53: Test 53

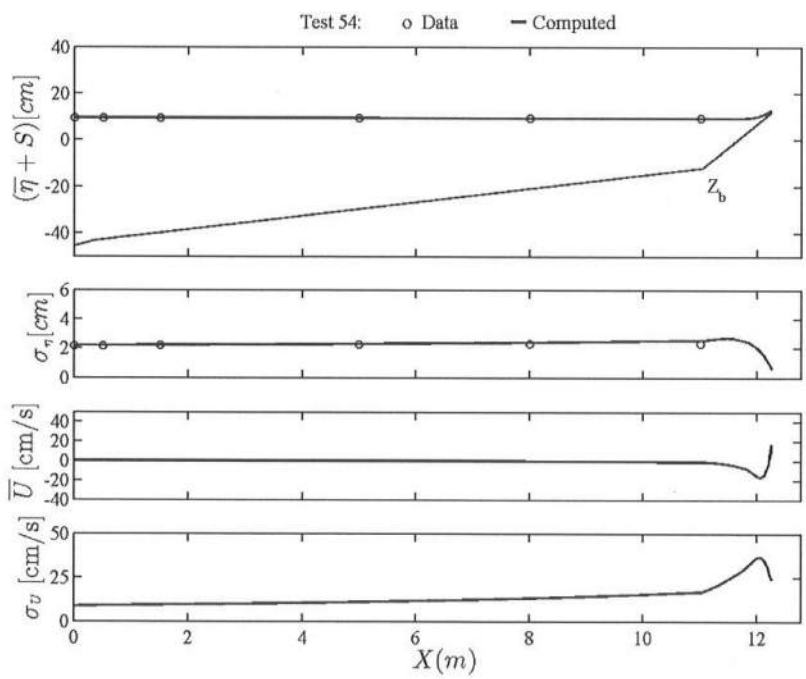

Fig. B.54: Test 54

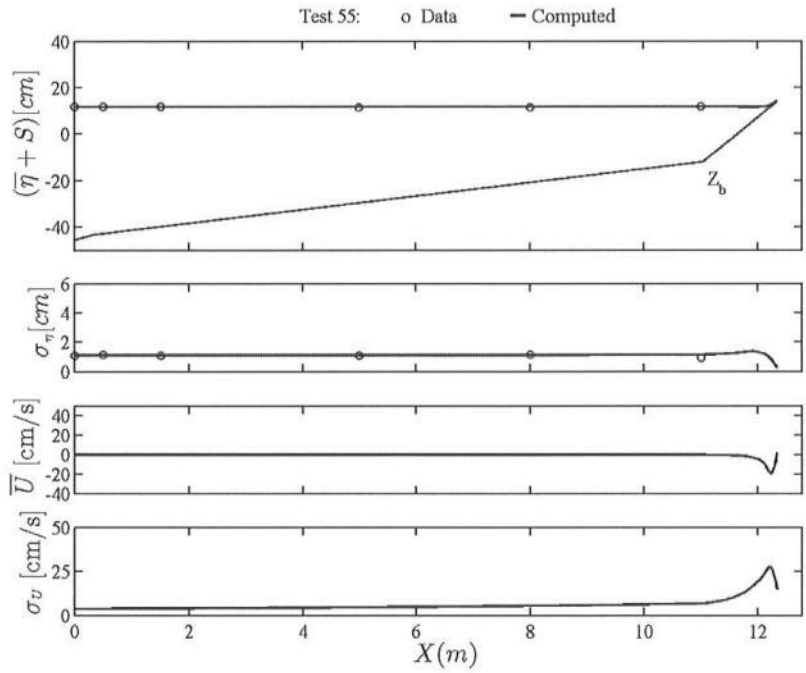

Fig. B.55: Test 55

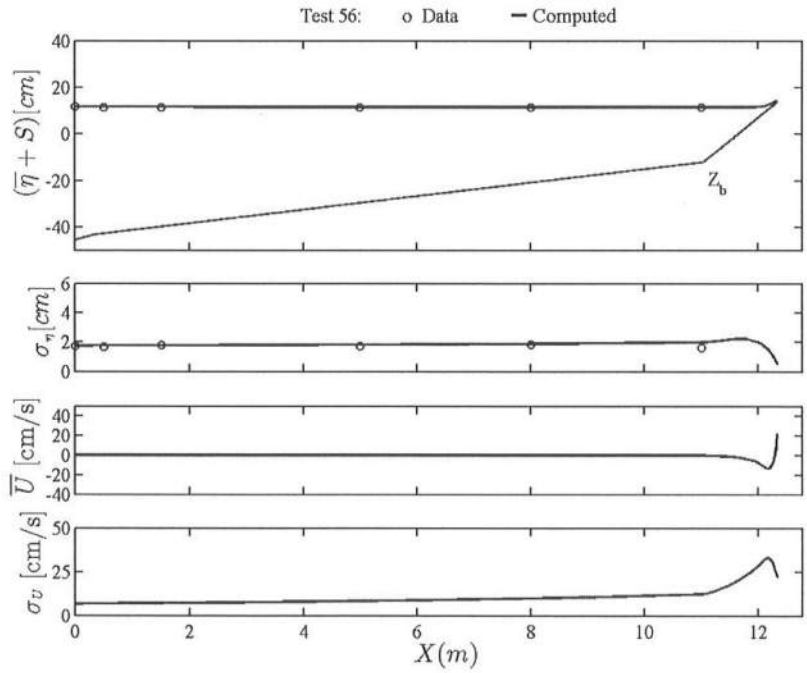

Fig. B.56: Test 56

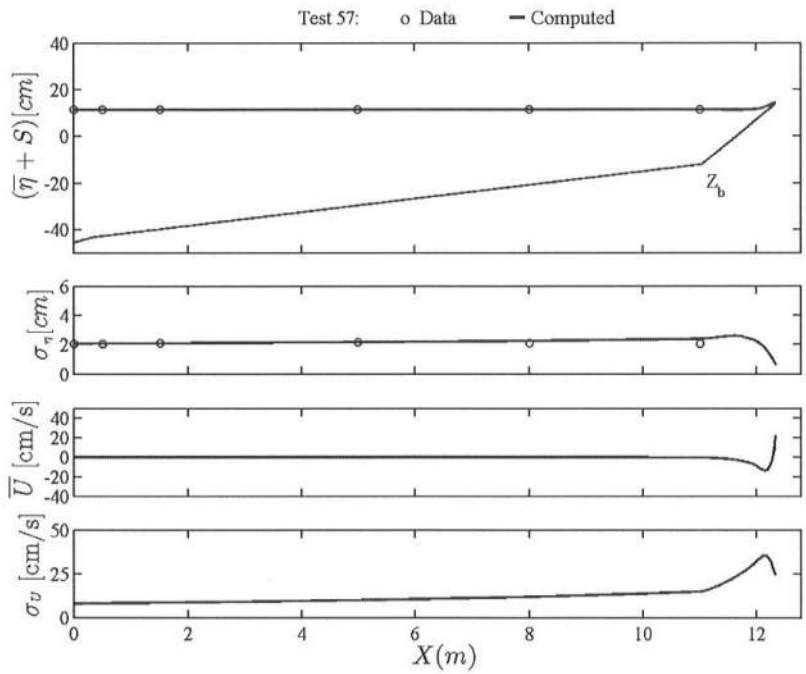

Fig. B.57: Test 57

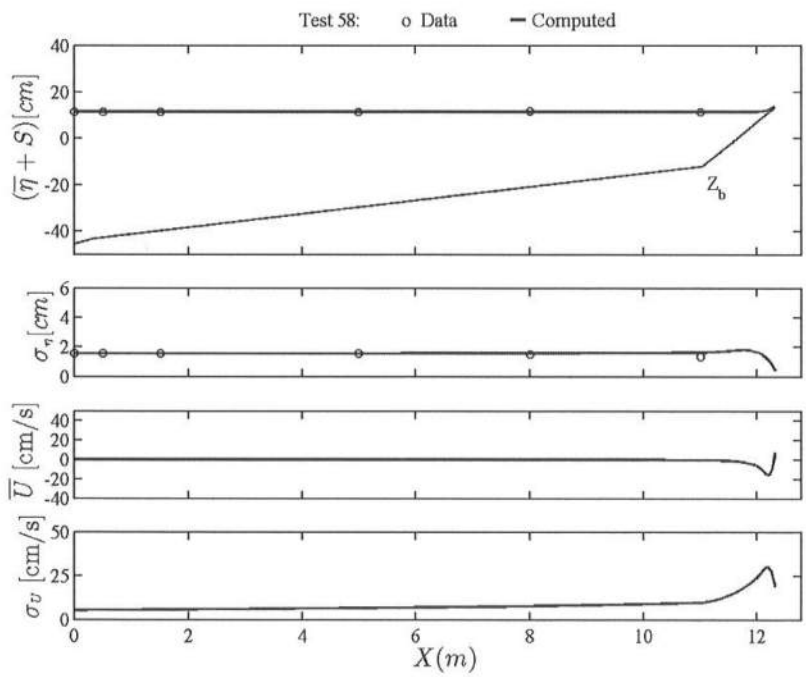

Fig. B.58: Test 58

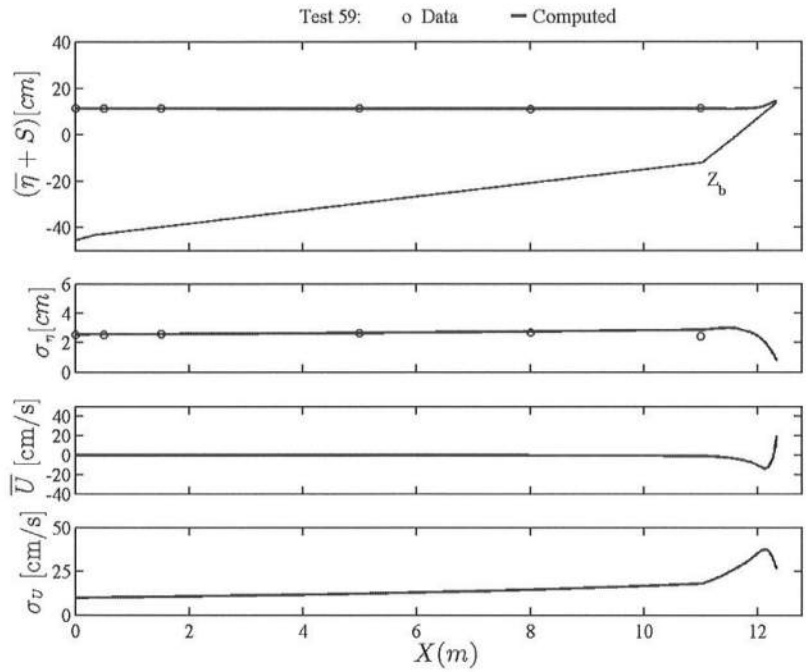

Fig. B.59: Test 59

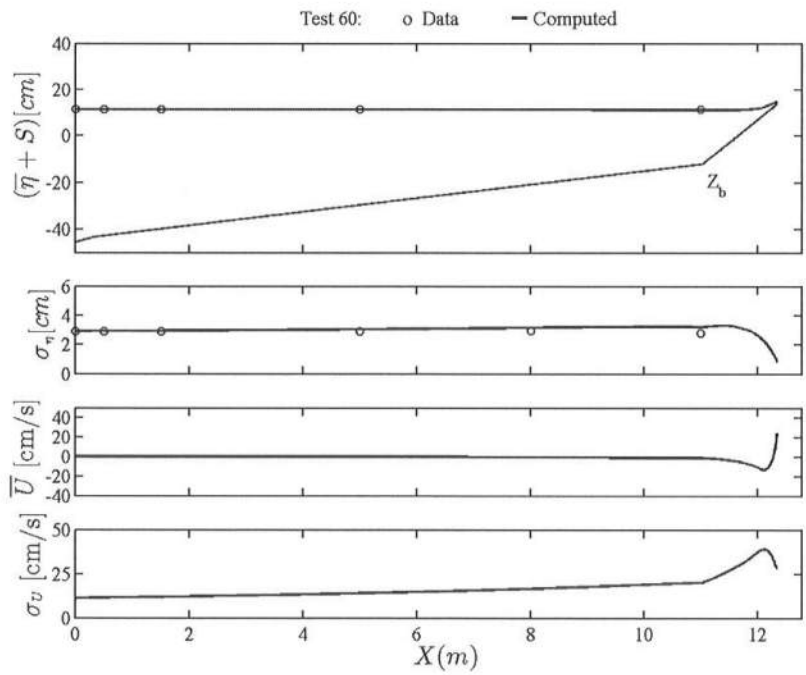

Fig. B.60: Test 60

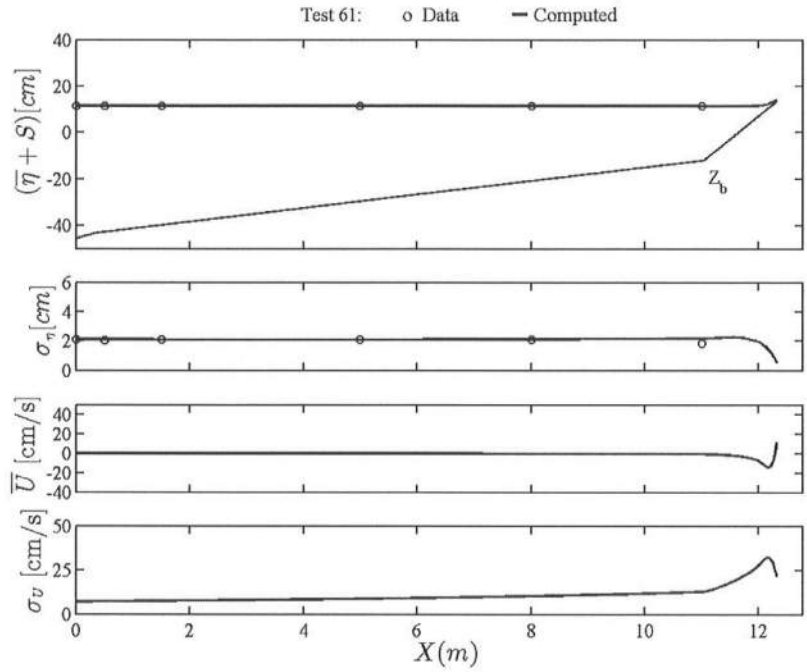

Fig. B.61: Test 61

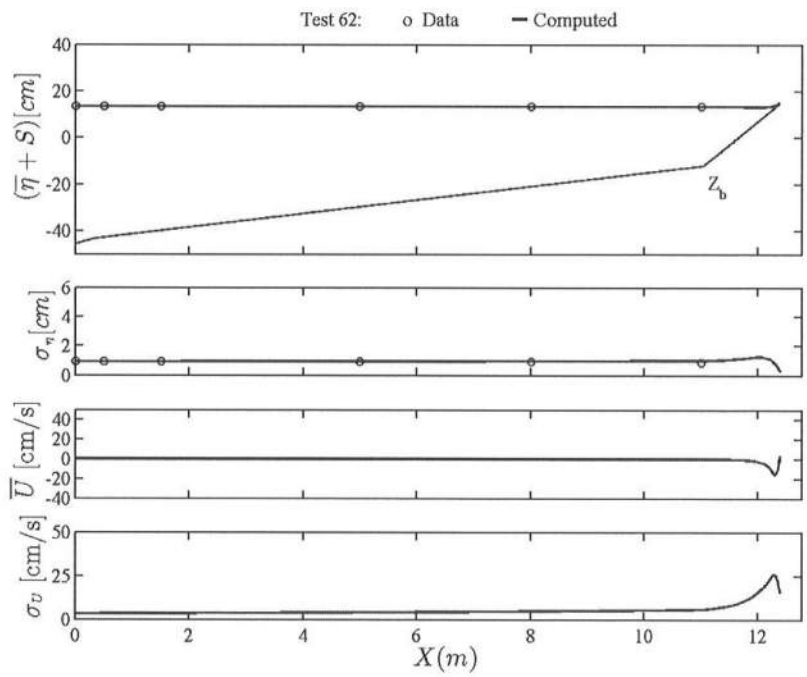

Fig. B.62: Test 62

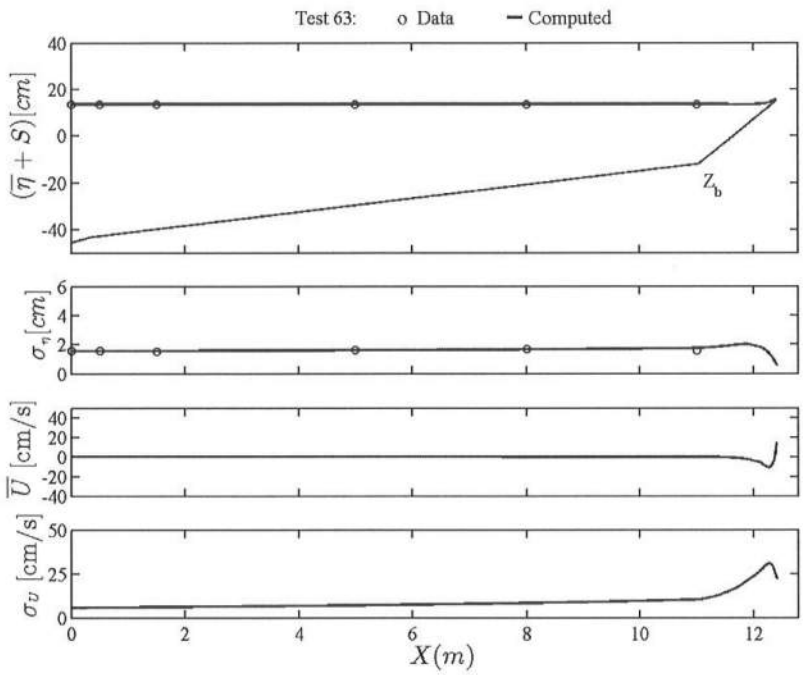

Fig. B.63: Test 63

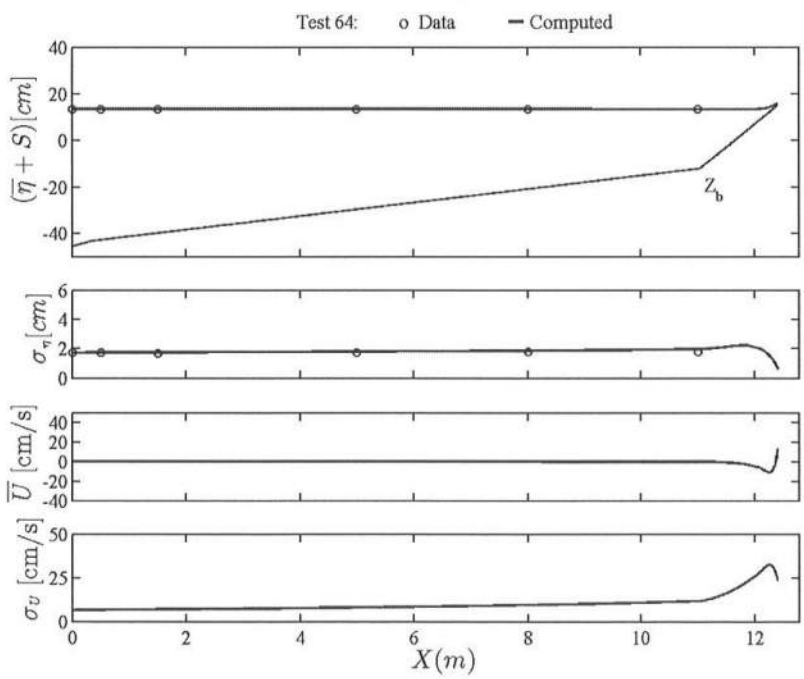

Fig. B.64: Test 64

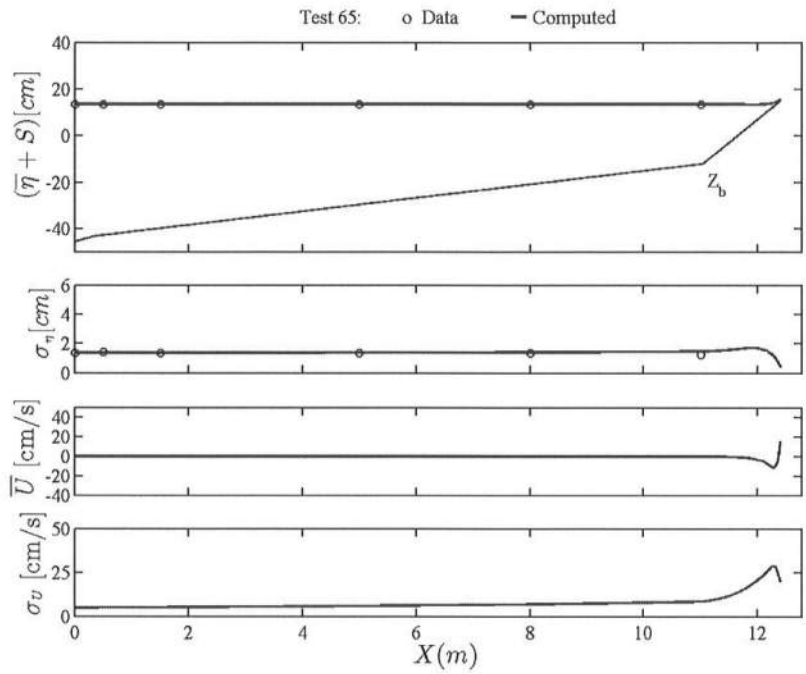

Fig. B.65: Test 65

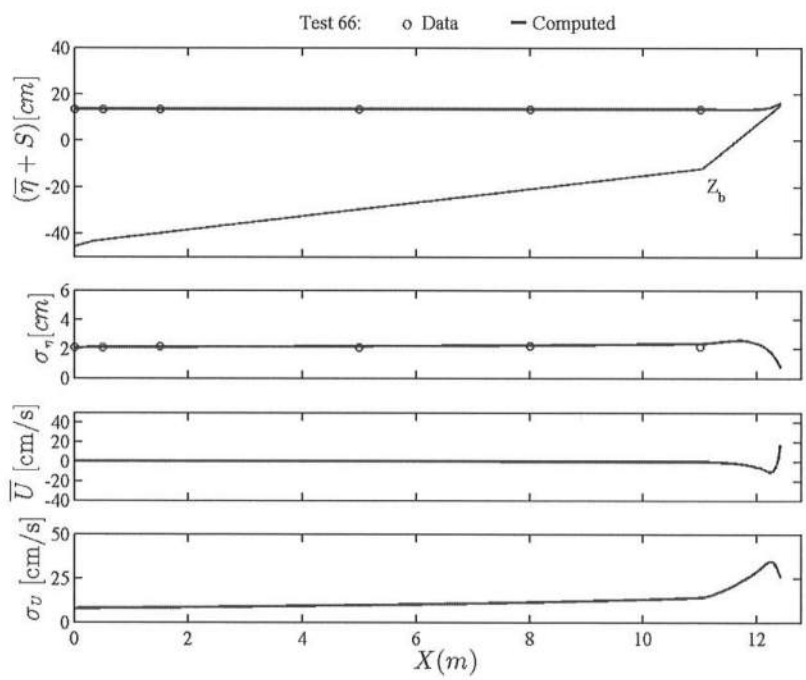

Fig. B.66: Test 66

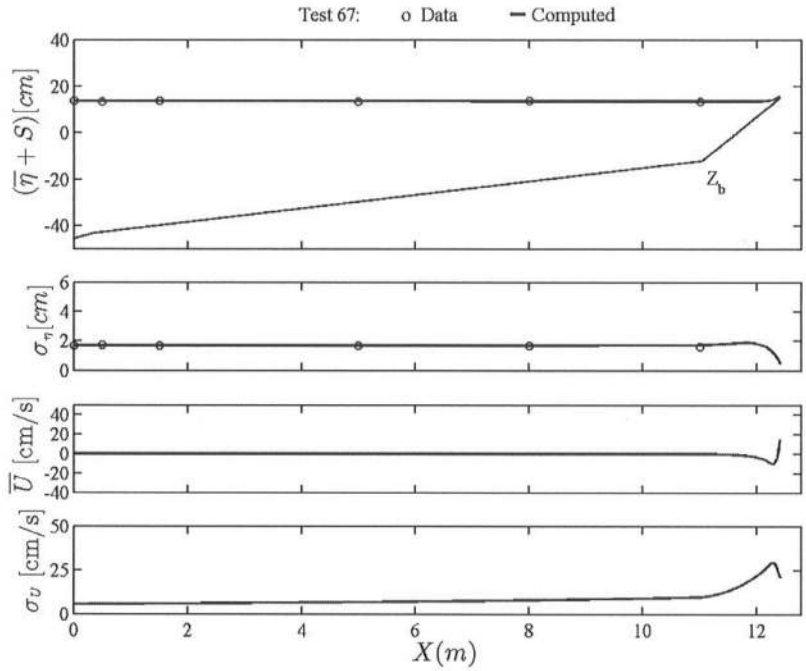

Fig. B.67: Test 67

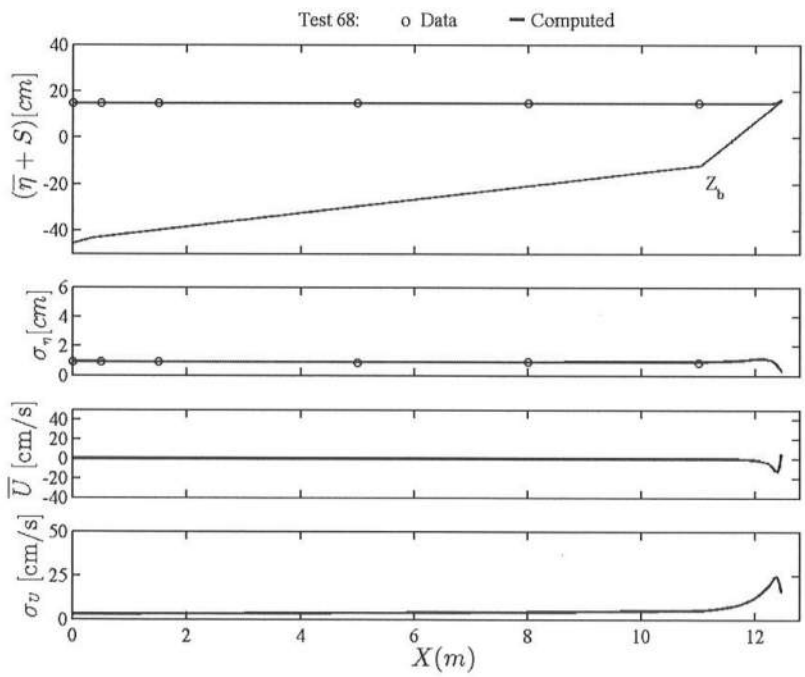

Fig. B.68: Test 68

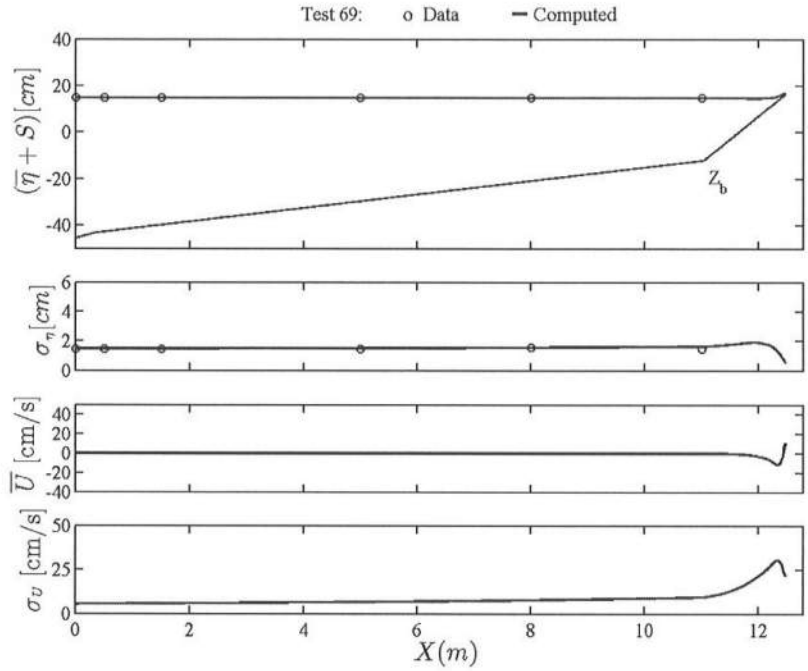

Fig. B.69: Test 69

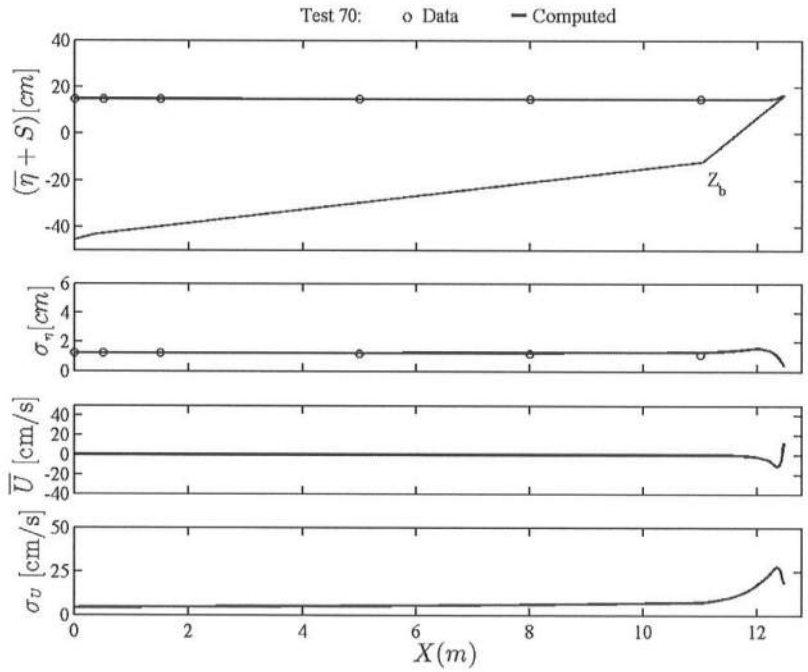

Fig. B.70: Test 70

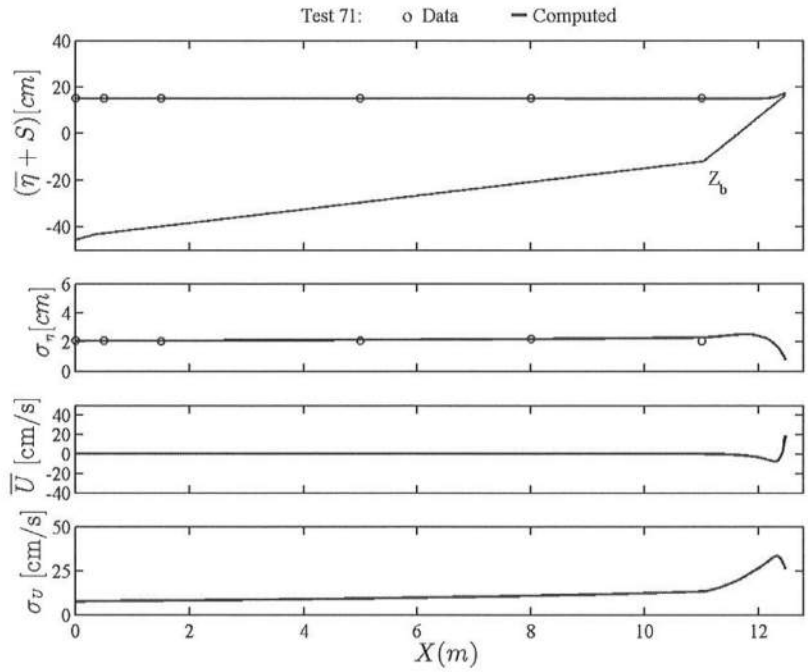

Fig. B.71: Test 71

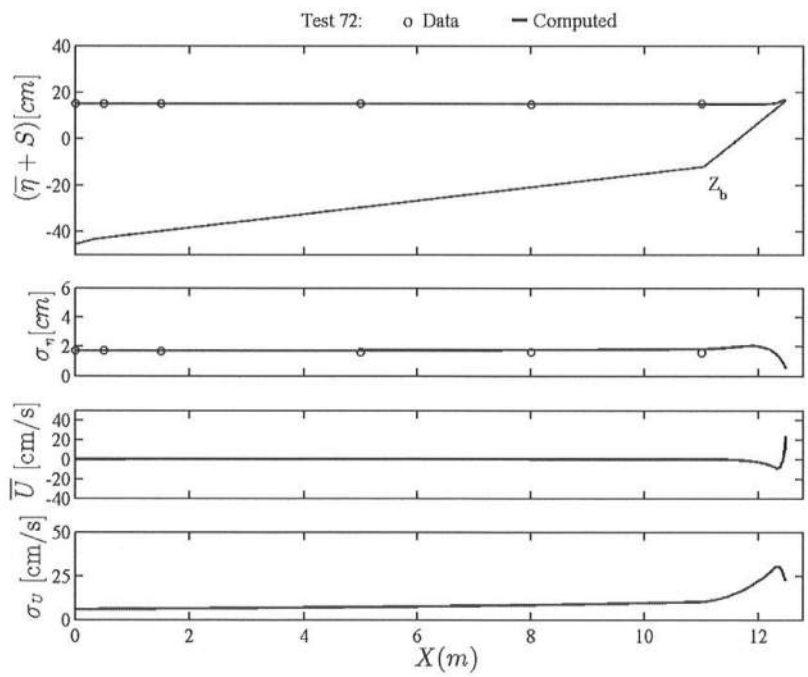

Fig. B.72: Test 72

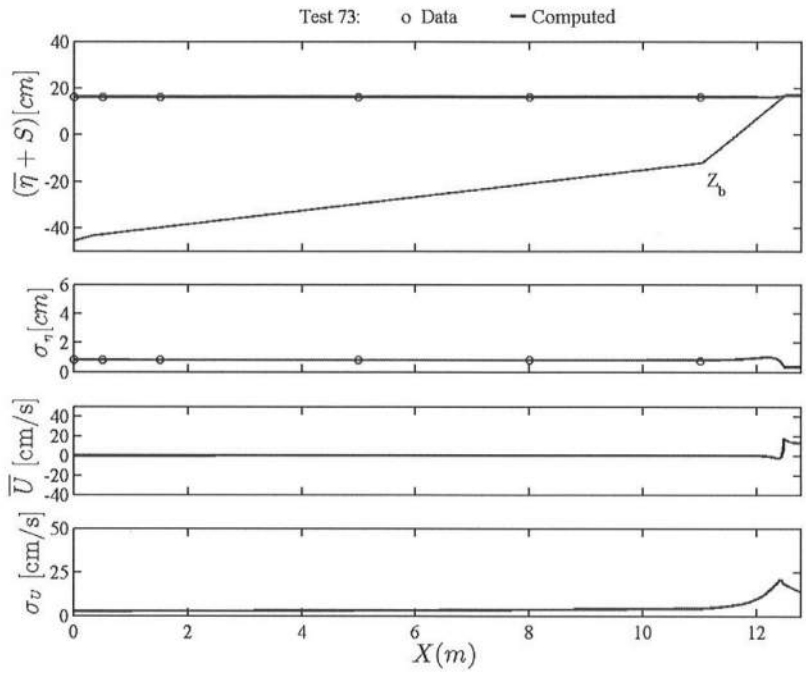

Fig. B.73: Test 73

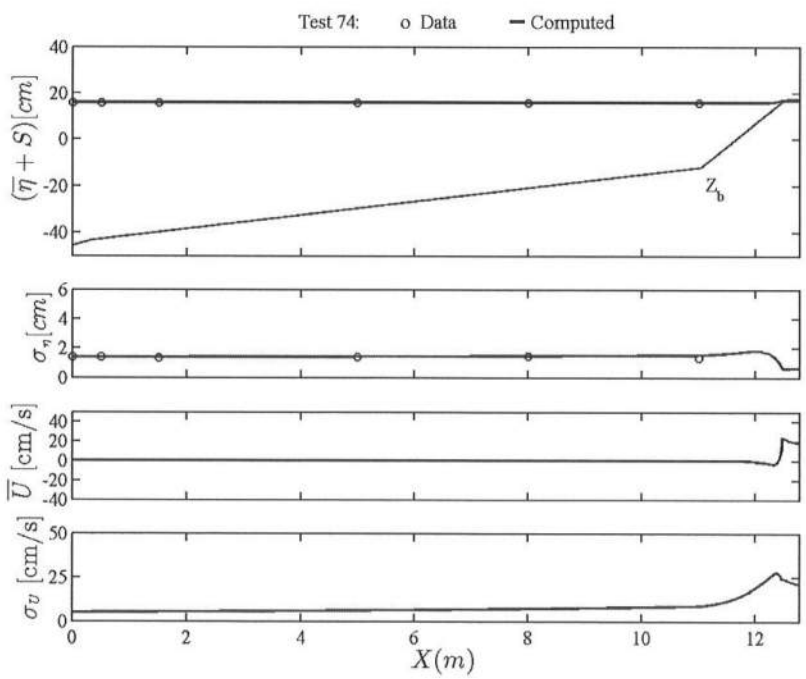

Fig. B.74: Test 74

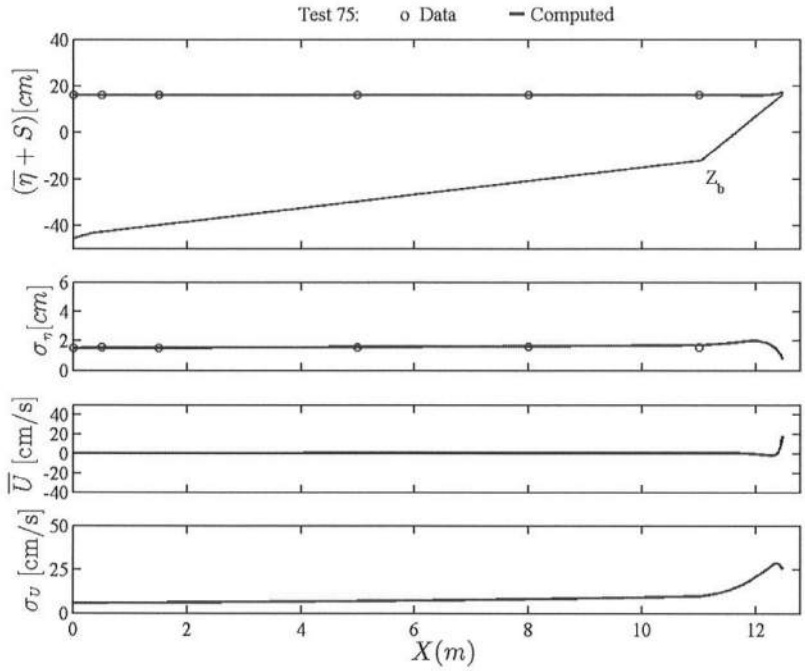

Fig. B.75: Test 75

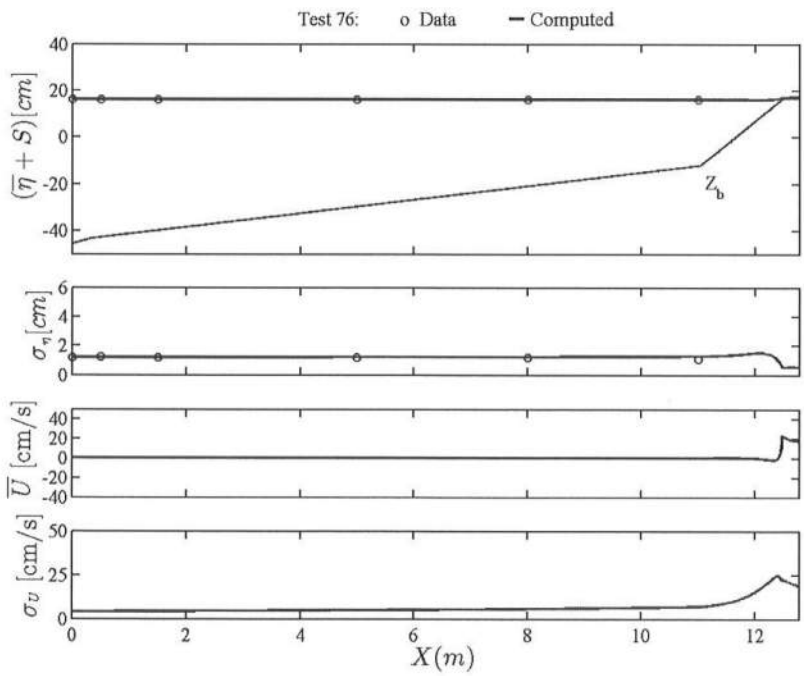

Fig. B.76: Test 76

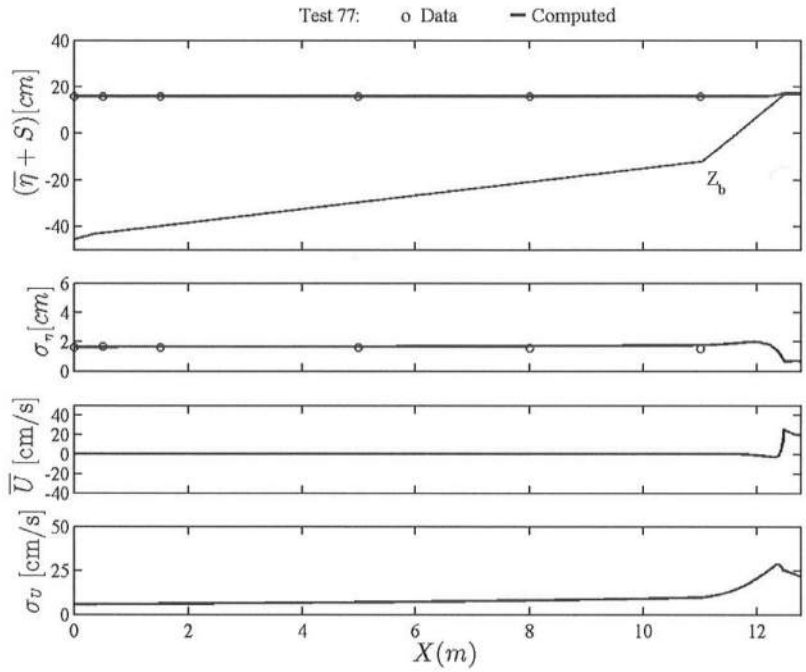

Fig. B.77: Test 77

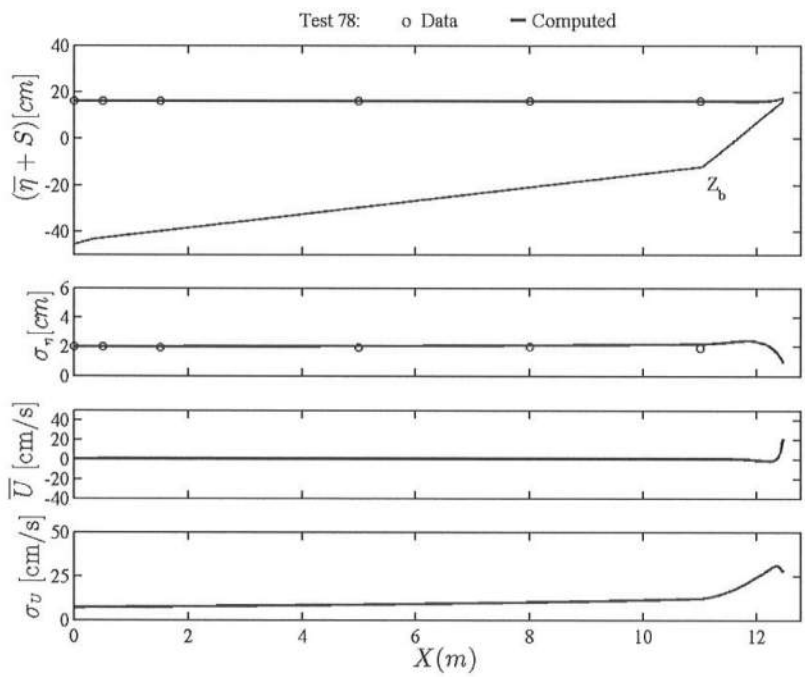

Fig. B.78: Test 78

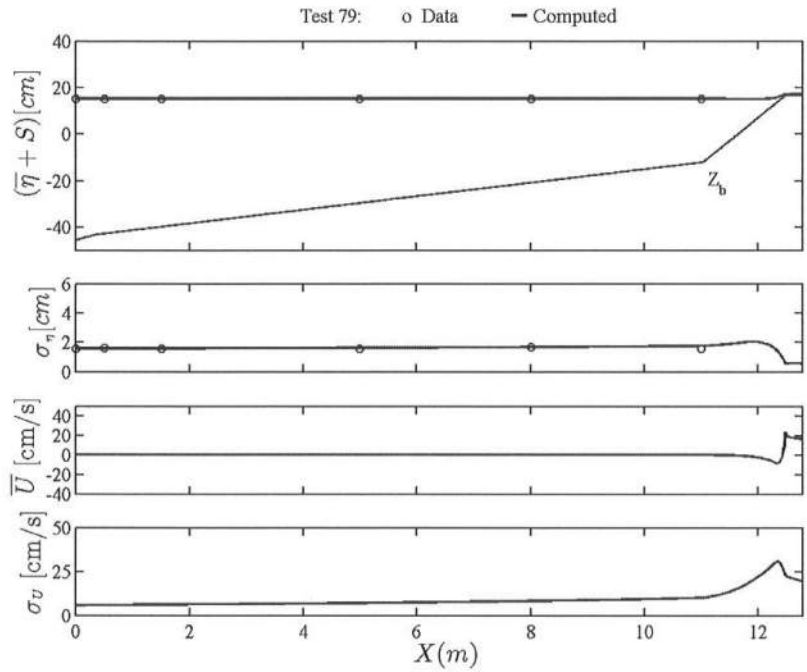

Fig. B.79: Test 79

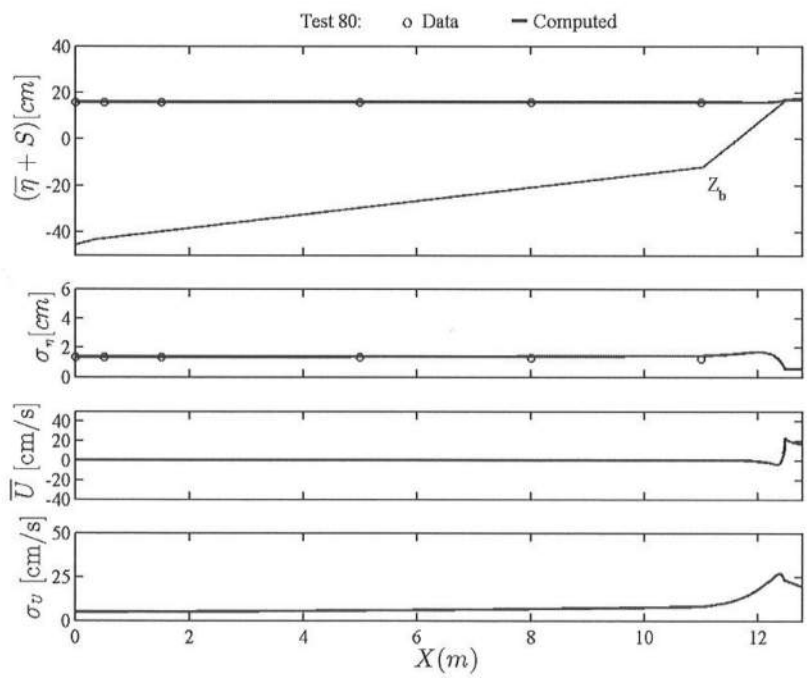

Fig. B.80: Test 80

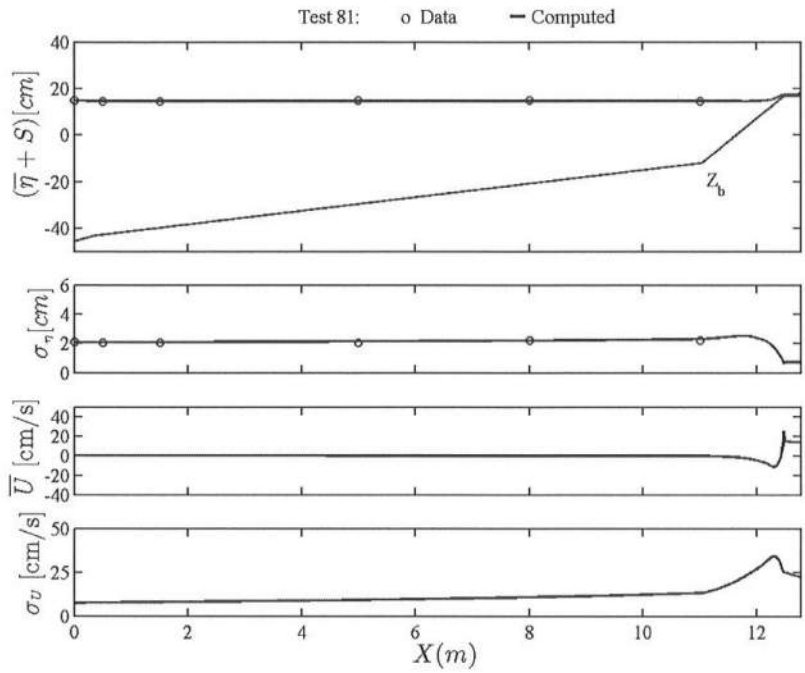

Fig. B.81: Test 81

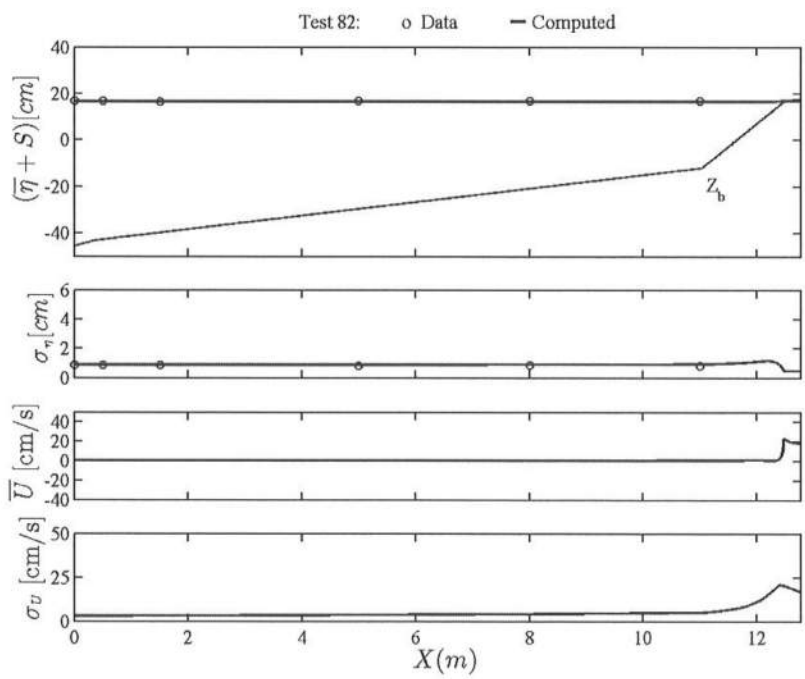

Fig. B.82: Test 82

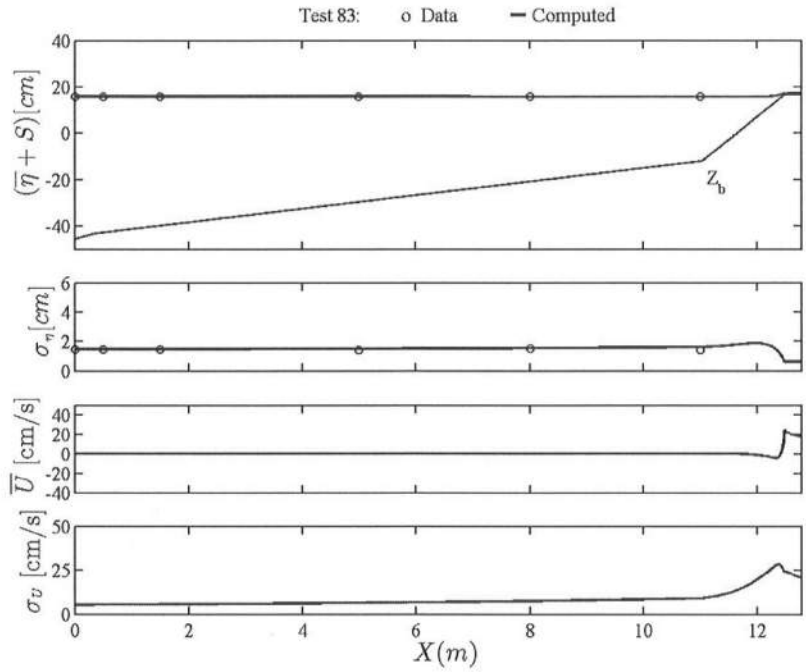

Fig. B.83: Test 83

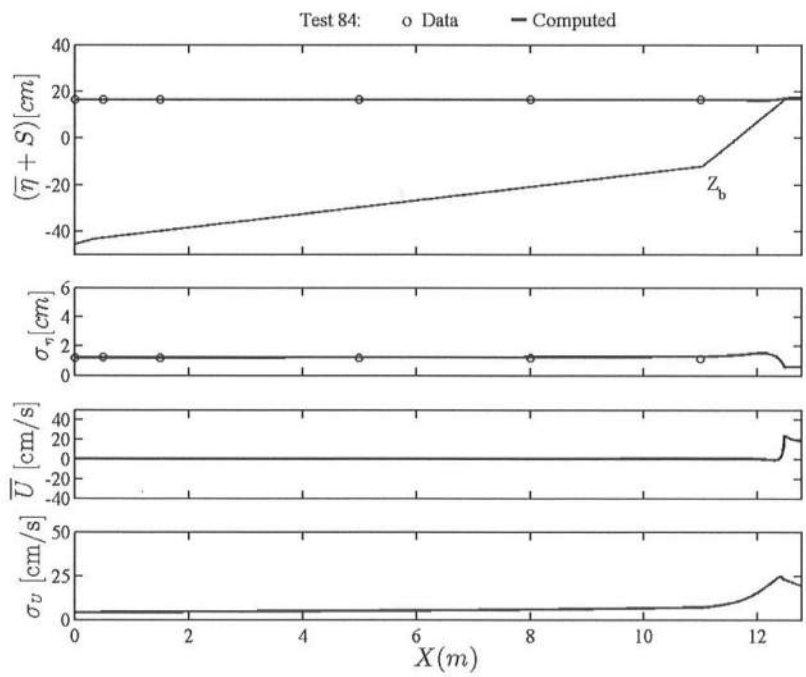

Fig. B.84: Test 84

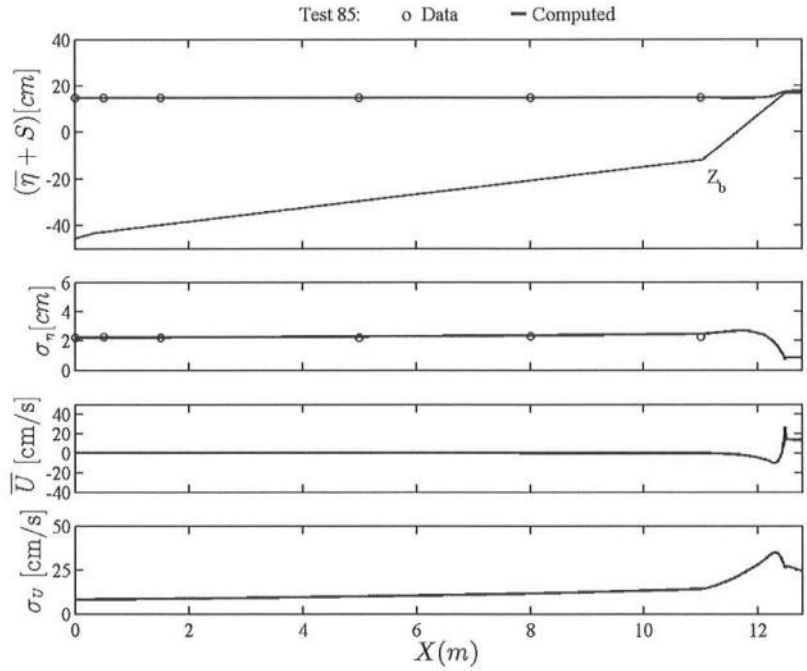

Fig. B.85: Test 85

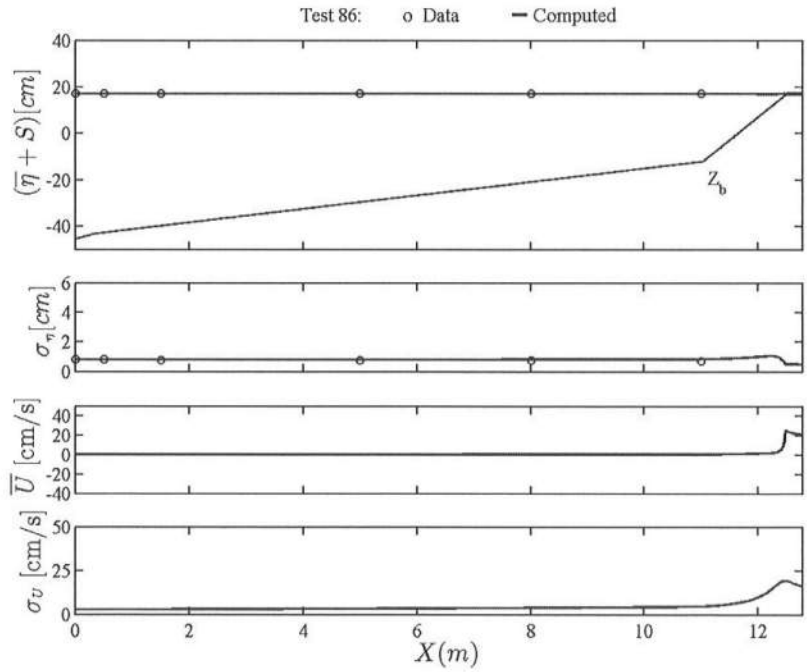

Fig. B.86: Test 86

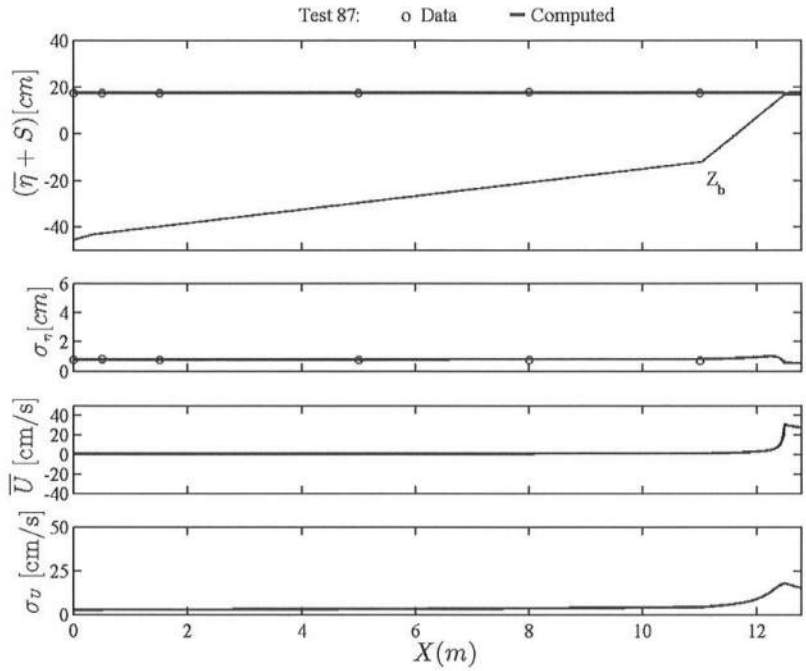

Fig. B.87: Test 87

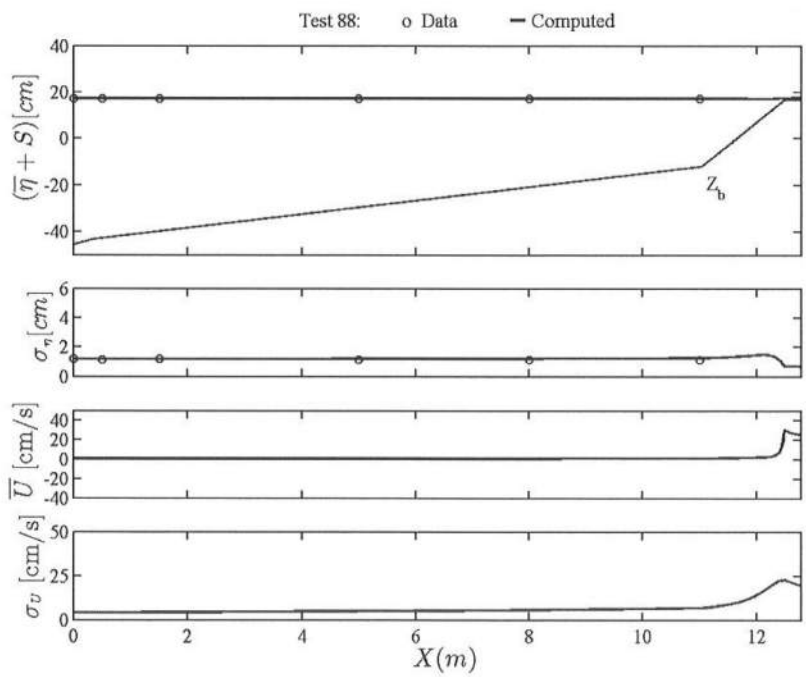

Fig. B.88: Test 88

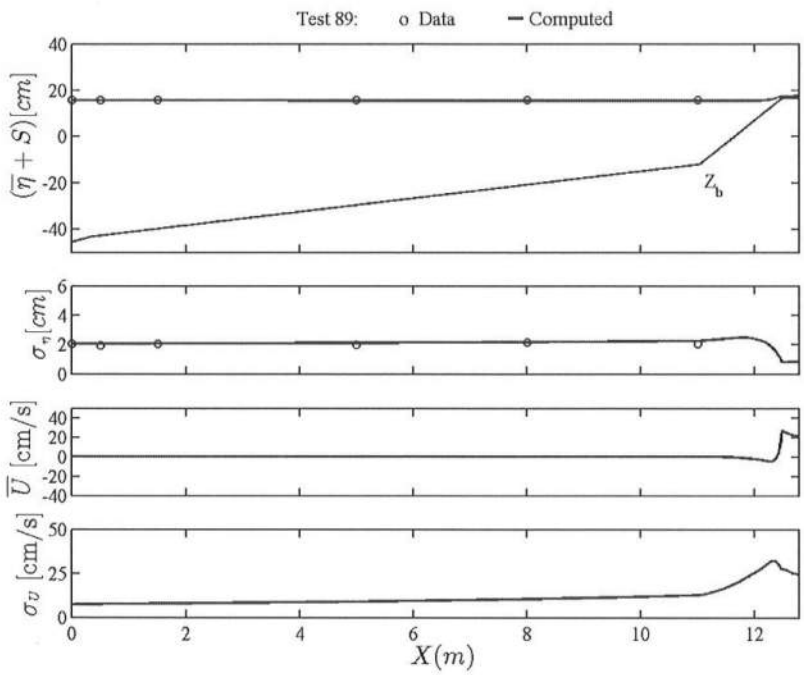

Fig. B.89: Test 89

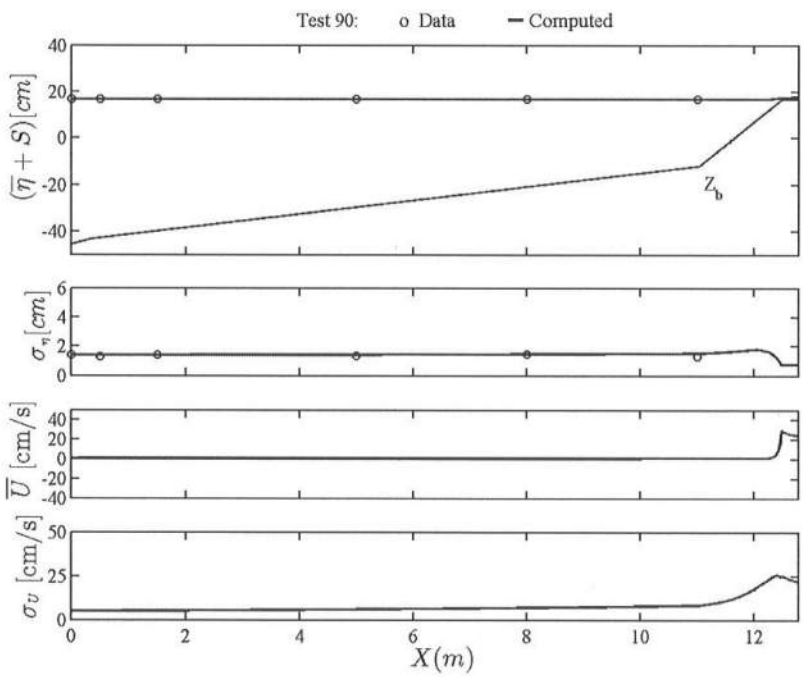

Fig. B.90: Test 90

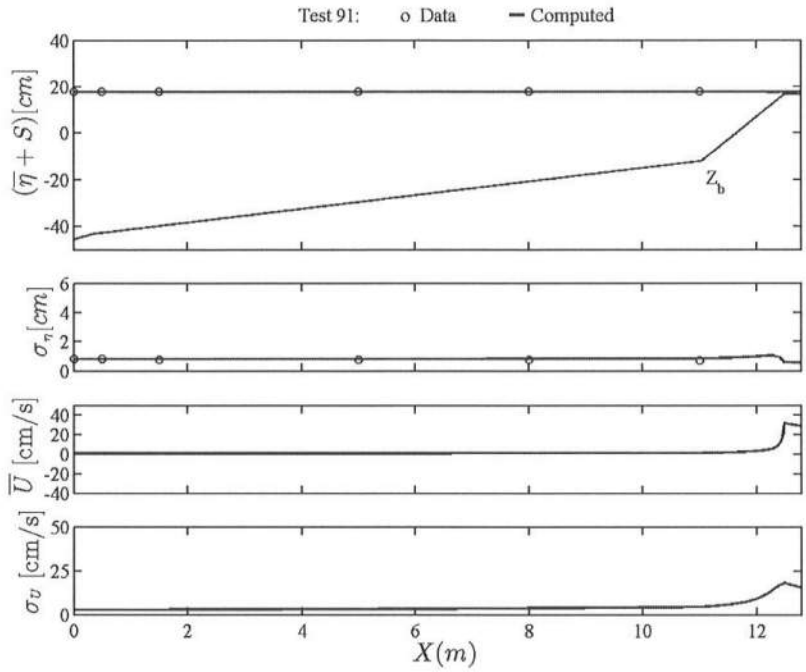

Fig. B.91: Test 91

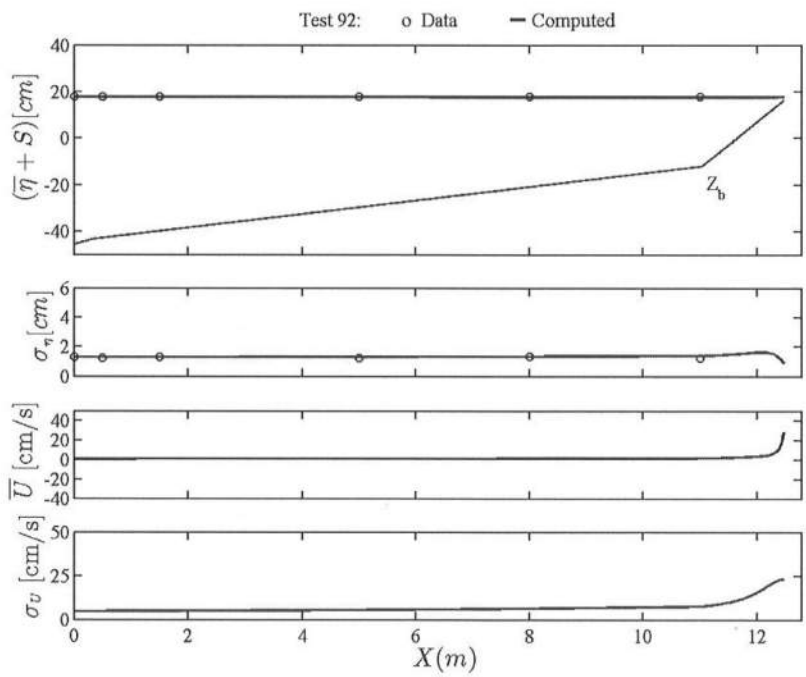

Fig. B.92: Test 92

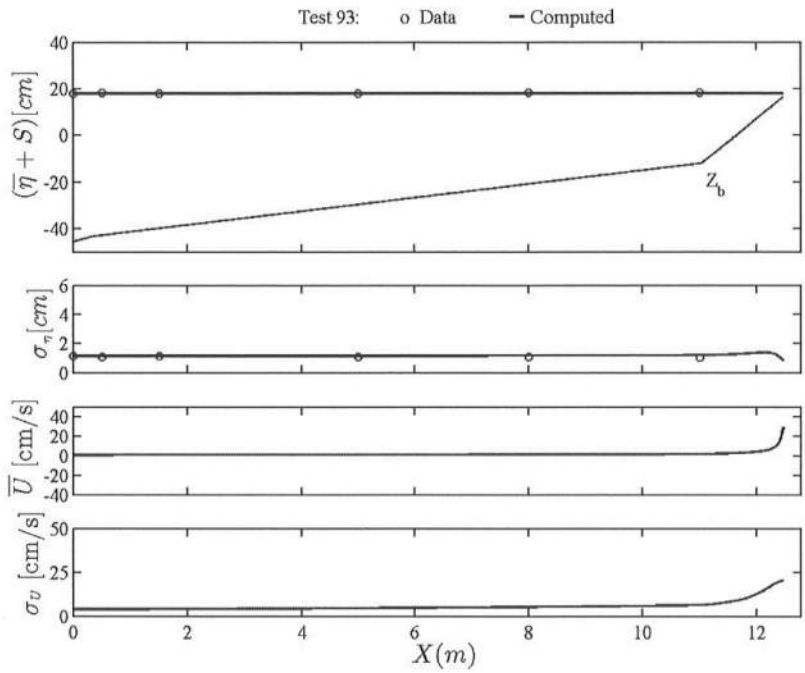

Fig. B.93: Test 93

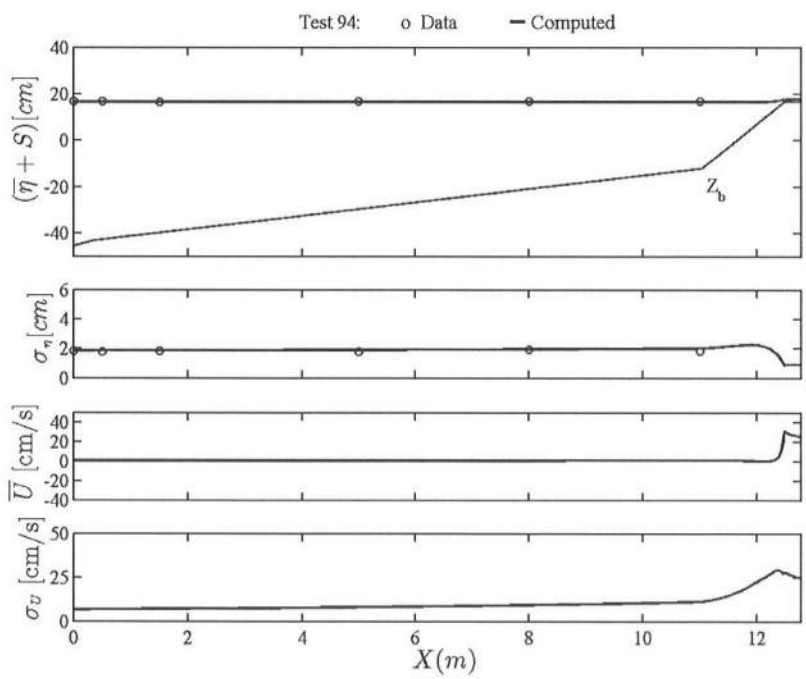

Fig. B.94: Test 94

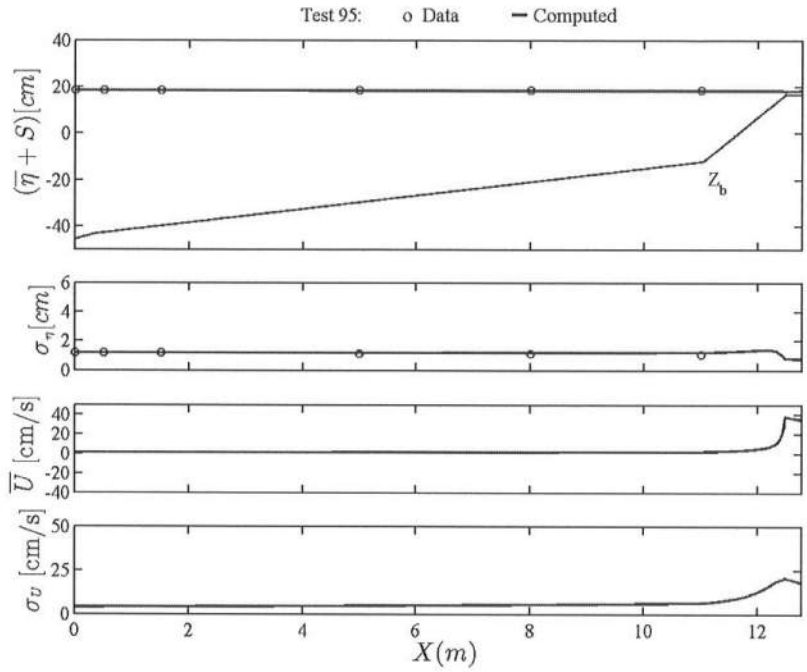

Fig. B.95: Test 95

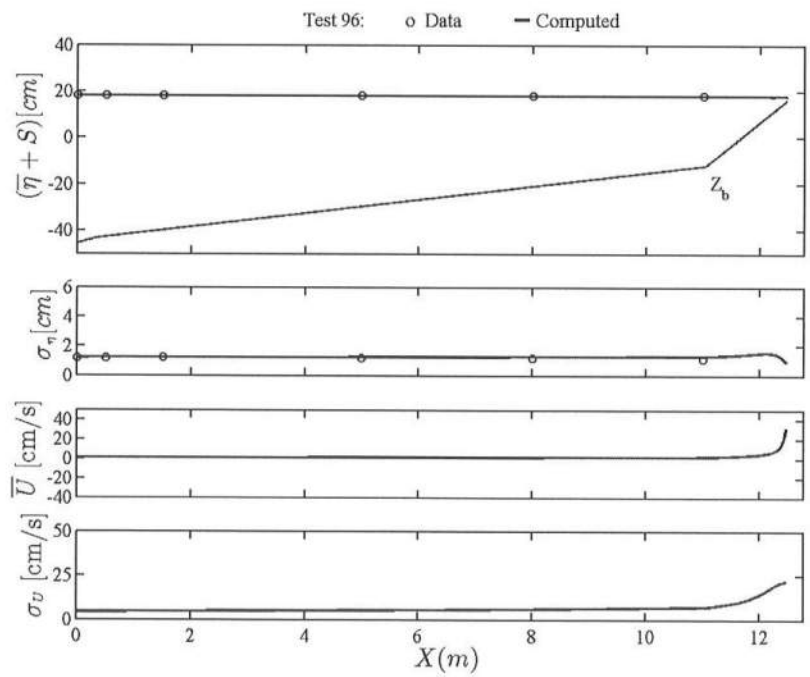

Fig. B.96: Test 96

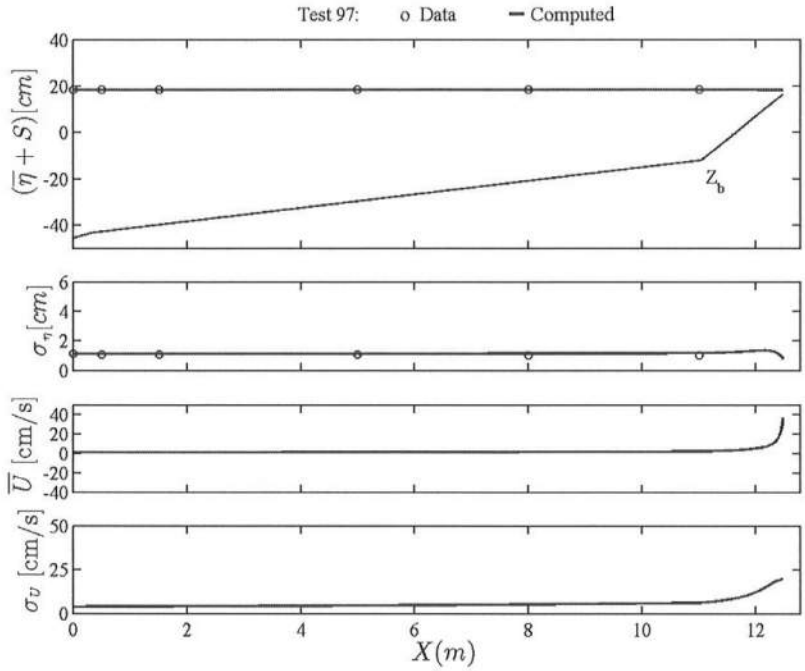

Fig. B.97: Test 97

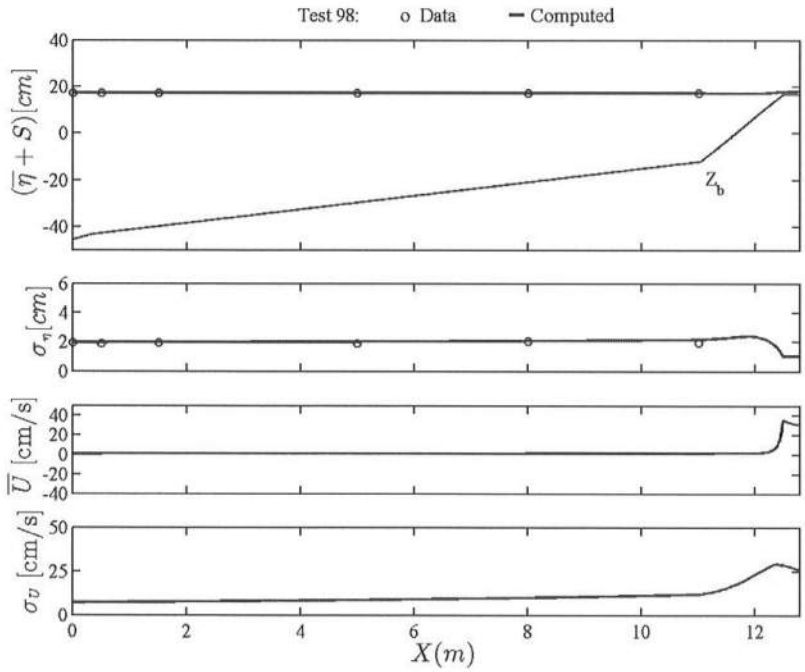

Fig. B.98: Test 98

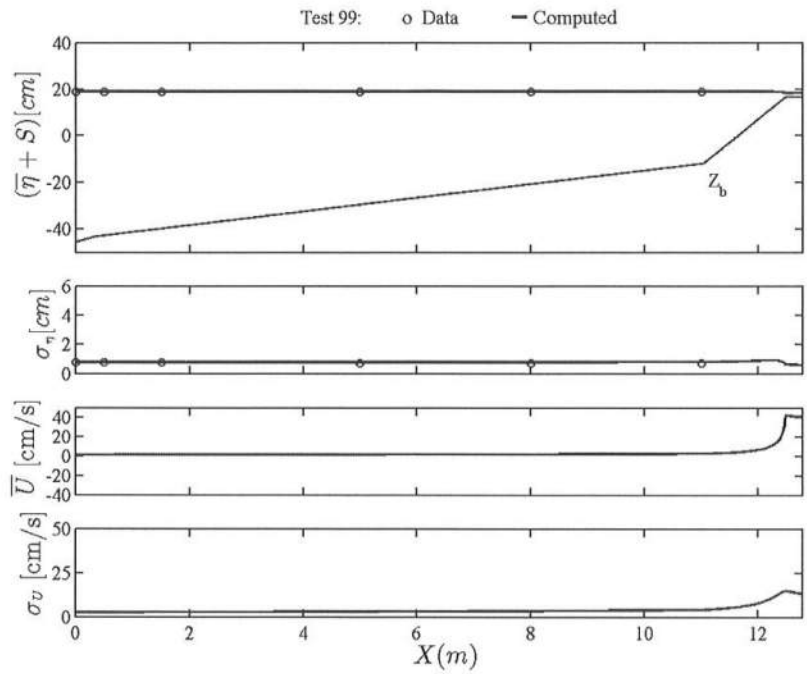

Fig. B.99: Test 99

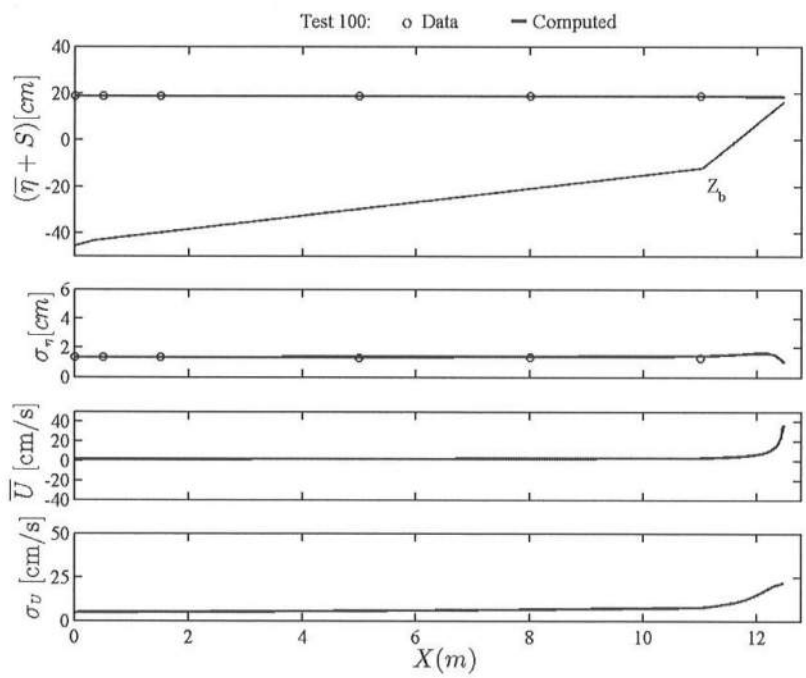

Fig. B.100: Test 100

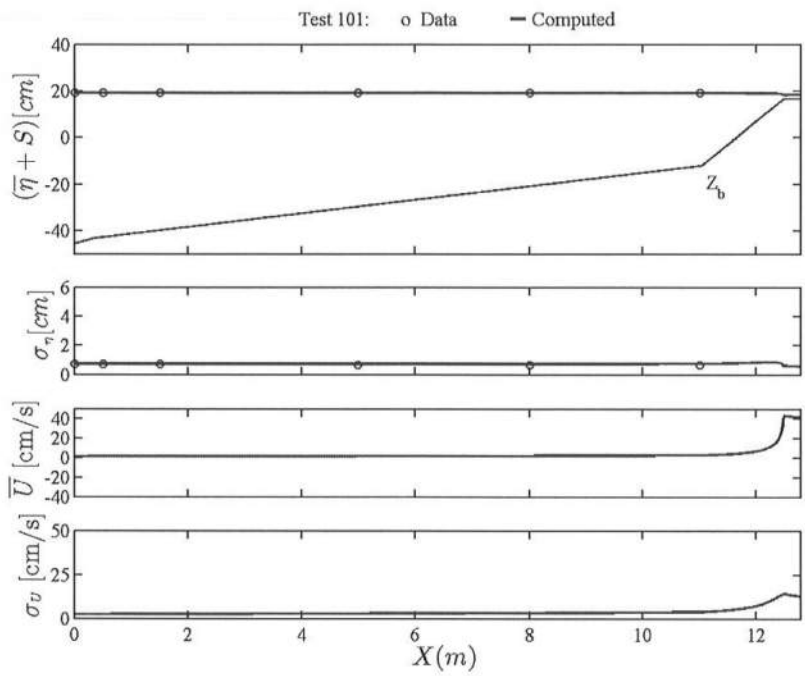

Fig. B.101: Test 101

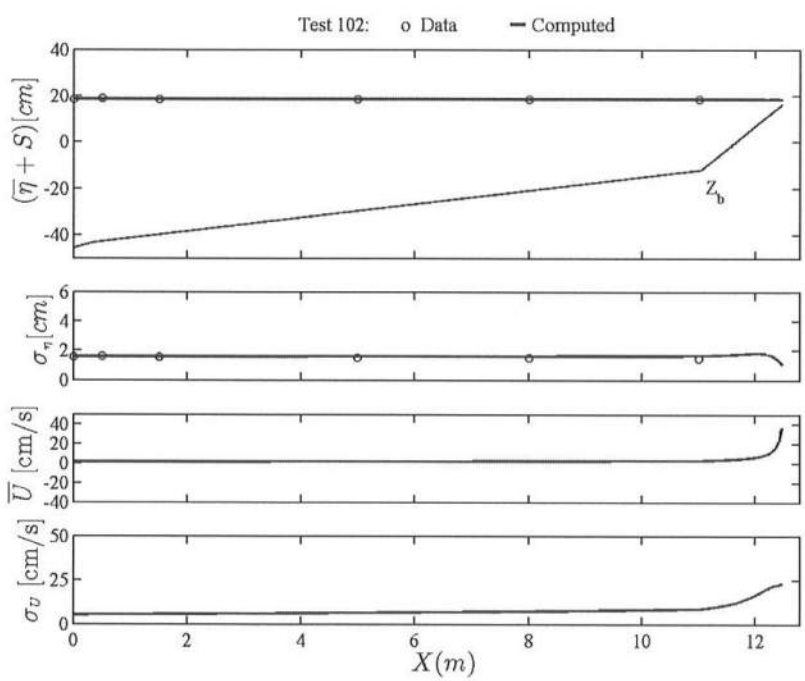

Fig. B.102: Test 102

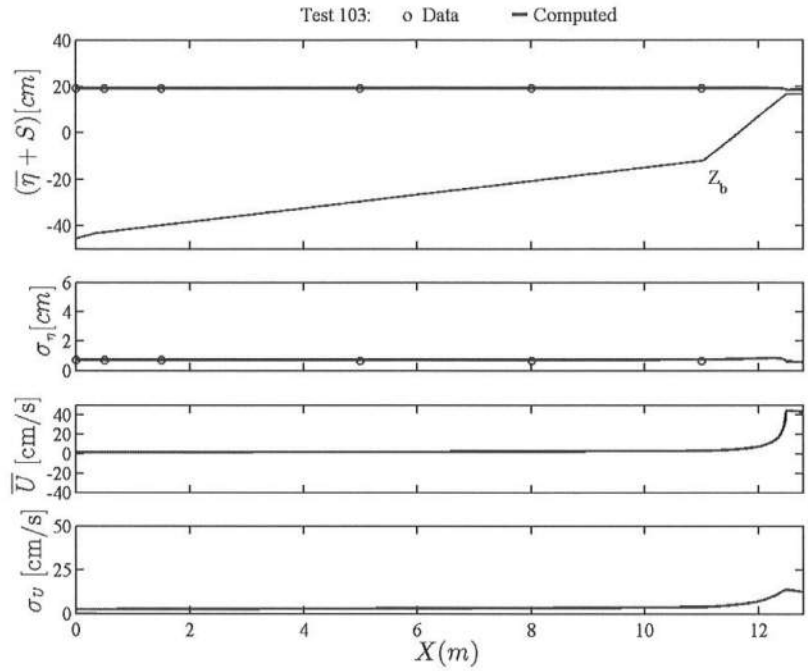

Fig. B.103: Test 103

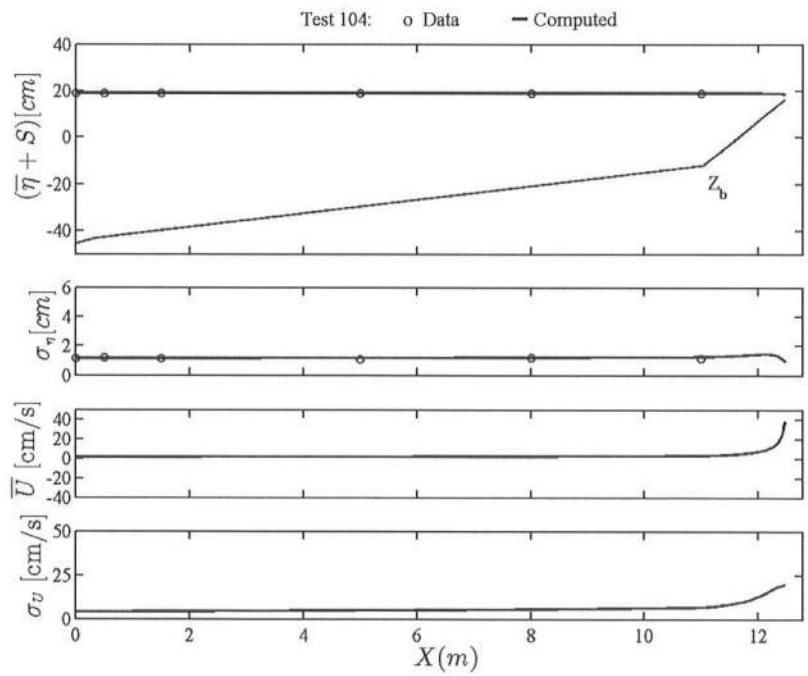

Fig. B.104: Test 104

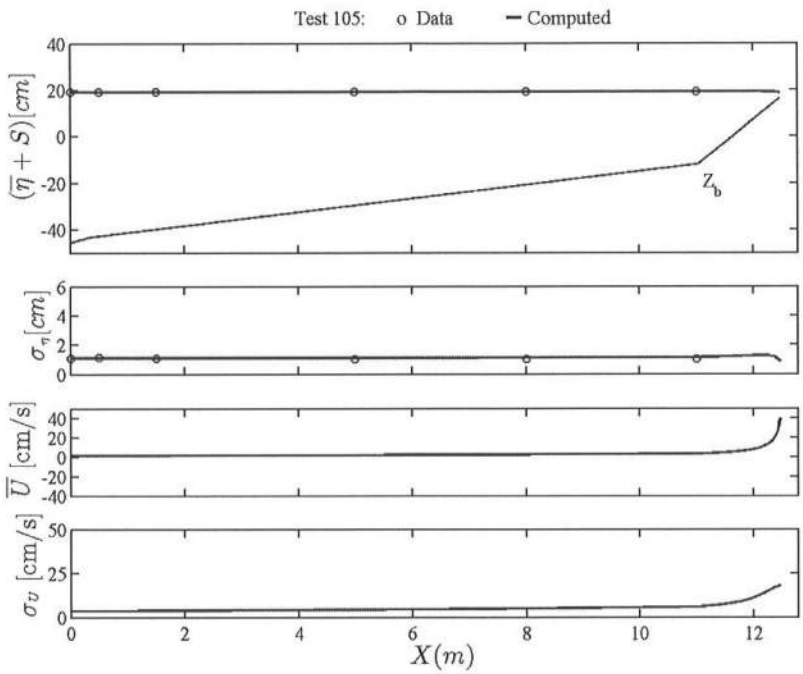

Fig. B.105: Test 105

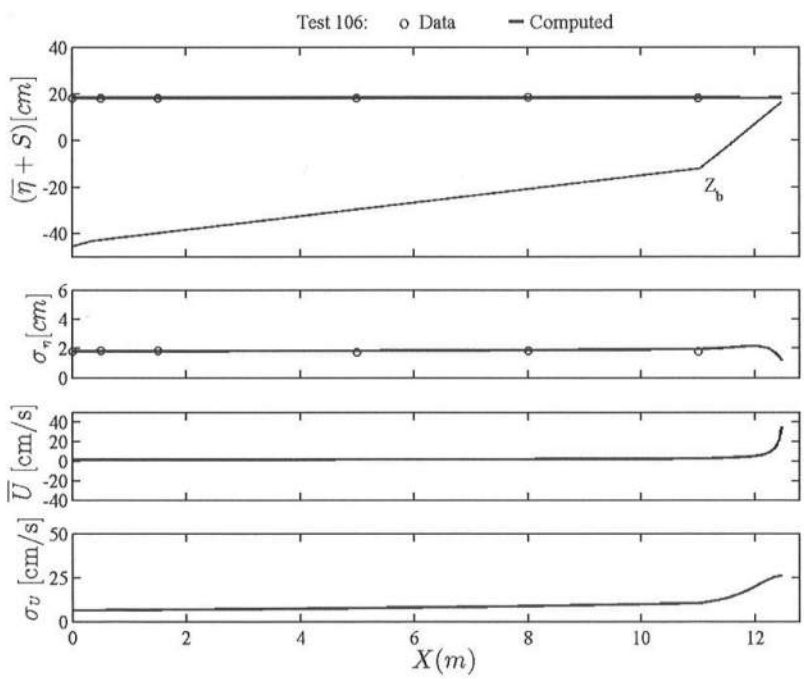

Fig. B.106: Test 106

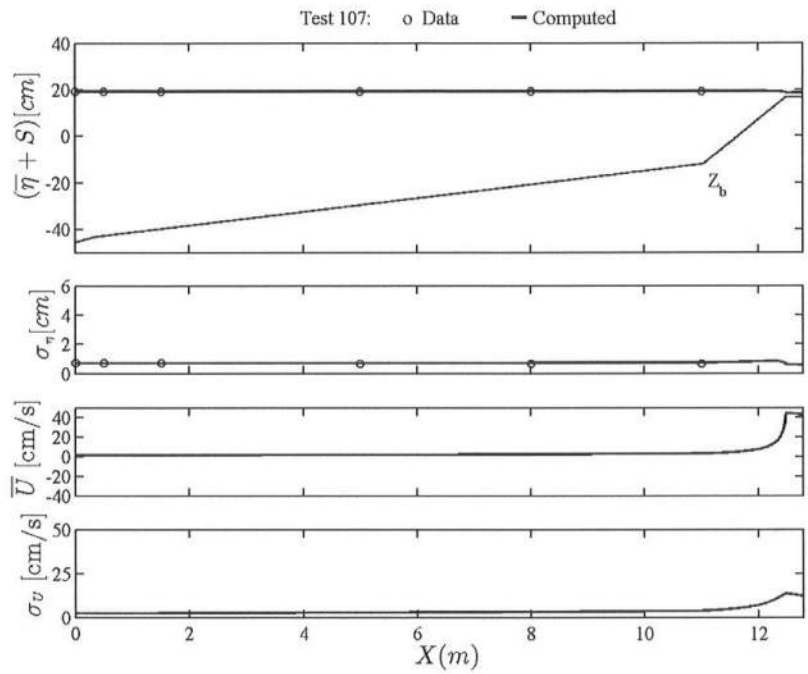

Fig. B.107: Test 107